FACULTY OF SCIENCES

Department of Chemistry
Raman Spectroscopy Reasearch Group

Raman Spectroscopy of Layered Cultural Heritage Materials

Anastasia Rousaki
Student number: 01312792

Supervisors: Prof. Dr. Luc Moens, Prof. Dr. Peter Vandenabeele, Dr. Jana Sanyova

A dissertation submitted to Ghent University in partial fulfilment of the requirements for the degree of Doctor of Science: Chemistry

Academic year: 2017 - 2018

GHENT UNIVERSITY

Acknowledgements

After more than four years my journey comes to an end. During this journey I have lived in a country completely different from my home, worked in one of the best groups worldwide on Raman spectroscopy and have met some wonderful and inspiring people whom I would like to thank.

First of all, I would like to thank my promoter, Prof. dr. Peter Vandenabeele. There are no words to describe how grateful I am for working with him, alongside him and for him. Thanks are due for his introducing and teaching me Raman spectroscopy, for supporting me without a second thought, for listening to my craziest ideas, for giving me all the right lessons and for giving me all the right reasons to love my job and the group. Thanks for the (first!) long list that was made during our first trip to Argentina and for all the discussions we have had these past four years.

Thanks to my promoter, Prof. dr. Luc Moens, who has been one of the most inspiring and caring people I have met. Thanks for the endless support to me and to every new project, for the new ideas, for the long talks and the amazing, even longer working hours when we were measuring spectra in Patagonia, Argentina. Thanks for listening to me and caring about my scientific and personal problems.

Thanks to Dr. Jana Sanyova (KIK-IRPA, Brussels, Belgium) for welcoming me in KIK-IRPA for the first months of my research, for sharing her expertise with our group and for working together on the project “Archaeometrical Study of the Ghent Altarpiece".

I would like to acknowledge Ghent University for its financial support through the concerted research action "Archaeometrical Study of the Ghent Altarpiece”. Through this project, I was able to study one of the world’s most magnificent paintings, the Ghent Altarpiece of the Van Eyck brothers, which also helped me complete my PhD research. Furthermore, I would like to thank

FWO for granting me a short stay abroad (project: K204416N) for analyzing, *in situ*, rock art paintings with portable Raman instrumentation in Patagonia, Argentina.

Thanks to dr. Claudia Conti (Istituto per la Conservazione e la Valorizzazione dei Beni Culturali, Milan, Italy) and Prof. dr. Pavel Matousek (Central Laser Facility, CCLRC Rutherford Appleton Laboratory, Oxfordshire, UK) for all the help, the support, their fruitful collaboration and their new ideas on the development of the new micro-SORS techniques.

Thanks to Prof. dr. Maximiliaan Martens, for his advice during the research campaign of the Ghent Altarpiece and for his collaboration and help during the measuring time on the cork masterpiece of the Pantheon of Rome made by Antonio Chichi.

Thanks to Prof. dr. Jan Jehlička (Charles University, Prague, Czech Republic) for his scientific advice on mineral-related questions, for his collaboration on the Patagonian rock art paintings and for some beautiful discussions during the last RAA (2017) conference.

Thanks to Prof. Dr. Laszlo Vincze, to dr. Bart Vekemans and Brecht Laforce for having shared with me their valuable expertise with X-rays. Thanks for the collaboration and measurements on beads from the Kongo King project and on samples from rock art paintings from Chubut province, Patagonia, Argentina.

Thanks to dr. Dimitri Vandenberghe for sharing his ideas on dating rock art with luminescence techniques and giving me new insights on characterizing iron oxides.

Thanks to Prof. dr. Danilo Bersani (University of Parma, Parma, Italy) for his advice concerning green earths and for his input on the analysis of ceramics from Ecuador.

Thanks to Prof. dr. Howell G. M. Edwards for upgrading and taking care of my PhD text and for the wonderful scientific conversation we had during the inArt (2016) conference in Ghent, Belgium.

Thanks to Prof. dr. Karel Strijckmans for all his support and organization since I first arrived in S12.

I would like to acknowledge dr. Eleni Kouloumpi (National Gallery-Alexandros Soutzos Museum, Athens, Greece) for being the first person to introduce me to archaeometry. Thanks for being my mentor and also one of my dearest friends. Thanks for all the support and all those endless nights we spent in discussions during my Bachelor and Master thesis work. But most of all, thanks for being there in one of my most troubled times in my life and for giving me unconditionally all the help I needed without a second thought. Thanks for inspiring me and for having you by my side. Without you, I wouldn't have gone so far.

Thanks to the Raman spectroscopy research group for welcoming me in the laboratory and to Ghent. Thanks to Alessia, Debbie and Mafalda for all the hours that we spent together working on projects and in the office. Special thanks to Jolien and Sylvia, two of my dearest people and my closest friends and colleagues. Thank you girls for making the working hours full of joy, for all the support and help, for all the problems that we solved together, for being there during my ups and downs but most of all thank you for really sharing your life with me the past four years. We had an amazing journey together and we shared a "notorious" office. Thanks to Possum for the support, the wonderful time we spent during her visits to S12 and for the great girls' night out we organized.

Thanks to our amazing Argentinian colleagues Emmanuel Vargas, Cristina Vázquez, Verónica Aldazábal, Cristina Bellelli, Mariana Carballido Calatayud, Adam Hajduk, Oscar Palacios, Emilio Eugenio, Lisandro Lopez and Graciella Custo for their support and trust on the characterization of Patagonian rock art paintings *in situ* and *in vitro*. Without their valuable expertise and commitment

none of the projects we carried out together would have been possible. I am really grateful for their hospitality and their big smiles during our first and second visits to Argentina.

Thanks to Prof. dr. Koen Bostoen, dr. Karlis Karklins and dr. Bernard Clist for their fruitful cooperation and valuable information on the glass beads from Democratic Republic of the Congo. I would like to acknowledge the KongoKing/BantUGent research groups for collaborating with us on the glass bead project that led to numerous publications.

Thanks to all the colleagues from University of Évora (Department of Chemistry, Hercules laboratory) for all the support during our common projects and for the analysis and detailed research on the glass beads.

Thanks to Prof. dr. Theodoros Ganetsos for all his help and for engaging me as a keynote speaker at the 2nd Pan-Hellenic Conference on Digital Cultural Heritage-EuroMed (2017).

Thanks to the colleagues from the laboratory of physicochemical analysis and research of National Gallery-Alexandros Soutzos Museum, Athens, Greece for their hospitality, help and knowledge provided to me during my training in 2009. Special thanks are due to dr. dr. Michail Doulgeridis, dr. Eleni Kouloumpi, dr. Anna P. Moutsatsou and Agni V. Terlixi.

Thanks to all the colleagues from my former research group in the Physics Department of the Aristotle University of Thessaloniki, Greece. Thanks to Prof. dr. Konstantinos M. Paraskevopoulos for sharing his knowledge, supporting and trusting me during my Bachelor and Master's years and to dr. Triantafyllia Zorba for being one of the greatest teachers in FTIR spectroscopy and for her friendship and support.

I would like to thank all the conservators from KIK-IRPA for their hospitality and help during the portable measurements made of the Ghent Altarpiece, in MSK.

Thanks to all the colleagues from S12 for the wonderful time we spent during the past four years and during Christmas lunches, barbeques and team-building exercises. Thanks to Sylvia and Kris for organizing all the common activities.

Thanks to all the Bachelor and Master students who worked with our group and for their dedication to the projects.

Thanks to my closest and dearest friends I met in Thessaloniki who became my family forever. Thanks to Aliki, Kleopatra, Anna, Renia, Nikos and Athina for sharing all these years together. You were the only ones that truly understood me and the only ones that supported me in every step I made (or still am making), stupid or not. Sorry for leaving you behind in 2014, sorry for breaking your heart some times, but thank you for all the love you still are giving me and I wish at some point to meet with you again all together in one place and be like we were at our 18th. There are no words to describe how grateful I am for meeting you and for sharing my life with you.

Thanks to Dimosthenes for being there all my life, for giving me his friendship and help during the most difficult periods of my life and for being my biggest supporter. Thanks for all the summers we spent together around Greece and thanks for being one of my closest friends and family.

Thanks to my friends from Thessaloniki, that I met during my Bachelor and Master's years. Thanks to Filitsa, Andy and Menti for their friendship and support and for all those countless days and nights we spent together. Thanks to Ilias, my eternal physics couple and my friend for everything he has done for me. Thanks to Thodoris, Nikos and Nikoleta for all the joyful moments we spent together.

Special thanks to my dearest friend Liana. Thanks for the past years that we spent together in Belgium, for the bad days that you made more than bearable, for giving me your love and friendship, for standing my stubbornness and helping me understand the world with your smile. I am lucky that I met you in Belgium and that we created together a small unit.

Thanks to the loving couple, Stavros and Melena, two of the first people I met on arrival in Ghent. Thanks for being there for me every time that I needed you, for all the trips, days and nights we spent together and for your valuable advice.

Thanks to Eutihia and Frederic for the countless joyful moments and the all the support they provided to me. Thanks to Themis, the amazing newcomer in the company. Thanks to Mirella, Vasilis, Grigoris, Ilias, Tonia and to my amazing new roommate Konstantina.

Thanks to my boyfriend Spiros for being always there for me. Thanks for all the love you unconditionally gave to me. Thanks for standing by my side even if we had thousands of kilometres distance between us. Thanks for all these late nights you were playing music to me in order to keep me company during my late working hours. Thanks for letting me be who I truly am with you, for supporting my dreams and respecting my decisions, for hearing my cry and loving my laugh. But most of all thank you for taking the leap of faith with me.

Thanks to Eleni, Panagiotis, Thanos, Eleutheria, Vasilis and the newest member Elena. Thanks for all the love that all these years gave and are still giving to me, for being there all my life guiding me, for opening your heart to me and for supporting me since I started to remember myself.

Special thanks and all my endless love to these people that my PhD thesis is dedicated to. My family. Thanks to my father George, my mother Konstantina and my little love of my life, my sister Nasia. Thanks to my family to whom I owe my entire existence. Thanks for letting me choose my path in life, for supporting me and being proud of the decisions I have made and for giving me so much precious advice. Thanks for giving me the kind of love that is hard to find. Thanks for wiping my tears every time that I was broken and for helping me stand on my feet. Thanks to George, Konstantina and Nasia that made me the person I am today.

Αναστασία Ρουσάκη

Γάνδη, 2018

Contents

Section β: Working in situ

Abbreviations and Acronyms

SORS	Spatially offset Raman spectroscopy
Fibre-optics micro-SORS	*Fibre-optics* microspatially offset Raman spectroscopy
Full micro-SORS	*Full* microspatially offset Raman spectroscopy
Defocusing micro-SORS	*Defocusing* microspatially offset Raman spectroscopy
CCD	Charge-Coupled Device
PB15	Copper phthalocyanine (pigment blue 15)
FT	Fourier-transform
Near-IR	Near infrared
SERS	Surface enhanced Raman spectroscopy
FTIR	Fourier-transform infrared spectroscopy
XRD	X-ray diffraction
p-XRD	Portable X-ray diffraction
SEM-EDX	Scanning electron microscopy coupled with energy dispersive X-ray spectroscopy
SCA	Structural and chemical analyser
XRF	X-ray fluorescence
hXRF	Handheld X-ray fluorescence
TXRF	Total reflection X-ray fluorescence
MA-XRF	Macro X-ray fluorescence
STD	Standard lens
LWD	Long working distance lens
HiNA	High numerical aperture lens
GPS	Global positioning system
SR-XRD	Synchrotron radiation X-ray diffraction

^{14}C dating	Radiocarbon dating
S/N	Signal-to-noise ratio
FC	Fibre-optic connector
PC	Physical contact connector
PVC	Polyvinyl chloride

List of Tables

List of Figures

α

Chapter 1 Introduction and outline

Over many years a theoretical framework in conservation science has been constructed based on practical experience. Skilled conservators and restorers have applied their treatment of cultural heritage objects and associated documentation with only limited access to analytical tools. As the demand for more scientific research grew, physicochemical techniques started to play an increasingly important role in the detailed documentation of the artefacts. From the merging of historical analysis, conservation practices and the natural sciences, a cross-disciplinary field was formed, namely, archaeometry. Archaeometrical research is dedicated to the historical and physicochemical documentation of works of art covering a wide chronological range, from prehistory to the modern era.

The high impact that archaeometrical research has on cultural heritage studies is underlined by the number of archaeometrical laboratories that can now be found around the world. Moreover, museums and national galleries have started to create their own, in house, analytical laboratories that assist the conservation teams towards a better documentation and preservation of their collections. It is worth noticing that scientific conservation in museums and national conservation/restoration centers had already started from the first half of the 20th century. On the other hand, dedicated scientific groups attached to universities, have created new analytical pathways and developed novel instrumentation in order to characterize art objects and identify the components associated with degradation and the state of preservation of the artifacts .

The subject of this PhD thesis is the contribution of the natural sciences, physics and chemistry, towards the analysis of components found in different layers of cultural heritage objects. The research is based on non-invasive and non-destructive analysis of works of art. “Non-invasive” means that no samples are required for the experiments. Mobile instruments can be employed and analyze the large scale artefacts inside their exposition area (museums, open air

environments) or inside laboratories without jeopardizing their intergrity. For smaller artworks, "non-invasive" analysis can be carried out in the analytical laboratories with the use of benchtop instruments, by positioning the object inside the configuration's chamber e.g Raman spectrometers and micro-X-Ray fluorescence (micro-XRF) spectrometers. "Non-destructive" refers to the fact that no alterations to the objects have been made or the samples have not been consumed. The main focus of this PhD is the contribution of Raman spectroscopy in cultural heritage studies and the development of the technique by proposing novel approaches for the chemical characterization of complex art structures.

This PhD research was accomplished in the Raman Spectroscopy Research group at Ghent University. The Raman research group is an internationally highly appreciated group dedicated to the applications and development of benchtop and mobile Raman spectroscopy in cultural heritage studies.

This work is dedicated to the application of Raman spectroscopy for the analysis of layered cultural heritage materials. Moreover, novel approaches and *state-of-the-art* Raman analysis are discussed. As a starting point, an extended review of the literature, dedicated to Raman spectroscopy and its use in archaeometrical investigations is provided in chapter 2. Furthermore, possible drawbacks and latest improvements of benchtop and mobile Raman spectroscopy are described along with its application in case studies dedicated to cultural heritage materials. The theoretical background of Raman spectroscopy and the Raman spectrometers used in this research are also discussed.

The main aim of this PhD research is the non-invasive analysis of works of art. In chapter 3, the first application of portable Raman instrumentation for the *in situ* analysis of prehistoric rock art paintings in Patagonian archaeological sites is illustrated. The *EZRaman-I dual* Raman analyser from TSI Inc. is employed for the analysis of rock art paintings from hunter-gatherers in different environments, in three different provinces in Argentinian part of Patagonia. (Neuquén, Río Negro, Chubut). This measurement campaign covered the investigation of 16 open air shelters and one

cave and resulted in one of the most comprehensive expeditions measuring directly on-site and rock art paintings. During this research the performance of the portable Raman spectrometer to characterise pigments, degradation products and substrata was evaluated. Moreover, the possible drawbacks of measuring under extreme conditions are underlined and several improvements are suggested.

The measurement campaign in Argentinian part of Patagonia revealed the pigments used by the indigenous population, as well as weathering products and components of the substrata (chapter 4). Different pigmented areas, namely red, green, white, black, yellow, blue/green etc., and encrustations found on top of the figures and rock surfaces were analysed. The applicability of the dual laser Raman system is underlined by the identification of green earth by both lasers. On-site macroscopical observations and data treatment revealed the existence of thin crusts that cover the rock paintings and the rock surface, entirely or partially. These crusts are the result of weathering, pollution and human activity. The weathering layers tend to encapsulate the pigmented ones and thus compromise the Raman signals. In some cases, the sites were so severely degraded that no Raman signal could be obtained. Raman spectroscopy, being a surface sensitive technique, does not normally allow the identification of components situated deeper than the top layer. In order to perform stratigraphic analysis, therefore, one has hitherto relied upon sampling and *in vitro* research. As the demand for non-invasive and non-destructive analysis is increasing, new scientific milestones should be accessed: the question needs to be addressed can Raman spectroscopy perform non-invasive stratigraphic analysis?

Fibre-optics micro-spatially offset Raman spectroscopy (*fibre-optics* micro-SORS) is proposed as a novel approach for non-invasive stratigraphic analysis on micrometer-thick turbid layers (chapter 5). The rationale behind this technique is that a spatial separation of the illumination zone and the Raman signal collection is achieved by the use of two bare glass fibres. *Fibre-optics* micro-SORS is complementary to *full* micro-SORS and *defocusing* micro-SORS modes recently described in the literature. Further development of the *fibre-optics* micro-SORS setup can contribute towards the development of a pioneering light sensor that can be applied to cultural heritage objects.

The next step towards probing deeper than the surface layer is the retrieval of subsurface chemical images. The connection between the chemical information and its spatial distribution is a concept known as mapping. Raman spectroscopy is an ideal technique for constructing such images by performing sequential Raman point measurements in a grid. In chapter 6, a *defocusing* micro-SORS approach is demonstrated and its capability of obtaining subsurface Raman mapping data is described. The *defocusing* micro-SORS variant is the most straightforward micro-SORS approach as it can be applied in any Raman spectroscopy configuration without further modifications. The latter is considered very important as the technique can be adopted and performed from any laboratory that utilizes Raman spectrometers for the analysis.

Finally, in chapter 7 (in English) and chapter 8 (in Dutch), the results obtained from this PhD research are summarized and future perspectives are discussed.

Chapter 2 Raman spectroscopy: theory and application

This chapter presents the basic theory of Raman spectroscopy. Moreover, the applications and possibilities of Raman spectroscopy on the archaeometrical field are extensively discussed and the instrumentation that is used for our research is described in detail.

2.1 Raman spectroscopy: an introduction

In 1928, C.V. Raman and K. S. Krishman discovered the inelastic scattering of light. A few years later, in 1930, C.V Raman was honoured with a knighthood and the Nobel Prize for Physics for his discovery.

Due to several instrumental improvements and technological advances, Raman spectroscopy has recently grown to become a well-appreciated molecular spectroscopic technique in a broad range of research areas (e.g. microbiology [1-2], mineralogy [1,3-4], cultural heritage studies [5-6], forensics [1,7-8], exobiology [1,9-10] and medicine [11-12]). Indeed, sensitive detectors now permit the use of low laser powers and short measuring times, which makes it possible to perform non-destructive analysis and mapping experiments. Using microscope optics on benchtop spectrometers means that a spatial (lateral) resolution down to less than 1 µm can be achieved , whereas the introduction of fibre-optic probe heads and the miniaturisation of spectrometers leads directly to mobile instrumental applications.

Before describing the applications and prospects of Raman spectroscopy in archaeometry, a brief fundamental description of the Raman effect is given. For a more detailed description we refer to the literature [13-17].

2.1.1 The Raman effect

The phenomenon known as the Raman effect is broadly described as the inelastic scattering of optical radiation by molecules. In Raman scattering, the scattered photon has a different energy to the incident photon. The Raman effect is observed when during a molecular vibration a change in the bond molecular polarizability occurs. [17] In other words, the electron cloud in a bond is distorted by the application of an external electric field [14].

The particle in a box model of quantum mechanics defines the allowed vibrational energy levels (E_v) :

$$\mathbf{E_v = (v + ½) \cdot h\nu_v} \qquad \textbf{[1]}$$

where v is the vibrational quantum number; ν_v, the molecular vibrational frequency; h, Planck's constant (h = 6.626 070 040(81) x 10^{-34} J·s).

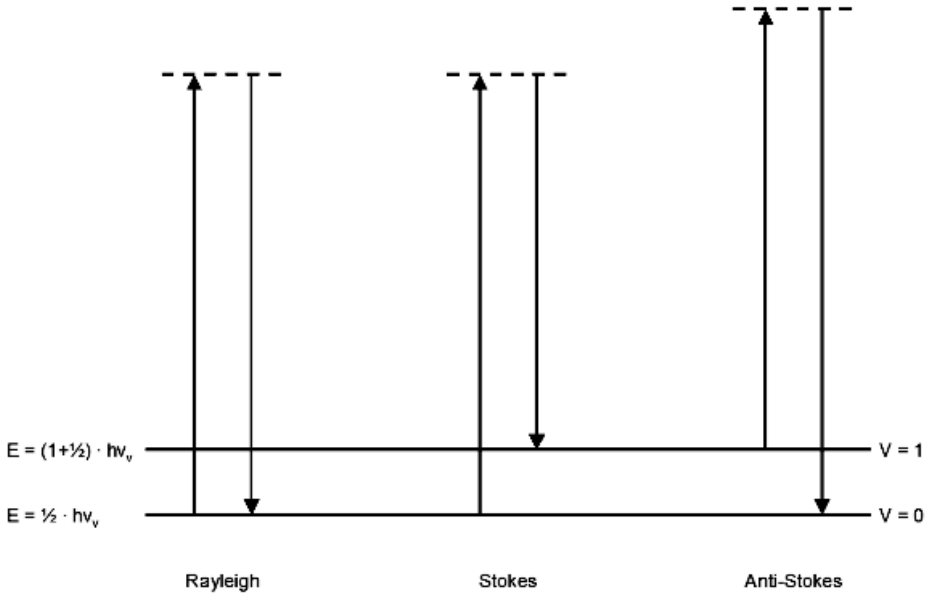

Figure 2.1. *Energy level diagram illustrating the spectroscopic transitions for Rayleigh and Raman scattering [17].*

If the energy difference between the emitted photon and the laser light is 0, Rayleigh scattering occurs. On the other hand, if the energy difference is different to 0, then Raman scattering takes place. In the case of Stokes Raman scattering, the scattered photon has a lower energy than the incident photon, while for anti-Stokes Raman scattering, the scattered photon has a higher energy that the initial photon. The energy difference between the ground state and the first vibrational excited state determines the Raman band position [Fig. 2.1]. [17].

2.1.2 The Raman spectrum

When performing Raman spectroscopy, a monochromatic laser is focused on the surface of the sample and/or object. The intensity of the scattered radiation is measured as a function of its wavelength [17]. In a Raman spectrum the intensity is plotted against the Raman wavenumber (in cm^{-1}), which represents the energy difference between the scattered and the incident radiation (Fig. 2.2) [17].

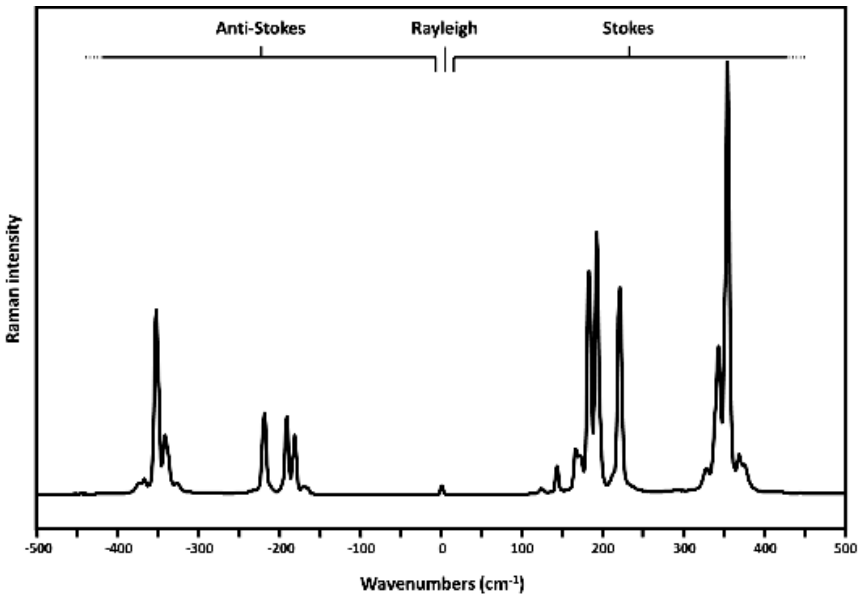

Figure 2.2. *The Raman spectrum of the mineral realgar (As_4S_4) recorded with a 785 nm laser [17].*

The 0 cm^{-1} band corresponds to Rayleigh scattering. This is usually suppressed by holographic filters in the spectrometer [17]. The pattern (symmetric band positions around the Rayleigh line) has positive wavenumbers (negative frequency shift) for Stokes and negative wavenumbers for anti-Stokes scattering [14].

The higher intensity of the Stokes bands compared with the anti-Stokes bands can be explained from Boltzmann's distribution law. At thermal equilibrium, lower states are more occupied than higher vibrational states, hence Stokes phenomena are more likely to occur than anti-Stokes.

2.2 Raman spectroscopy in archaeometry: an introduction

Based on: A. Rousaki, L. Moens, P. Vandenabeele, in *Micro-Raman Spectroscopy Theory and Application*, (Ed.: J. Popp), Physical Sciences Reviews, De Gruyter, Berlin, Germany, **2018**, submitted.

Archaeometry is a research area at the interface between the humanities and natural sciences: it uses and optimises methods from chemistry, spectroscopy, physics, biology, etc. to help answer research questions in the humanities, especially archaeology and the arts. In general, archaeological and art objects are investigated for several reasons. Besides the fundamental interest in the search for knowledge about materials that were used in the past, the study of artefacts can support their preservation, particularly by helping to select their optimal storage or display conditions and by investigating decay pathways and suggesting solutions for their conservation. Other reasons for art analysis include provenance studies, and potentially assisting in the dating of the artefact and for identifying forgeries.

In recent years, Raman spectroscopy has been increasingly applied for the investigation of objects of art and in archaeology [5, 18-19]. The technique is well-appreciated for the limited (or even nonexistent) sample preparation, the relatively straightforward interpretation of the spectra (by spectral fingerprinting – that is, undertaking a comparison of spectral data signatures against

a database of reference pigments, for example) and its speed of analysis. Moreover, the small spectral "footprint" – which allows the recording of a molecular spectrum of particles down to 1 µm in spatial diameter, the typical size of fine pigment grains – is certainly a positive advantage of the technique. Raman spectroscopy is also rather versatile as inorganic as well as organic materials can be studied without extraction or separation and the technique can acquire information on crystalline as well as non-crystalline phases. As a consequence, Raman spectroscopy can be used to study antique objects and 20th century synthetic (organic and inorganic) materials – illustrating a potentially wide range of applications. [5] Finally, the technique is non-destructive, provided the laser power is kept sufficiently low not to damage the artwork. In literature, the terms 'non-invasive' and 'non-destructive' are used, where the first term means that no sampling is involved, and the latter term indicates that no further sampling of a specimen is taken and that during analysis the sample is not consumed (destroyed), so this then and remains available for further analysis.

In the next few paragraphs, some recent applications of Raman spectroscopy in archaeometry will be discussed. Firstly, an overview will be given of some novel trends involving *in vitro* (laboratory) research of samples or small objects. Secondly, non-invasive applications, involving mobile Raman instrumentation, will be illustrated, followed by a discussion on the combination of Raman spectroscopy with other analytical techniques.

2.2.1 Benchtop Raman instrumentation and possibilities

New applications in Raman spectroscopy were often driven by instrumental changes. Thus, the introduction of confocal Raman microscopy and the application of Charge-Coupled Device (CCD) detectors have triggered the application of Raman spectroscopy in art and archaeology [20]. In general, benchtop Raman instruments share some favourable characteristics such as the ability of coupling multiple monochromatic light sources (single, dual or multiple laser systems), optimal wavenumber stability, high spectral resolution (depending on the laser excitation within the same

configuration), focusing through high magnification objectives and the incorporation of calibrated motorised stages.

The first realisation of the application of Raman spectroscopy in the art area was pigment identification in mediaeval manuscripts [21-23]: an important application which demonstrated some different possibilities of the technique. Soon, it was realised that this approach could be extended towards other applications, including paintings [24], corrosion products [25], gems [26], glass [27] and ceramics [28]. The artefacts that can be studied via Raman spectroscopy date from prehistory through to contemporary art. A credible example is the chemical characterization of rock art paintings, which are considered as one the most ancient forms of human expression. In general, rock art is considered to encompass the painted, engraved or carved natural rock surfaces made by indigenous people. The pictographs or petroglyphs found on stone surfaces can stylistically vary from the abstract to geometric or more naturalistic forms and can be can be found widely in Europe, Africa, America, Latin-America, Asia, and Oceania. Their preservation and documentation is considered highly important in order to understand the technological level of the societies that created them. Several studies can be found in the literature highlighting the use of Raman spectroscopy on the characterization of the mainly red, yellow, green, white and black pigmented layers [29-30]. With particular reference to their preservation state, Raman spectroscopy is employed to study (bio)degradation products associated with weathering and human activity. For modern art studies, Raman spectroscopy was used for the investigation of the characteristic spectral signatures of azo pigments [31] and copper phthalocyanine (PB15). The latter is often identified as an important pigment in 20th century artworks. However, PB15 is used in different polymorphic forms (α-CuPc, β-CuPc and ε-CuPc). Raman spectroscopy is a very valuable technique for the detection of this pigment in paint systems and it is able to distinguish between these polymorphs. [32] The discrimination of PB15 polymorphs can be used to date and authenticate artworks [32] as they appeared at different times on the paint market. [33-34] The Raman spectra of α-CuPc and β-CuPc differ only in the relative intensities of some bands. Furthermore, using linear discriminant analysis (LDA), the α-, β- and ε-CuPc pigments could be discriminated using the Raman intensity ratios as variables [32].

The analytical Raman spectroscopic approach was also increasingly applied for the study of natural organic products, although, due to its inherent fluorescence suppression, this was often related to Fourier-transform (FT-RS) applications. It was realised that by shifting to near-IR excitation lasers (typically 1064 nm), the contribution of fluorescence emission which is significantly stronger than Raman scattering is minimised and its swamping effect can therefore be partially avoided. However, simultaneously the Raman scattering capability is decreased, and as a consequence, the adoption of a higher irradiance together with larger measuring times should be applied, with the added risk of overheating the sample [35-36]. Moreover, the use of FT-Raman technology implies the use of solid state detectors (usually low-bandgap semiconductors), as silica based CCD detectors are less sensitive in the near IR region (for wavelengths larger than 1.1 μm) [36]. Despite possible drawbacks, FT-Raman spectroscopy is a very powerful tool with many applications in cultural heritage, such as (among others) the study of native American Indian rock art [37], the characterization of Egyptian pigments [38] investigation of thioindigo–palygorskite mixtures resembling Maya blue [39]. Furthermore, elaborate and comprehensive FT-Raman spectral databases can be found in the literature [40-41].

Today, Raman spectroscopy has proven to be a versatile approach in archaeometry, and it is often considered as a first choice technique when it comes to art analysis. Unfortunately, compared with other spectroscopic methods, the Raman effect is relatively weak. On the other hand, it has an excellent spatial resolution, and by focussing the laser beam on, for instance, a single pigment grain, it is possible to obtain good quality spectra. Unfortunately, not all molecules yield intense Raman spectra, which depend upon the molecular scattering coefficients. However, on occasions when several laser wavelengths are available for selection, one can choose a laser that has a frequency close to the electronic absorption region of a specimen, thus resulting in an enhancing of the spectral signal by several orders of magnitude. This resonance enhancement produced, for instance, interesting results when studying lazurite, ultramarine blue, chrome based pigments [42-43] and carotenoids (including corals) [44-46]. Although, lasers that have excitation in the blue and green regions of the electromagnetic spectrum are considered optimal for the Raman signal enhancement of carotenoids [47], red and near IR laser excitation can also be used

for the identification of these molecules [revealing at least the two strongest Raman bands (namely the in-phase ν(C=C) and ν(C—C) stretching vibrations) and one medium intensity feature (the in-plane ρ(C—CH_3) rocking mode) [47]] even with the use of portable Raman instrumentation [48]. However, when selecting a laser, it is important to consider that the intrinsic Raman intensity is proportional to the 4^{th} power of the laser frequency. For resonance Raman spectroscopy, the laser wavelength should be compatible with the vibrations of the target molecule under study. On the other hand, the spectroscopist should be aware that theoretically when selecting shorter, higher energetic wavelengths, fluorescence emission is also increasing even though the Raman signal is significantly enhanced.

Moreover, some materials, such as dyes, are not present in high local concentrations, but are rather found to occur in a dispersed way, which makes it difficult to focus the laser on specific regions of the sample. Surface enhanced Raman spectroscopy (SERS) [49-50] can here be of help for identifying the dye molecules present. Indeed, by adsorbing analyte molecules onto noble metal nanostructures, the observed Raman signal can be significantly enhanced, while the accompanying fluorescence emission is reduced. This is achieved by combined electromagnetic [51] and charge-transfer [52] mechanisms. Silver nanoparticles can be produced in different ways. In cultural heritage research, often silver nanoparticles are obtained by reduction of silver nitrate using citrate [53]. Another approach starts from silver sulfate that is reduced by glucose under microwave irradiation [54]. In that case, very reproducible results could be obtained, while sodium citrate is used as a capping agent. Also photoreduction [55] and laser-ablation [56] have been proposed as promising alternatives for the production of silver nanoparticles. Silver island films (AgIFs) or thin films of silver over nanospheres were also proposed as SERS substrates. In that case, these substrates were either directly deposited [57] on a coloured surface, or firstly adsorbed onto a silver-alumina support [58] on which the analyte was adsorbed afterwards.

The SERS technique was discovered in 1974 [49], but its application in artworks started only in 1987 [59] by the identification of madder on an historical textile.[60] SERS proved to be very successful for the identification of pure, commercial dyes, the detection of natural organic

colorants [54, 60] such as anthraquinones, flavonoids, naphthoquinones, and rhodamines, as they are the main components in dyes found on works of art. However, some challenges should also be recognised; for example , lake pigments or mordant dyes require hydrolysis as the first step towards the extraction of the dye from the inorganic substrate or the textile fibre, respectively [36].

Raman spectroscopy is known to be a surface sensitive technique as the molecular information that is retrieved during Raman experiments typically originates from the uppermost layer, since the (visible) laser light does not penetrate deep into the sample. When using a confocal set-up it is possible to focus through a transparent layer and thus to obtain information from deeper areas of the specimen. If the surface layer is not transparent one typically has to rely on embedding an excised sample in resin, then cutting and polishing it to achieve an overview of the different stratigraphic layers. However, as in many cases sampling is considered undesirable (damage, time consuming sample preparation, contamination, etc.) and in 2005, spatially offset Raman spectroscopy (SORS) was proposed by Matousek et al. [61-62]. By collecting the Raman signal from an area that is spatially offset from the laser spot, it is possible to retrieve molecular information from the subsurface underneath a highly turbid top layer [63]. The larger a spatial offset selected, the deeper the information that can be retrieved, but consequently the weaker the collected signal is. Typically high power infrared lasers are used with a spatial offset of few millimetres and penetration depths of up to several cm. SORS has, amongst others, proven to be successful for analysing pharmaceuticals through their packaging [64], in cancer research [65] and for other medical applications [66].

In works of art, the painted layers are typically a few micrometres thick. Moreover, one can say that in most of the cases these layers are turbid (non-transparent). However, exceptions of non-turbid layers can be found on cultural heritage objects (glazes, varnished layers etc.). One example of transparent layers is coming from the complex stratigraphy of Ghent Altarpiece made by the Van Eyck brothers where layers of glazes, isolation layers and underlayers can be found. In order to achieve non-invasive stratigraphic analysis of turbid layers, an alternative to the SORS

technique was proposed namely, microscale-spatially offset Raman spectroscopy (micro-SORS). This approach is favourable for analytical research into cultural heritage objects [67]. In micro-SORS, the laser power, spot size and collection area for the scattered radiation are reduced, as well as the (small) spatial offset, which allows one to combine the advantageous lateral resolution of Raman microscopy with the retrieval of molecular information on the stratigraphy. Although the transition from SORS to micro-SORS might seem a simple case of miniaturisation, special spatial constraints do apply. Moreover, the experimental set-up for *full* micro-SORS requires the laser to be focused on the sample through a different lens for the collection of the Raman signal, which is not directly compatible with commercially available Raman spectroscopic instrumentation [67]. Therefore, alternative approaches were proposed, such as a *defocusing* micro-SORS arrangment, which uses a commercially available Raman microscope. During this approach, the spatial offset is obtained by defocusing the (collection) optics, and thus probing an area which contains a large fraction of the spatially offset signal [68-69]. The more defocused the spectra are, the more information that can be obtained from the deeper layers; spectral post-processing involves the scaled subtraction of the in-focus spectrum from the out-of-focus one to diminish the contribution of the surface [36]. It should be remarked that, despite being straightforward in use, *defocusing* micro-SORS does not yield optimal separation between layers, as can be achieved with the *full* micro-SORS. To overcome some of the practical constraints of *full* micro-SORS, *fibre-optics* micro-SORS was recently proposed [70]. The technique utilizes two parallel glass fibres that are in contact with the sample. The excitation fibre is mounted on a stationary part of the system, whereas the collection fibre is mounted on a translation stage, allowing one to select the required spatial offset. *Fibre-optics* micro-SORS was successfully demonstrated on compounds with thicknesses of the top layer ranging from 50 to 500 μm [70]. Despite this successful proof-of-concept, this approach still needs further optimisation such as the addressing of the fibre brittleness, optimal fibre thickness and the application of the appropriate filters.

The applicability of the micro-SORS technique, in respect of cultural heritage studies, has been demonstrated on thin-layered, mock-up samples [69] and real artefacts such as stucco and terracotta sculptures and painted plaster in combination with cross-section analyses [71].

Moreover, micro-SORS chemical interrogations on mock-up samples, among others, consist of an examination of the sequence of which the layers are made [72] and if two components are situated within the same or different layers [73].

Besides the successful application of micro-SORS on cultural heritage studies and thin paint layers, this newly developed technique can also have applicability in other fields.

The study of thin stratified polymers and probing through packaging for quality control are some of the domains where micro-SORS could potentially be applied for non-invasive structural analysis [68]. Moreover, high scattering biological tissues can be investigated with micro-SORS [74] and generally, the technique can be applied on biological samples.

Conti et al., in 2015 [72] demonstrated the application of micro-SORS technique in three different specimens namely: an artificially two-layer polymeric system (top layer: polytetrafluoroethylene (PTFE) tape (75 μm thick), sublayer: plastic drinking cup made of polypropylene (PP) (150 μm thick), a single-side coated paper sheet with multiple thin layers and a wheat seed of the variety “Olivin” [72]. For the latter two, cross sectional analysis was applied in order to compare and evaluate the micro-SORS technique. The results of this study are very significant as they provide data of applications of micro-SORS other than art analysis and underline its wide range of application.

Another possible application of micro-SORS can be found on the field of geoscience. In geological samples thin crusts can be observed on the surface of the actual rocks blocking the Raman signal from the mineral. Moreover, inclusions can be found under the surface. By investigating deeper than the visible surface, it should be possible to overpass thin crusts and obtain molecular information of the geological specimen while simultaneously inclusions can be studied.

Laboratory Raman spectrometers can be coupled with calibrated automated positioning stages, allowing movement of the specimen on the XY and XYZ axes. This facility makes micro-Raman spectrometers suitable for undertaking molecular mapping and thus correlating chemical information with the spatial distribution. By focusing the objective at one point on the sample, the automated stage can be moved inside a preset, well-defined area collecting sequences of Raman spectra, which can be stored as sequential point measurements (movement along the X and Y axes). An advantage of acquiring full wavenumber range spectra is that the construction of the Raman mapping image can be decided according to the need of the analysis. For surfaces that are not completely flat, an autofocusing option (movement along the Z axis) can be applied for each analysed point. Autofocusing is a very crucial requirement when mapping cultural heritage objects and for cross sections that are not completely flat. It increases the spectral quality and thus the image eventually obtained. Lofrumento et al. [75] used Raman mapping in a study dedicated to Ethiopian prehistoric rock painting, for the investigation of the possible origin of calcium oxalate crusts. Conti et al. [77] applied micro-Raman mapping for the study of calcium oxalate films from samples taken from the north façade of the Cathedral of Trento. For subsurface Raman mapping, recently, two studies have explored the possibilities of *full* micro-SORS mapping on samples mimicking real situations found in artworks with hidden layers [77] and a *defocusing* micro-SORS mapping experiment on a 19th century porcelain card [78].

Point-to-point mapping can consume several working hours (this time is even more increased when autofocussing is involved). Linear lasers can significantly decrease the overall measuring time by simultaneously recording a series of points in a row. Opposite to mapping, Raman imaging uses larger illumination areas and filters to obtain the desired image usually acquired by the selection of one component, characterised by the adoption of a specific Raman band [17]. Raman imaging seems to be little used in cultural heritage studies, as Raman mapping can produce more detailed information of the area under investigation and where even the entire dataset can be used later for chemometrical analysis.

2.2.2 Direct Raman analysis

Raman spectroscopy is considered traditionally as a non-destructive technique as the laser power can be kept low in order to avoid alteration and permanent thermal damage to the object/sample. Technological evolutions and development of fibre optics brought Raman spectrometers out of the laboratory and into the field or inside museums. The latter helped towards the improvement of direct, non-invasive analysis as large scale monuments or art works started to be investigated in their natural environment or in dedicated museum collections without sampling and thus jeopardising the integrity of the artefact. Compared with benchtop Raman spectrometers, instruments dedicated to this *in situ* analysis have, in general, a decreased wavenumber stability (due to vibrations, thermal fluctuations etc.), thus they need frequent calibration during operation. They usually have a larger spectral footprint and poorer spectral resolution; focusing is achieved through the evaluation of the signal-to-noise ratio, the number of observed Raman bands and their shapes and intensities in the spectra of the unknown in a given position or through the use of fixed focal distances (when using light blockers).

Before discussing the use of mobile Raman spectrometers in archaeometrical research, one should be aware of definitions found in the literature about not only the kind of analysis performed but also the kind of the instrument used. On site, in-field or *in situ* analysis is proposed when the study is performed in the environment where the work of art is found or displayed, whereas non-invasive refers to the fact that no sampling is necessary [36, 79-81]. A wide range of definitions exist for characterizing the mobility of a Raman instrument. Previous studies have [79-81] distinguished the type of instrument as follows: (i) Transportable: instruments that are usually not designed for their mobility. Benchtop Raman instruments can hence be referred as transportable; (ii) Mobile: a general term applied to stable spectrometers designed for mobility; (iii) Portable: compact, usually battery-operated Raman spectrometers that can be carried by a single person; (iv) Handheld: low weight spectrometers, which can be held in one hand whilst performing measurements; (v) Palm: ultra-light, ultra-mobile Raman spectrometers, very small in size.

The first attempts in analysing works of art with fibre-optic probe heads was performed on easel paintings by probing through the top varnish layers [82]. Fibre-optics where attached to a FT-Raman instrument first allowed the direct analysis of the artefact to be carried out, so avoiding the rather cramped spatial restrictions of the sample illuminator compartment. Following this, in 2004 [83], a new more compact portable Raman instrument was introduced, coupled with a 785 nm diode laser, camera and adjustable power device. This instrument allowed for direct, *in situ* Raman analysis as demonstrated successfully by investigating the tomb of Menna, Theban Necropolis, Egypt [84], folios from the breviary of Arnold of Egmond [85], vault paintings in the Antwerp cathedral [86] and others. In 2007 [87], a short comparative review on commercially available Raman instruments was published.

In cultural heritage studies, portable Raman spectrometers are more favoured due to their coupling with long fibre optic cables which allows the remote investigation of art objects or the easy access to larger artefacts. Moreover, such Raman instruments allow the freedom for the operator to choose the spectral and measuring parameters. For the handheld and ultra-mobile instruments the probehead is directly attached to the small spectrometer. These types of instruments are usually found to be described in mineralogy studies [88] but also in the gems and gemstones [89] literature.

Portable Raman spectrometers are equipped with one or two lasers, while handheld instruments have one laser and a fixed spectral wavenumber range. In 2015, Bruker introduced a new handheld instrument on the market, using different lasers and a shifted wavelength algorithm to correct for fluorescence background, with low laser power and a wide spectral wavenumber range [90-92]. This instrument has been evaluated on laboratory specimens and painted sculptures [89], on pigments, organic materials and binders in modern art [92] but also on minerals and carbons relevant to exobiology and geobiology [91].

Although, handheld and palm-sized Raman instruments are not widely used in the art analysis field, great attention should be given in their applicability on geosciences and astrobiology.

An important advantageous property of handheld Raman instruments is that the weight of their packaging often is quite below the weight of portable Raman configurations. Moreover, these systems are very autonomous as batteries are used for their operation. A review on the role of mobile Raman instrumentation on the fields of archaeometry, geosciences and forensics shares a deep insight on the applicability of the technique and instrumentation also on mineralogy [81].

One of the most noticeable applications of mobile Raman spectroscopy in geoscience is planetary exploration and astrobiology. Light-weighted Raman spectrometers were proposed for remote measuring on space missions [93]. Although considerable problems are arising from the total weight of the configuration, spectral fingerprinting, fluorescence in respect to the laser wavelength used and laser stability [81], elaborated research and novel Raman instrumentation were developed in order to be adapted on the ExoMars mission [94-95].

From the one hand, in the field of mineralogy, portable Raman instruments with long fibre-optic probeheads were used for the identification of earth materials. Kelloway et al., in 2010 [96], investigated a collection of obsidian samples from the West New Britain (WNB), Manus and Banks Islands, Vanuatu by using of a benchtop (Renishaw Raman inVia Reflex microscope, Renishaw plc., Wotton-under-Edge, UK, 785 nm diode laser) and a portable (EZRaman-i portable Raman spectrometer, Enwave Optronics Inc., Irving, USA, 785 nm diode laser) Raman instrument. The comparison of the benchtop and portable Raman instrument data set and the use of principal component analysis revealed minor differences and underline the potential of using portable spectrometers for the study of obsidian provenance on site.

From the other hand, handheld Raman instruments have been more frequently used for the investigation of minerals. Elaborated studies on mineral specimens from collections, conducted indoors and outdoors with both handheld and benchtop Raman instruments successfully showed that different sulfates and organic minerals [97-98] can be examined.

Furthermore, research on the evaluation of handheld instruments on low temperatures and high altitudes revealed the applicability of miniaturized, low-weighted, commercially available Raman instruments under extreme conditions. Spectra from organic acids [99], biomolecules [10] and organic compounds [100] were collected, under cold, high-mountain conditions in order to evaluate the performance of the spectrometers used for exobiology applications.

Mobile Raman spectroscopy has grown to be a first choice technique in many cultural heritage studies. Besides wall painting analysis [79], mobile Raman spectroscopy has found a noteworthy application in the study of prehistoric rock art paintings. Raman researchers investigated many rock sites situated around the world, e.g., South Africa [101], France [102], India [103], Spain [104-106], Argentinian part of Patagonia [48]. For the former two studies, a transportable instrument was used [48]. Other applications include the direct analysis of glyptics [107], paintings and mortars from the Marcus Lucretius Pompeian house [108], stone building materials suffering environmental deterioration [109], the on site analysis of enamel porcelains and stoneware [110-111] and others.

In contrast to benchtop instruments, focusing the probe heads of portable spectrometers can be rather challenging. Without visual inspection through coupled objective lenses, one needs to rely on the evaluation of the Raman spectra. Positioning systems need to assure stability and thus optimal focusing. These usually involve the use of tripods, articulating arms etc. For works of art that are situated in elevated positions above the ground, the probe heads can be positioned on scaffolding or long fibre optic cables can be mounted on extended tripod devices. If, bringing these positioning accessories into the field is rather time consuming and sometimes limits the equipment mobility, special cups with fixed focal distances can be used [48, 79]. These cups, whose tips are covered with protective foam, are slid over the probe heads and measurement of the surface can be achieved by placing them in contact with the surface under investigation. Moreover, the cups serve also as light blockers (blocking the signal of ambient light) when working in open air environments during daylight hours.

As the Raman signal suffers environmental interference from ambient light it is advisable to perform *in situ* measurements preferably in complete darkness or during night. When studying a range of artistic objects with multiple techniques, e.g. in a museum, when the measurements are undertaken during restoration campaigns or when the analysis is carried out in public places double cloth tents can be used and the object together with the Raman spectrometer can be placed inside them.

Although benchtop Raman spectrometers are often found to perform better compared with their mobile counterparts, mobile/portable/handheld Raman instruments are used extensively in the field of cultural heritage because of their non-invasive characteristics. Recently, an *in situ* Raman mapping configuration has been published in the literature, for the analysis of porcelain cards [112]. Even though the results were very promising, several milestones still should be reached in order for the technique to be more widely applicable. Furthermore, the firsts steps towards subsurface mobile Raman mapping have been taken by the development of *defocusing* micro-SORS in a mobile set-up [113] and the development of a prototype of a *full* micro-SORS probe head [114], both of these suggesting future possibilities for *in situ* experiments in several fields of application, including archaeometry.

2.3 Raman spectroscopy in combination with other techniques

Elaborate physicochemical protocols for cultural heritage analysis often use a wide range of techniques. Artistic artefacts comprise complex compositions that require both elemental, molecular and separation techniques in order for the different components to be identified. The analytical approaches can yield qualitative or quantitative results. Ideally, the documentation should be noninvasive but this is not always achievable. The evaluation of the artefacts can carried out with several macro-imaging techniques, such as X-ray radiography, infrared reflectography, 2D- and 3D- digital microscopy etc. If the ethics and the state of the object allow the sampling then invasive, laboratory techniques can be employed. For laboratory measurements, the analysis should be non-destructive and thus, the same sample needs to be investigated with a variation of

techniques and finally kept intact for future studies. If destructive techniques (with sample consumption) are employed these should be scheduled towards the end of the analytical protocol and used only where the analytical information obtained therefrom is essential.

Since combined methodological approaches are usually preferable, Raman spectroscopy can be used in combination with other molecular or elemental analytical techniques. One popular approach is its combination with Fourier-transform infrared spectroscopy (FTIR) [115]. This technique, gives rise to vibrations due to a change in dipole polarization, while Raman spectroscopy requires changes in bond polarisability [17]. In general, intense infrared active modes are weak in Raman spectroscopy except if, in some cases, structural changes occur inside the matrices e.g. lowering of crystallinity, distortion of stuctures etc. FTIR spectroscopy is especially suitable for both organic binders/varnishes and inorganic pigments [116]. Moreover, it can be applied non-invasively using reflectance infrared portable instruments [117]. FTIR analysis is sometimes combined with thermal analysis methods for the discrimination of historic plasters and mortars [118].

X-ray diffraction (XRD) is another technique that is highly suitable for the analysis of crystalline phases and can complement Raman spectroscopy for the analysis of inorganic molecules. For example, the identification of feldspars can be sometimes challenging with Raman spectroscopy, as high spectral resolution and exact wavenumber calibration are necessary to identify the correct end member of a mineral series. Portable XRD (p-XRD) instruments can also be used for the analysis of cultural heritage objects [119] but in some cases positioning and alignment can be quite time-consuming procedures [120].

Scanning electron microscopy coupled with energy dispersive X-ray spectroscopy (SEM-EDX) allows for the characterization of the morphology and the elemental distribution of cross sections of untreated samples, or even small objects. Depending on the electrical conductivity of the sample, it should either be coated or measured as it is. For the instrumental coupling between an SEM and a Raman spectrometer a hybrid system has emerged called the structural and chemical

analyser (SCA) [121]. In cultural heritage research such a system was used for the identification of the degradation products of archaeological gilded irons [121].

One of the most frequently discussed combinations is the coupling of X-ray fluorescence data with Raman spectroscopic data in cultural heritage studies for the provision of molecular and elemental information. Although the complementarity of the two techniques is considered successful, one should be aware of the different sampling volumes and penetration depths of both techniques when interpreting the results. Visible light does not penetrate deeper than the surface while X-rays can penetrate significant depths into the sample and object. For the latter, the information received is a sum of the same or different elements found in the entire stratigraphy. In archaeometry, micro-Raman and micro-XRF can be combined [122] and both have mobile counterparts [123]. Analysis of powdered samples or scrapings taken from artifacts allow the use of another XRF technique [124], namely total reflection X-ray fluorescence (TXRF) for fast and sensitive (down to trace elements) analysis. Combined XRF-XRD [125] and XRF-Raman [126] mobile configurations are also reported in the archaeometrical research field. The evolution of macro-XRF (MA-XRF) imaging and its applications for art analysis are well established and demonstrated in numerous published studies [127].

2.4 Conclusions

Raman spectroscopy has grown to be one of the most appreciated techniques in the study of art and archaeology. Technical advantages have shaped the technique and moreover, initiated the expected development of more novel Raman techniques subsequently. For cultural heritage studies, advanced approaches involve the development of new methods such as micro-SORS, new instrumentation such as dispersive instruments equipped with an IR laser, enhancement of Raman signals for optimal identification, upgraded benchtop and portable systems, subsurface and *in situ* molecular mappings, and so on. Raman spectroscopy hence seems to be the perfect technique for novel developments in the interesting research field of archaeometry.

The first attempt to explore the possibilities of mobile Raman spectroscopy for the analysis of Patagonian rock art is illustrated in the next chapter. A specific portable Raman system was evaluated by its applicability on rock art paintings in Argentinian part of Patagonia. Moreover, possible drawbacks and solutions when measuring on-site and in extreme conditions are proposed.

2.5 References

[1] P. Vandenabeele, *Spectrochim. Acta A* **2011**, *80*, 27.

[2] K. De Gussem, P. Vandenabeele, A. Verbeken, L. Moens, *Spectrochim. Acta A* **2005**, *61*, 2896.

[3] A.V. Korsakov, P. Vandenabeele, K. Theunissen, *Spectrochim. Acta A* **2005**, *61*, 2378.

[4] J. Jehlicka, P. Vitek, H.G.M. Edwards, M. Hargreaves, T. Capoun, *Spectrochim. Acta A* **2009**, *73*, 410.

[5] P. Vandenabeele, H.G.M. Edwards, L. Moens, *Chem. Rev.* **2007**, *107*, 675.

[6] P. Colomban, A. Tournie, P. Ricciardi, *J. Raman Spectrosc*. **2009**, 40, 1949.

[7] J. De Gelder, P. Vandenabeele, F. Govaert, L. Moens, *J. Raman Spectrosc.* **2005**, *36*, 1059.

[8] V. L. Brewster, H. G. M. Edwards, M. D. Hargreaves, T. Munshi, *Drug Test. Anal.* **2009**, *1*, 25.

[9] H. G. M. Edwards, P. Vandenabeele, S. E. Jorge-Villar, E. A. Carter, F. Rull Perez, M.D.Hargreaves, *Spectrochim. Acta A* **2007**, *68*, 1133.

[10] J. Jehlicka, P. Vandenabeele, H. G. M. Edwards, A. Culka, T. Capoun, *Anal. Bioanal. Chem.* **2010**, *397*, 2753.

[11] M. de Veij, P.Vandenabeele, T. De Beer, J. P.Remon, L.Moens, *J.Raman Spectrosc.* **2009**, *40*, 297.

[12] M. de Veij, A. Deneckere, P. Vandenabeele, D. de Kaste, L. Moens, *J. Pharm. Biomed. Anal.* **2008**, *46*, 303.

[13] E. Smith, G. Dent, Modern Raman Spectroscopy: A Practical Approach, John Wiley & Sons, Chichester, UK, 2005.

[14] R.L McCreery, *Raman Spectroscopy for Chemical Analysis,* John Wiley & Sons, New York, USA, **2000**.

[15] J.R Ferraro, K. Nakamoto, C.W Brown, Introductory Raman Spectroscopy, 2nd Edition, Academic Press, Amsterdam 2003.

[16] D.A. Long, *Raman Spectrosopy*, McGraw-Hill, Maidenhead, UK, **1977**.

[17] P. Vandenabeele, *Practical Raman spectroscopy: an introduction*, John Wiley & Sons, Chichester, UK, **2013**.

[18] H.G.M Edwards, J.M. Chalmers, Eds. *Raman Spectroscopy in Archaeology and Art History*, The Royal Society of Chemistry, Cambridge, UK, **2005**.

[19] Ph. Colomban, *J. Raman Spectrosc.* **2012**, *43*, 1529.

[20] P. Dhamelincourt, F. Wallart, M. Leclercq, A.T. Nguyen, D.O. Landon, *Anal. Chem.* **1979**, *51*, 414A.

[21] B. Guineau, C. Coupry, M.T. Gousset, J.P. Forgerit, J.Vezin, *Scriptorium* **1986**, *40*, 157.

[22] R.J.H. Clark, *Chem. Soc. Rev.* **1995**, *24*, 187.

[23] P. Vandenabeele, B. Wehling, L. Moens, B. Dekeyzer, B. Cardon, A. Von Bohlen, R. Klockenkamper, *Analyst* **1999**, *124*, 169.

[24] C. Andalo, M. Bicchieri, P. Bocchini, G. Casu, G.C. Galletti, P.A. Mando, M. Nardone, A. Sodo, M.P. Zappala, *Anal. Chim. Acta* **2001**, *429*, 279.

[25] V. Hayez, J. Guillaume, A. Hubin, H. Terryn, *J. Raman Spectrosc.* **2004**, *35*, 732.

[26] L. Kiefert, H.A. Hänni, J.P. Chalain, W. Weber, *J. Gemmol.* **1999**, *26*, 501.

[27] P. Colomban, H.D. Schreiber, *J. Raman Spectrosc.* **2005**, *36*, 884.

[28] R.J.H. Clark, M.L. Curri, *J. Mol. Struct.* **1998**, *440*, 105.

[29] A. Rousaki, C. Bellelli, M. Carballido Calatayud, V. Aldazábal, G. Custo, L. Moens, P. Vandenabeele, C. Vázquez, *J. Raman Spectrosc.* **2015**, *46*,1016.

[30] A. Hernanz, J.M. Gavira-Vallejo, J.F. Ruiz-López, H.G.M. Edwards, *J. Raman Spectrosc.* **2008**, *39*, 972.

[31] P. Vandenabeele, L. Moens, H.G.M. Edwards, R. Dams, *J. Raman Spectrosc.* **2000**, 31, 509.

[32] C. Defeyt, J. Van Pevenage, L. Moens, D. Strivay, P. Vandenabeele, *Spectrochim. Acta A* **2013**, *115*, 636.

[33] F.H. Moser, A.L. Thomas, *Phthalocyanine Compounds*, Reinhold Publishing Corporation, New York, USA, **1963**.

[34] W. Herbst, K. Hunger, G. Wilker, H. Ohleier, R. Winter, *Industrial Organic Pigments*, third ed. Wiley-VCH Verlag GmbH & Co. KGaA, Weinheim, FRG, **2004**.

[35] D. Bersani, P.P. Lottici, *J. Raman Spectrosc.* **2016**, *47*, 499.

[36] D. Bersani, C. Conti, P. Matousek, F. Pozzi, P. Vandenabeele, *Anal. Methods* **2016**, *8*, 8395.

[37] H.G.M. Edwards, L. Drummond, J. Russ, *Spectrochim. Acta Part A* **1998**, *54*, 1849.

[38] R. David, H.G.M. Edwards, D.W. Farwell, D.L. De Faria, *Archaeometry* **2001**, *43*, 461.

[39] F.S. Manciu, A. Ramirez, W. Durrer, J. Govani, R.R. Chianelli, *J. Raman Spectrosc.* **2008**, *39*, 1257.

[40] K. Castro, M. Pérez-Alonso, M.D. Rodríguez-Laso, L.A. Fernández, J.M. Madariaga, *Anal. Bioanal. Chem.* **2005**, *382*, 248.

[41] L. Burgio, R.J.H. Clark, *Spectrochim. Acta Part A* **2001**, *57*, 1491.

[42] A.M. Correia, M.J.V Oliveira, R.J.H. Clark, M.I. Ribeiro, M.L. Duarte, *Anal. Chem.* **2008**, *80*, 1482.

[43] P. Colomban, *J. Raman Spectrosc.* **2003**, *34*, 420.

[44] I.V. Ermakov, M. Sharifzadeh, M. Ermakova, W. Gellermann, *J. Biomed. Opt.* **2005**, *10*, 861.

[45] L. Bergamonti, D. Bersani, D. Csermely, P.P. Lottici, *Spectrosc. Lett.* **2011**, *44*, 453.

[46] D. Gill, R.G. Kilponen, L. Rimai, *Nature* **1970**, *227*, 743-4.

[47] J. Jehlička, H.G.M. Edwards, A. Oren, *Appl. Environ. Microbiol.* **2014**, *80*, 3286.

[48] A. Rousaki, C. Vázquez, V. Aldazábal, C. Bellelli, M. Carballido Calatayud, A. Hajduk , E. Vargas, O. Palacios, P. Vandenabeele, L. Moens, *J. Raman Spectrosc.* **2017**, *48*, 1459.

[49] M. Fleischmann, P.J. Hendra, A.J. McQuillan, *Chem. Phys. Lett.* **1974**, *26*, 163.

[50] R. Aroca, *Surface-Enhanced Vibrational Spectroscopy*, John Wiley & Sons, Chichester, UK, **2006**.

[51] D.L. Jeanmaire, R.P. Van Duyne, *J. Electroanal. Chem.* **1977**, *84*, 1.

[52] M.G. Albrecht, J.A. Creighton, *J. Am. Chem. Soc.* **1977**, *99*, 5215.

[53] P.C. Lee, D.J. Meisel, *J. Phys. Chem.* **1982**, *86*, 3391.

[54] M. Leona, *Proc. Natl. Acad. Sci. USA* **2009**, *106*, 14757.

[55] M.V. Cañamares, J.V. Garcia-Ramos, J.D. Gómez-Varga, C. Domingo, S. Sanchez-Cortes, *Langmuir* **2007**, *23*, 5210.

[56] M.V. Cañamares, J.V. Garcia-Ramos, S. Sanchez-Cortes, M. Castillejo, M. Oujja, *J. Colloid. Interface Sci.* **2008**, *326*, 103.

[57] A.V. Whitney, R.P. Van Duyne, F. Casadio, *J. Raman Spectrosc.* **2006**, *37*, 993.

[58] K. Chen, M. Leona, K.-C. Vo-Dinh, F. Yan, M.B. Wabuyele, T. Vo-Dinh, *J. Raman Spectrosc.* **2006**, *37*, 520.

[59] B. Guineau, V. Guichard, in *ICOM Committee for Conservation: 8th triennial meeting*, 6-11 September, Sydney, Australia, 1987 Preprints, The Getty Conservation Institute: Marina del Rey, CA, **1987**, *Vol. II*, 659.

[60] F. Casadio, M. Leona, J.R. Lombardi, R. Van Duyne, *Acc. Chem. Res.* **2010**, *43*, 782.

[61] P. Matousek, I.P. Clark, E.R.C. Draper, M.D. Morris, A.E. Goodship, N. Everall, M. Towrie, W.F. Finney, A.W. Parker, *Appl. Spectrosc.* **2005**, *59*, 393.

[62] P. Matousek, M.D. Morris, N. Everall, I.P. Clark, M. Towrie, E. Draper, A. Goodship, A.W. Parker, *Appl. Spectrosc.* **2005**, *59*, 1485.

[63] K. Buckley, P. Matousek, *Analyst* **2011**, *136*, 3039.

[64] C. Eliasson, P. Matousek, *Anal. Chem.* **2007**, *79*, 1696.

[65] N. Stone, R. Baker, K. Rogers, A. William Parker, P. Matousek, *Analyst* **2007**, *132*, 899.

[66] P. Matousek, N. Stone, *Chem. Soc. Rev.* **2016**, *45*, 1794.

[67] C. Conti, M. Realini, C. Colombo, P. Matousek, *Analyst* **2015**, *140*, 8127.

[68] P. Matousek, C. Conti, M. Realini, C. Colombo, *Analyst* **2016**, *141*, 731.

[69] C. Conti, C. Colombo, M. Realini, G. Zerbi, P. Matousek, *Appl. Spectrosc.* **2014**, *68*, 686.

[70] P.Vandenabeele, C. Conti, A. Rousaki, L. Moens, M. Realini, P. Matousek, *Anal. Chem.* **2017**, *89*, 9218.

[71] C. Conti, C. Colombo, M. Realini, P. Matousek, *J. Raman Spectrosc.* **2015**, *46*, 476.

[72] C. Conti, M. Realini, C. Colombo, K. Sowoidnich, N.K. Afseth, M. Bertasa, A. Botteon , P. Matousek, *Anal. Chem.* **2015**, *87*, 5810.

[73] C. Conti, M. Realini, A. Botteon, C. Colombo, S. Noll, S.R. Elliott, P. Matousek, *Appl. Spectrosc.* **2016**, *70*, 156.

[74] Z. Di, B. H. Hokr, H. Cai, K. Wang, V. V. Yakovlev, A. V. Sokolov, M. O. Scully, *J. Mod. Opt.* **2014**, *62*, 97.

[75] C. Lofrumento, M. Ricci, L. Bachechi, D. De Feo, E.M. Castellucci, *J. Raman Spectrosc.* **2012**, *43*, 809.

[76] C. Conti, I. Aliatis, C. Colombo, M. Greco, E. Possenti, M. Realini, C. Castiglioni, G. Zerbi, *J. Raman Spectrosc.* **2012**, *43*, 1604.

[77] A. Botteon, C. Conti, M. Realini, C. Colombo, P. Matousek, *Anal. Chem.* **2017**, *89*, 792.

[78] A. Rousaki, A. Botteon, C. Colombo, C. Conti, P. Matousek, L. Moens, P. Vandenabeele, *Anal. Methods* **2017**, *9*, 6435.

[79] D. Lauwers, A. Garcia Hutado, V. Tanevska, L. Moens, D. Bersani, P. Vandenabeele, *Spectrochim. Acta Part A* **2014**, *118*, 294.

[80] P. Vandenabeele, M.K. Donais, *App. Spectrosc.* **2016**, *70*, 27.

[81] P. Vandenabeele, H.G.M. Edwards, J. Jehlička, *Chem. Soc. Rev.* **2014**, *43*, 2628.

[82] P. Vandenabeele, F. Verpoort, L. Moens, *J. Raman Spectrosc.* **2001**, *32*, 263.

[83] P. Vandenabeele, T.L. Weis, E.R. Grant, L.J. Moens, *Anal. Bioanal. Chem.* **2004**, *379*, 137.

[84] P. Vandenabeele, R. Garcia-Moreno, F. Mathis, K. Leterme, E. Van Elslande, F.-P. Hocquet, S. Rakkaa, D. Laboury, L. Moens, D. Strivay, M. Hartwig, *Spectrochim. Acta A.* **2009**, *73*, 546.

[85] A. Deneckere, M. Leeflang, M. Bloem, C.A. Chavannes-Mazel, B. Vekemans, L. Vincze, P. Vandenabeele, L. Moens, *Spectrochim. Acta A.* **2011**, *83*, 194.

[86] A. Deneckere, W. Schudel, M. Van Bos, H. Wouters, A. Bergmans, P. Vandenabeele, L. Moens, *Spectrochim. Acta Part A*, **2010**, *75*, 511.

[87] P. Vandenabeele, K. Castro, M. Hargreaves, L. Moens, J.M. Madariaga, H.G.M. Edwards, *Anal. Chim. Acta* **2007**, *588*, 108.

[88] J. Jehlička, A. Culka, P. Vandenabeele, H.G.M. Edwards, *Spectrochim. Acta Part A* **2011**, *80*, 36.

[89] Z. Petrová, J. Jehlička, T. Čapoun, R. Hanus, T. Trojek, V. Goliáš, *J. Raman Spectrosc.* **2012**, *43*, 1275.

[90] C. Conti, A. Botteon, M. Bertasa, C. Colombo, M. Realini, D. Sali, *Analyst* **2016**, *141*, 4599.

[91] J. Jehlička, A. Culka, F. Košek, *J. Raman Spectrosc.* **2017**, *48*, 1583.

[92] M. Vagnini, F. Gabrieli, A. Daveri, D. Sali, *Spectrochim. Acta Part A* **2017**, *176*, 174.

[93] A. Ellery, D. Wynn-Williams, J. Parnell, H. G. M. Edwards and D. Dickensheets, *J. Raman Spectrosc.* **2004**, *35*, 441

[94] G. M. H. Edwards, I. Hutchinson, R. Ingley, *Anal. Bioanal. Chem.* **2012,** *404*, 1723.

[95] H.G.M. Edwards, I.B. Hutchinson, R. Ingley, Parnell J, P. Vítek, J. Jehlička, *Astrobiology* **2013**, 13, 543.

[96] S. J. Kelloway, N. Kononenko, R. Torrence and E. A. Carter, *Vib. Spectrosc.* **2010**, *53*, 88.

[97] J. Jehlička, P. Vítek, H. G. M. Edwards, M. Hargreaves and T. Čapoun, *J. Raman Spectrosc.* 2009, **40**, 1082.

[98] J. Jehlička, P. Vítek, H. G. M. Edwards, M. Hargreaves and T. Čapoun, *J. Raman Spectrosc.*, 2009, **40**, 1645.

[99] J. Jehlička, P. Vítek, H. G. M. Edwards, *J. Raman Spectrosc.* **2010**, *41*, 440.

[100] J. Jehlička, H. G. M. Edwards, A. Culka, *Phil. Trans. R. Soc. A* **2010**, *368*, 3109.

[101] A. Tournié, L.C. Prinsloo, C. Paris, P. Colomban, B. Smith, *J. Raman Spectrosc.* **2011**, *42*, 399.

[102] S. Lahlil, M. Lebon, L. Beck, H. Rousselière, C. Vignaud, I. Reiche, M. Menu, P. Paillet , F. Plassard, *J. Raman Spectrosc.* **2012**, *43*, 1637.

[103] T.R. Ravindran, A.K. Arora, M. Singh, S.B. Ota, *J. Raman Spectrosc.* **2013**, *44*, 108.

[104] M. Olivares, K. Castro, M.S. Corchón, D. Gárate, X. Murelaga, A. Sarmiento, N. Etxebarria, *J. Archaeol. Sci.* **2013**, *40*, 1354.

[105] A. Hernanz, J.F. Ruiz-López, J.M. Madariaga, E. Gavrilenko, M. Maguregui, S. Fdez-Ortiz de Vallejuelo, I. Martínez-Arkarazo, R. Alloza-Izquierdo, V. Baldellou-Martínez, R. Viñas-Vallverdu, A. Rubio i Mora, A. Pitarch, A. Giakoumaki, *J. Raman Spectrosc.* **2014**, *45*, 1236.

[106] A. Pitarch, J.F. Ruiz, S. Fdez-Ortiz de Vallejuelo, A. Hernanz, M. Maguregui, J.M. Madariaga, *Anal. Methods* **2014**, *6*, 6641.

[107] D. Lauwers, A. Candeias, A. Coccato, J. Mirao, P. Vandenabeele, L. Moens, *Spectrochim. Acta A* **2016**, *15*, 146.

[108] M. Maguregui, U. Knuutinen, I. Martínez-Arkarazo, A. Giakoumaki, K. Castro, J.M. Madariaga, *J. Raman Spectrosc.* **2012**, *43*, 1747.

[109] H. Morillas, M. Maguregui, O. Gómez-Laserna, J. Trebolazabala, J.M. Madariaga, *J. Raman Spectrosc.* **2012**, *43*, 1630.

[110] P. Colomban, V. Milande, *J. Raman Spectrosc.* **2006**, *37*, 606.

[111] B. Kırmızı, P. Colomban, B. Quette, *J. Raman Spectrosc.* **2010**, *41*, 780.

[112] D. Lauwers, P. Brondeel, L. Moens, V. Vandenabeele, *Philos. Trans. R. Soc. A* **2016**, *374*, 20160039.

[113] M. Realini, A. Botteon, C. Conti, C. Colombo, P. Matousek, *Analyst* **2016**, *141*, 3012.

[114] M. Realini, C. Conti, A. Botteon, C. Colombo, P. Matousek, *Analyst* **2017**, *142*, 351.

[115] D. Bikiaris, Sister Daniilia, S. Sotiropoulou, O. Katsimbiri, E. Pavlidou, A.P. Moutsatsou, Y. Chryssoulakis, *Spectrochim. Acta Part A* **1999**, *56*, 3.

[116] V. Ganitis, E. Pavlidou, F. Zorba, K.M. Paraskevopoulos, D. Bikiaris, *J. Cult. Herit.* **2004**, *5*, 349.

[117] C. Miliani, F. Rosi, A. Burnstock, B.G. Brunetti, A. Sgamellotti, *Appl. Phys. A* **2007**, *89*, 849.

[118] M. Anastasiou, Th. Hasapis, T. Zorba, E. Pavlidou, K. Chrissafis, K.M. Paraskevopoulos, *J. Therm. Anal. Cal.* **2006**, *84*, 27.

[119] I. Nakai, Y. Abe, *Appl. Phys. A* **2012**, *106*, 279.

[120] L. Van de Voorde, J. Van Pevenage, K. De Langhe, R. de Wolf, B. Vekemans, L. Vincze, P. Vandenabeele, M.P.J. Martens, *Spectrochim. Acta Part* B **2014**, *97*, 1.

[121] M. Veneranda, I. Costantini, S. Fdez-Ortiz de Vallejuelo, L. Garcia, I. García, K. Castro, A. Azkarate, J.M. Madariaga, *Philos. Trans. A Math. Phys. Eng. Sci.* **2016**, *374*, 20160046.

[122] A. Deneckere, B. Vekemans, L. Van de Voorde, P. De Paepe, L. Vincze, L. Moens, P. Vandenabeele, *Appl. Phys. A* **2012**, *106*, 363.

[123] L. Van de Voorde, M. Vandevijvere, B. Vekemans, J. Van Pevenage, J. Caen, P. Vandenabeele, P. Van Espen, L. Vincze, *Spectrochim. Acta Part B* **2014**, *102*, 28–35.

[124] B. Wehling, P. Vandenabeele, L. Moens, R. Klockenkiimper, A. Von Bohlen, G. Van Hooydonk, M. de Reu, *Microchim. Acta* **1999**, *130*, 253.

[125] L. Beck, H. Rousseliere, J. Castaing, A. Duran, M. Lebon, B. Moignard, F. Plassard, *Talanta* **2014**, *129*, 459.

[126] K.S. Andrikopoulos, Sister Daniilia, B. Roussel, K. Janssens, *J. Raman Spectrosc.* **2006**, *37*, 1026.

[127] G. Van der Snickt, H. Dubois, J. Sanyova, S. Legrand, A. Coudray, C. Glaude, M. Postec, P. Van Espen, K. Janssens, *Angew. Chem.* **2017**, *129*, 4875.

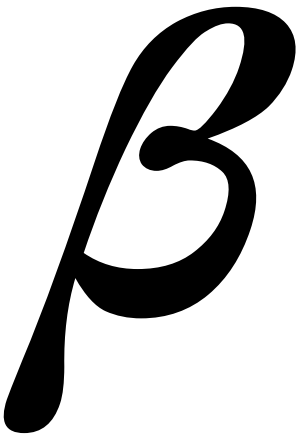

Chapter 3 The first use of portable Raman instrumentation for the *in situ* study of prehistoric rock paintings in Patagonian sites

Based on the paper: A. Rousaki, C. Vázquez, V. Aldazábal, C. Bellelli, M. Carballido Calatayud, A. Hajduk, E. Vargas, O. Palacios, P. Vandenabeele, L. Moens, *J. Raman Spectrosc.* **2017**, *48*, 1459.

In the previous chapter theoretical considerations of Raman spectroscopy are discussed in respect of applications to cultural heritage objects. In the current chapter, we describe the first use of portable Raman instrumentation for the in situ analysis of rock art paintings from hunter-gatherer sites in three different provinces in Argentinian part of Patagonia *(Neuquén, Río Negro, Chubut). During a single research campaign 16 shelters and 1 cave were investigated which makes this study one of the most comprehensive expeditions undertaken on the analysis of rock art paintings. In this work the coordinates of the archaeological sites are not given, as a measure against looting, illegal trafficking or damaging. The main aim is to evaluate the use of the EZRaman-I Dual Raman spectrometer to analyse rock art paintings (pigments, alteration products and substrata) under extreme conditions in Patagonia. Finally, several improvements are proposed, to maximize the quality of the research output in such comprehensive expeditions. The current chapter focuses on technical aspects of Raman spectroscopy, without introducing an extensive archaeological background.*

3.1 Introduction

Archaeometrical studies in Patagonia (Argentina) reveal useful information about the materials used by the population that inhabited the area: the North Patagonian region was occupied by hunter-gatherer populations from the transition between late Pleistocene-early Holocene (at least 10.000 years B.P.) to the last century. When crossing the landscape from West to East, relatively low temperatures in the Andes region are found, followed by the wet forest of the mountain, dry steppes and, finally the moderate temperatures and humidity of the Atlantic coast. Through the study of different archaeological contexts and materials (i.e. the geochemical analysis of obsidian tools and sources), it has been established that these groups of hunter-gatherers had broad mobility or exchange systems that could include these varied environments, which are hundreds of kilometres distant from each other [1]. In Patagonian archaeological sites lithic materials, pottery and faunal remains are commonly found, as well as paintings or engravings on rocks, leather or textiles. The current work focuses on the direct investigation of prehistoric rock art paintings at 17 sites, in two different environmental regions of Patagonia, the forest at Neuquén and Río Negro and the steppe at Chubut. More specifically, we shall study their pigments, the alteration products and the substrata.

Rock art paintings are relatively common in the Patagonian scenery and thus they play an important role in understanding the population dynamics of local hunter-gatherer groups. However, little information is available based on physicochemical investigation to better understand their manufacturing techniques and to identify the painting materials.

The pioneering work on using X-ray methods for the investigation of south Patagonian rock art was carried out among others by Gradin et al. in 1977 [2], Aschero in 1985 [3] and Barbosa et al. in 1985 [4] and 1988 [5], all using X-ray Diffraction (XRD) (details on these studies in Patagonia can be found at Boschin et al. (2011) [6]). Other studies determined the composition of pigments from Southern and Northern rock art sites [7] and analysed the organic and inorganic fractions of pigments and coloured sediments recovered in excavations from Tierra del Fuego island [8].

In 2000, Wainwright et al. [9] analysed seven samples from forest sites in North Patagonia and one sample from Campo Moncada 1, a site located in the same steppe (Chubut province) as will be discussed in this chapter. Samples of rock art from the El Trébol site, close to Bariloche (Río Negro province), were studied before, by Vázquez et al., in 2007 [10]. The span of human occupation in the El Trébol site is dated around 10600 ± 130 BP to 5731 ± 70 BP [11]. Furthermore, other North Patagonian rock art studies can be found in the literature, referring the analysis of pigments [12, 13], rock art samples and nearby outcrops [14] and pottery, pigmented raw materials and some rock art fragments [15].

The first report of the use of Raman spectroscopy in North Patagonia has been published by Maier et al. in 2005 [16] and 2007 [17], combining spectroscopic and chromatographic methods to determine the composition of two archaeological pastes recovered at a stratigraphic layer of Loncoman cave (Río Negro province). An extensive analysis from 13 sites in the Río Negro province and one sample from a leather blanket preserved in the Bariloche city museum, was published by Boschin et al. in 2011 [6]. They analysed 107 samples of rock art, pastes, rocks, artifacts, leather fragments and control samples with X-ray Diffraction (XRD), Energy-dispersive X-ray spectroscopy (SEM EDX), Fourier Transform Infrared Spectroscopy (FTIR) and Raman spectroscopy. Furthermore, pigments found on leather artefacts from the archaeological site at Campo Moncada 2 (Piedra Parada, Chubut province) were analysed using Raman spectroscopy by Bellelli et al., in 2015 [18]. Finally, in 2015 Rousaki et al. [19] reported the analysis of pigments, beads, grinding tools and pottery from archaeological excavation of hunter-gatherer archaeological sites from the Traful Lake (Neuquén province) and Manso River areas (Río Negro province) using the combination of micro-Raman spectroscopy and X-ray fluorescence (XRF).

The pictographs found on the stone surfaces can stylistically vary from abstract to geometric or more naturalistic and can be dated back to prehistory. For these painted surfaces the main components consist of mostly different haematitic compositions, natural green pigments, yellow ochres, manganese oxides, carbon blacks, gypsum and (post)depositional degradation components.

Physicochemical research in the Argentinian part of Patagonia play an important role on documentation of these magnificent works of art. The contribution of the analytical techniques on the rock art documentation is twofold: concluding on the "palette" used by indigenous people, and thus unravel one of the most ancient forms of human expression, and investigating weathering processes that affect these magnificent works of art.

Pigments were important resources used for rock art, body painting and objects decoration. Often they were of mineral origin, although in some cases, they could also be synthesized (intentionally as a by-product of an existing mineral). For example, if goethite is fired under appropriate conditions, haematite is formed. [19] The investigation and successful identification of the minerals and the minerals' origin plays an important role on understand the technological level and resources of the local hunter-gatherer population.

On the other hand monitor the degradation procedures on the painted rock surfaces can be very helpful for the better preservation of particularly open-air Patagonian rock paintings. The latter can be quite significant as some of the rock paintings are doomed to be consumed by nature or aggressive human activity.

Raman spectroscopy has proven to be a powerful approach to study rock art paintings, substrata and alteration products on the rock surface. The technique was either used as a single approach [20-24] or, in combination with complimentary techniques [25-36].

The use of portable instrumentation in rock art painting research has expanded the field of non-destructive and non-invasive investigation. Also, portable Raman instruments can be carried on-site, to perform analysis of the artefacts without disturbing the work of art. In 2011 Tournié et al. [37] managed to study *in situ* San rock art in South Africa with an HE532 micro-Raman spectrometer (Jobin-Yvon-Horiba, Villeneuve d'Ascq, France). They positively identified red and white pigments, accretions, and alteration products while testing their portable Raman instrument in extreme conditions. Although the analysis of the San rock art was successful the portability of

the instrument can be reasonably questioned as its total weight including the supporting tripod was approximately 60 kg, and therefore, we would rather classify the instrument as transportable [38]. In 2012, Lahlil et al. [39] used the same instrument for the analysis of prehistoric cave art in Rouffignac St-Cernin, France, characterising the minerological nature of manganese pigments and underlining the presence of organic materials. In 2012, Ravidran et al. [40] reported the on-site analysis of rock-shelter paintings at the Bhimbetka site (India) using a B&WTek portable Raman spectrometer. The spectra collected from the portable instrument were compared with those obtained from *in-vitro* Raman laboratory equipment. It is worth mentioning that on-site analysis revealed mainly the inorganic components of the rock art paintings and a possible organic binder was found from an extracted pigment sample. Olivares et al. [41] discussed the analysis of paintings in La Peña Cave in San Roman de Candamo, Spain with a similar portable spectrometer, identifying red earths, amorphous carbon, and manganese (with a handheld EDXRF instrument) as the main pigments along with products that indicate the presence of cyanobacterial growth (parietin, beta-carotene and lycopene), while a recent study [42] reported the use of a B&WTek InnoRam 785H portable Raman microscope in selected open air rock shelters in the Iberian Penisula, highlighting the difficulties of measuring in open-air environments and presenting the analysis of pigments and crusts from the rock art paintings. In 2014, Pitarch et al. [43] analysed *in situ* the rock substrate and paintings of the Los Chaparros shelter (Albalate del Arzobispo, Teruel, Spain), again with the use of a B&WTek portable Raman spectrometer, obtaining information from the rock substrate and identifying alteration and accretion products and also investigating the Mn-bearing minerals of the pigments used. The last five studies used in addition to Raman spectroscopy other auxiliary portable or laboratory instruments for combining the data. It is worth mentioning that the B&WTek portable Raman spectrometers were significantly lower in weight (ca. 10 kg) compared with the instrument that Tournié et al. [37] used. The total weight of the instrument and the packaging could play a very important role in site-to-site transportation, especially when the rock shelters are difficult to reach or when the measurements must be undertaken over a large number of sites that need to be studied in a short time. This is also an issue that has been encountered in the current study.

The problem of weight can be solved by the use of ultramobile or handheld, battery-operated instruments (< 2kg). These Raman spectrometers can perform analyses whilst being held by one person [44]. Although these ultra light Raman spectrometers have not been discussed hitherto in the literature of the analysis of rock art paintings, there are many studies that highlight their use outdoors, on-site and in extreme conditions. Moreover, handheld and palm-sized instruments have typically a single, fixed grating, in comparison with other portable Raman instruments [44]. In some of the studies, handheld Raman instruments were used for detecting biomarkers in complex samples in a host geological matrix under Alpine conditions [45], for the *in-situ* identification of arsenate minerals at outcrops [46], for field identification of several minerals [47], for the analysis of stones and gemstones mounted in a jewelled sceptre in the Faculty of Science of Charles University in Prague [48], and for the detection of common gemstones in several complex religious artefacts and the Ring Monstrance from the Loreto treasury [49]. For the latter study a 0.8 kg palm-sized device was used.

The total weight of the analytical devices, along with other drawbacks that might be faced when analysing rock art with portable instrumentation, will be extensively discussed in this work and possible solutions are suggested to circumvent this. In this work, we also report for the first time the use of *in situ* Raman spectroscopy in the rock art painting of 16 shelters and one cave in archaeological regions in three different Patagonian provinces (Neuquén, Río Negro, Chubut) (Fig. 3.1). The focus of this study is on the use of portable Raman spectroscopy for the analysis of the rock art materials, accretions, alteration products and substrata.

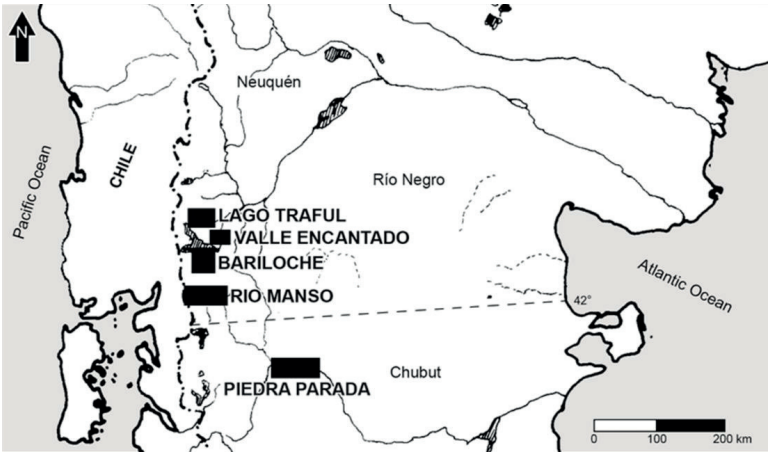

Figure 3.1. *Map indicating the location of the different archaeological sites in three different Patagonian provinces (Neuquén, Río Negro, Chubut).*

3.2 Experimental

Sixteen shelters and one cave in Argentinian part of Patagonia were investigated with portable Raman spectroscopy during a 9-day measuring campaign (Fig. 3.2 (a)-(c)). An overview of these sites is given in Table 3.1. The instrument was carried into the field and used on painted rock surfaces, alteration and substrata. Reaching the sites was certainly not straightforward, as usually these sites were not accessible by car.

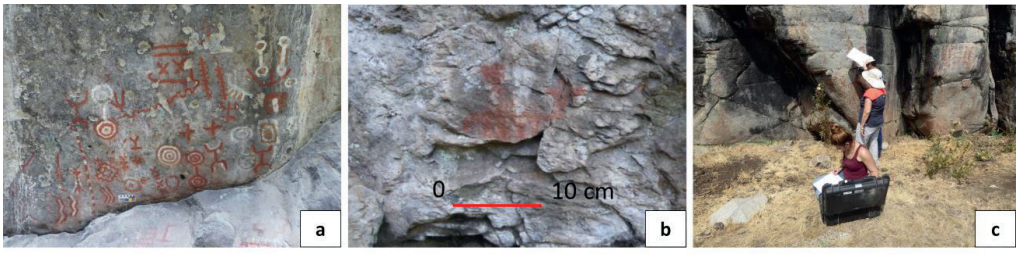

Figure 3.2. *(a) Rock art painting from the shelter Las Mellizas (Neuquén). (b) Figure representing a man horse riding from the shelter Lago Moreno East (Río Negro). (c) Raman portable instrument setup in the shelter at Paredón Lanfré (Río Negro).*

Table 3.1. *An overview of the archaeological sites that were investigated with the portable Raman EZRAMAN-I Dual analyser.* ^{14}C *chronology indicates the span of human occupation in each site and not the rock art painting age (ª Denotes the relative chronology).*

Area	Province	Number	Site	Sites Chronology
Traful	Neuquén	1	Shelter Cueva Olate	Late Holocene[a]
Traful	Neuquén	2	Shelter Alero Las Mellizas	590 ± 90 BP
Valle Encantado	Río Negro	3	Cave Mirador de Castillo	Not dated
Valle Encantado	Río Negro	4	Shelter Alero Maqui	Not dated
San Carlos de Bariloche (Gutiérrez Lake)	Río Negro	5	Shelter Queutre Inalef	Not dated
San Carlos de Bariloche (Guillelmo Lake)	Río Negro	6	Shelter Guillelmo Lake	Not dated
San Carlos de Bariloche (Mascardi Lake)	Río Negro	7	Shelter Los Rápidos	Not dated
San Carlos de Bariloche	Río Negro	8	Shelter Cerro Campanario	Not dated
San Carlos de Bariloche	Río Negro	9	Shelter Cerro Campanario 2	Not dated
San Carlos de Bariloche	Río Negro	10	Shelter Lago Moreno East	Not dated
San Carlos de Bariloche	Río Negro	11	Shelter El Trébol	10600 ± 130 BP – 5731 ± 70 BP
Río Manso	Río Negro	12	Shelter Paredón Lanfré	1570 ± 60BP – 330 ± 50BP
Río Manso	Río Negro	13	Shelter Campamento Argentino	560 ± 60 BP – 230 ± 70 BP
Piedra Parada Valley	Chubut	14	Shelter Angostura Blanca	2960 ± 60 BP – 450 ± 110 BP
Piedra Parada Valley	Chubut	15	Shelter Piedra Parada 1	1330 ± 50 BP
Piedra Parada Valley	Chubut	16	Shelter Campo Moncada 1	Late Holocene[a]
Piedra Parada Valley	Chubut	17	Shelter Campo Cerda 1	2850 ± 50 BP – 580 ± 60 BP

All spectra, were recorded using a portable *EZRaman-I Dual* Raman analyser from TSI Inc. (Minnesota, USA) [38]. The fibre-optics-based spectrometer is coupled with two lasers, a red diode laser (785 nm) and a green Nd:YAG laser (532 nm). The spectrometer is equipped with three interchangeable lenses for each wavelength: a standard lens (STD), a long working distance lens (LWD) and a high numerical aperture lens (HiNA). Most measurements were performed using the standard objective lens, with a typical experimental working distance of 7 or 8 mm and a circular spot size of 74 ± 2 µm and 88 ± 2 µm for the 785 nm and 532 nm laser, respectively. The spectrometer is equipped with adjustable power controllers for each laser, with a maximum output power of 300 mW and 50 mW for the 785 nm and 532 nm lasers, respectively.

The spectrometer is equipped with two gratings, allowing one to record spectra with a spectral resolution of 6-7 cm^{-1} (the official bandwidth as reported by the manufacturer) and projecting the spectra onto a TEC-cooled (-50°C) charge-coupled-device (CCD) detector, allowing for the recording of spectral wavenumber ranges of 100 – 2350 cm^{-1} and 100 – 3200 cm^{-1}, for the red and green laser, respectively. 5m long fibre-optic cables permit the recording of spectra remotely from the instrument. A trigger is built into each probe head for convenient commencement of the measurements. The instrument is controlled by a built-in laptop, allowing the visualisation of the spectra while performing the measurements. An internal and an external Li-ion battery allows for a total running time of ca. 12 h. The instrument was modified with a built-in GPS tracking device that reports the coordinates of the system.

A plastic tube with a foam layer was slid over the objective lens tube to minimise the interference from the ambient sunlight. Typically, the laser power was kept low, to avoid possible laser damage: namely, ca. <30 mW (785 nm) and <8mW (532 nm). Measurement times and the number of accumulations were determined to obtain spectra with acceptable signal-to-noise (S/N) ratios, bearing in mind that focussing was performed manually, without rigid positioning equipment, and knowing that the available time on site was limited. The entire system is encased in a unit (55 x 35.5 x 24 cm, ca. 17 kg), which was carried on a metallic exoskeleton, to allow for transportation by a single person.

Before starting the measurements with the portable Raman spectrometer, and after each deployment of the instrument, wavenumber calibration was performed for both lasers. Five materials were used for this calibration: sulphur, epsilon-caprolactone (Acros Organics), cyclohexane (Kaiser), polystyrene pellets (Aldrich) and acetonitrile (Panreac)/ toluene (UCB) (mixed in 50/50 volume%). The selection of five products for calibration, or an elaborated calibration as suggested by R. L McCreery in 2000 [50], shares advantageous features compared to one-product-calibration as the Raman bands are spread over an extended spectral region (covering the low and high wavenumber region), the procedure is more robust and as the number of bands positions are increasing the calibration curve tends to have a better fit.

The instrument was positioned on an even ground or a gentle slope. The probehead with the light blocker covered with foam was placed perpendicular to and in contact with the selected spot for examination. The foam layer protected the rock art from any superficial damage. Positioning of the probehead was achieved by hand or by using a stick to reach the highest rock art paintings. Thus, for every single shelter or cave, spectra from the rock surface, the pictograms, the encrustations or alterations and the surrounding environment were collected. Although positioning of the probehead and thus focusing was difficult to be achieved, the quality of the Raman results was not significantly affected.

Post-measurement data treatment was performed by using Thermo Grams/AI 8.0® suite of software (Thermo Fischer Scientific).

3.3 Results and discussion

3.3.1 Practical considerations for the *in situ* Raman spectroscopic analysis of Patagonian rock art

The purpose of this work is to describe possible difficulties that could be encountered during *in situ* Raman measurement of Patagonian prehistoric rock art, and some possible improvements are thereby suggested. The portable Raman spectrometer used in this project had also been applied in previous studies, covering a broad range of artefacts, such as the analysis of a mediaeval wall painting [38], glass glyptics [51], illuminated mediaeval manuscripts [52], 16th century majolica tiles [53] , the 'Mad Meg' oil painting by Pieter Bruegel the Elder [54] and the identification of different minerals [55, 56]. Its application for the direct analysis of rock art paintings from Patagonia, Argentina is described and discussed for the first time in this study. Noteworthy for the current research project is that 17 sites were investigated in a single expedition, which makes this study one of the most comprehensive ever carried out on the measurement of rock art paintings. Consequently, some challenges were identified in bringing the equipment on site and reaching the areas of interest.

During this campaign, the first site was the Cueva Olate shelter in Neuquén province, Patagonia. The shelter was situated high in the mountains and it was not easy accessible. This site was the only one that had been surveyed in the area. The materials recovered from the archaeological site in combination with the actual rock art motifs, suggest a later chronology. The shelter at Las Mellizas (Neuquén) is situated on the north bank of Lago Traful (Traful lake) and is reachable first by boat and then on foot. This shelter was previously excavated and the results indicated an occupation dating from around 590 ± 90 BP. Dating of the archaeological site was based on the ^{14}C analysis on charcoal. The boat trip to the north bank was itself a challenge taking into account that the instrument could not suffer severe vibrations or water penetration. Also, a calm boat trip was necessary to reach the cave at Mirador de Castillo and the shelter at Alero Maqui in Valle

Encantado in the Río Negro province. The rest of the shelters in Río Negro province were much more accessible as they could be reached on foot and were at a relatively moderate distance from the main roads .

Another obstacle that was faced in attempting to reach the shelters was the thick vegetation which sometimes covered the path. This problem was more evident in a number of archaeological sites in the provinces of Neuquén and Rio Negro as they are located inside forests. In contrast, the shelters in the Chubut province located in Piedra Parada were more easy to reach because they are near the roads and in an open steppe environment. Moreover, at the time of the campaign, which was conducted during the summer, the expedition needed to take place under extreme heat, which not only hampered transport to the site but meant that intense sunlight also interfered with the measurements.

When arriving on site, the rock art paintings were first evaluated and discussed with the archaeologists to understand the current knowledge on how the hunter-gatherer population created the rock art paintings. In some cases, the hunter-gatherers used to paint on top of already degraded rock surfaces to achieve a better contrast. This information was very helpful in understanding the paintings and their stratigraphy, which is obviously also of interest when interpreting the results. Pictograms that needed to be investigated were selected and measurement points were determined with the help of a small microscope. Preferentially, thick paint layers were selected for Raman spectroscopic analysis, if possible without the presence of any superficial degradation crusts. In some cases, finding an appropriate spot was difficult, as some paintings, and particularly yellow and green areas, were severely damaged or degraded. Some shelters, such as that at Campanario 2, Río Negro, were completely covered with a white weathered crust.

The evaluation of the portable instrument EZRaman-I Dual Raman laser spectrometer was undertaken on rock art paintings in three different provinces in Patagonia, from which the capability for its transportation from site to site, or from panel to panel within the same site, was

considered as this could interfere with wavenumber stability. The problem of transportation was partially due to the weight of the instrument (ca. 17 kg) and its associated additional components (e.g. the external battery, calibration products, sample holder to record calibration products, lenses and light blockers). The instrument, is constructed in a suitcase, that was mounted on a metallic exoskeleton for ease of backpack carrying. Moreover, in some cases, when steep slopes and climbing are involved, vibrations can affect the geometry of the internal components and thus contribute to wavenumber instability, underlining the need for regular spectral calibration. Transport not only involved rough and steep paths but also travelling by boat to reach the shelters at the north bank of the Traful Lake.

Most of the shelters and the cave in the provinces of Neuquén and Río Negro were situated in the forests and were located at long walking or climbing distances from roads or main cities. In the Río Manso area, in shelters at the Paredón Lanfré and Piedra Parada sites (Chubut province), the environmental conditions were dramatically different. The environment there was dry and warm and most of the shelters were facing the sun. The spectra were recorded in direct sunlight and metallic components and the laptop of the instrument were exposed to direct solar heating.

On all the examined archaeological sites, before starting measurements, the instrument was calibrated for both lasers. It is known that changing the lasers (hence changing the grating position) could potentially affect the observed wavenumber stability. [38] In the case of the Patagonian sites, measurements were made at three to four archaeological sites per day and this involved the use of both lasers at each site.

In conclusion, different sources can be distinguished which contribute to slight shifts in the observed Raman band positions encountered during measurements of Patagonian rock art paintings. These include: (1) vibrations generated by the moving of the instrument as a backpack from site to site or caused by its transportation on rough roads, boat and so on, and (2) temperature fluctuations coming from different environmental conditions experienced when measuring in the forests of Neuquén and Río Negro to the dry steppes of the Chubut province.

Whilst these wavenumber variations should normally be addressed by the calibration procedure, small shifts can be observed if changes in the instrument occur between the calibration and the recording of the spectrum of the unknown.

Another important aspect of measuring in the Patagonian field is the availability of an electrical power supply. The portable *EZRaman-I Dual* Raman analyser has an internal battery and an external lithium-ion source. The latter has a lifetime of ca. 6 h 30 min. before charging is required. However, frequently changing between the different lasers decreases this time. As has been reported by Lauwers et al. [38], the laser output power decreases slightly with time and this can influence the Raman signal intensity. After 2 h, a constant power output of 230 mW is reached until the battery is discharged. The time needed for the batteries to be fully charged is 8.30 h. Working remotely with batteries in Patagonian rock art painting is, hence, a challenge. Furthermore, it is not possible to fully recharge the batteries with no access to electrical power whilst being far away from major cities. When visiting the shelters at the Chubut province, this problem was more evident as the team stayed in an organized campsite in the Piedra Parada Valley where the only source of electricity was a generator that was shut down at midnight and repowered at 7:00 h. Except from the first measuring day in the Chubut province, the spectra were collected with only half-charged batteries, which might have influenced the overall Raman signal intensity.

The spectrometer is equipped with two 5-m long fibre-optic cables. This was particularly favourable for use in the analysis of rock art paintings located at a higher level in shelters such as Alero Las Mellizas (Neuquén province). To collect spectra from these elevated figures the probehead was attached to a stick. Moreover, the positioning of the probehead in all the archaeological sites studied was accomplished by hand. Although it is necessary that the probehead should be sufficient stable in order to properly focus the laser beam on the rock art painting, this could not be definitely ensured in every case. In spectra that were recorded from the same spot under different measuring conditions, broader bands and low intensity spectra were observed which required longer measuring times as this focusing by hand is unavoidable while

working in the Patagonian sites. The alternative use of positioning equipment such as tripods would be advantageous but would also slow down the setting up process when limited site time was available and would introduce additional problems in mobility. Moreover, some shelters, like Cueva Olate (Neuquén province), are located on slopes in the mountains and it is difficult to find flat areas that are suitable for positioning the tripod.

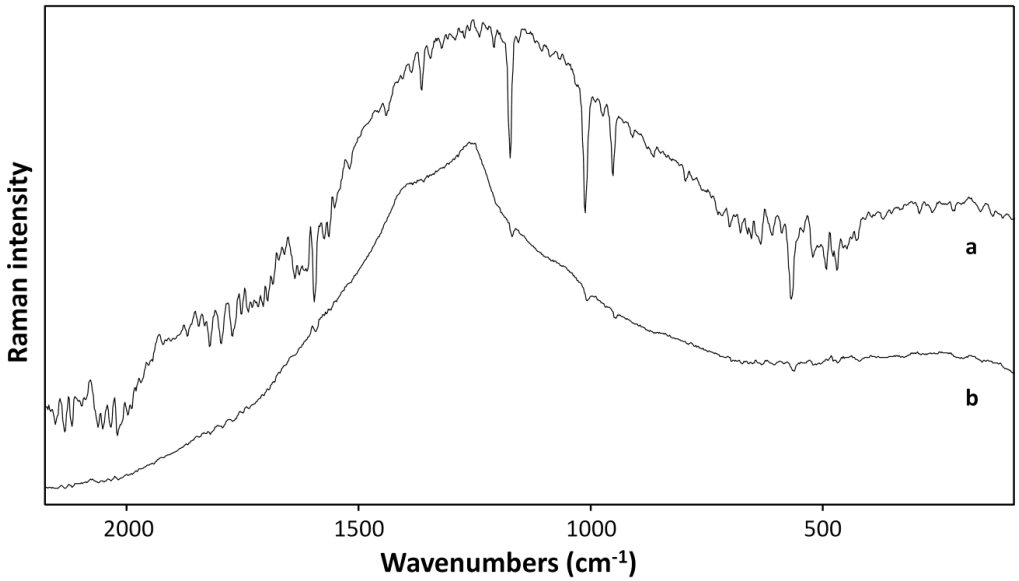

Figure 3.3. *Raman spectra demostrating the problem of light penetration during measurements. Spectrum (a) represents an environmental measurement while spectrum (b) was recorded during the last measuring day at a black rock art painting from the shelter at Piedra Parada 1, Chubut province.*

An important aspect when measuring rock painting is the interference of ambient light. When measuring in the field with portable Raman spectrometers, it is advisable to work at night or in darkness. In the case of the Patagonian rock art paintings, all the shelters except that at the Mirador de Castillo cave (Río Negro) were exposed directly to light. In the Chubut province, most of the shelters were directly facing the sun. For these reasons and in order to perform most of the

measurements during daytime, a plastic tube with a foam layer (to prevent damage to the painting) was slid over the objective lens tube to avoid sunlight interference. These light blockers performed well in the field. The only problem occurred during the last measuring day in the Piedra Parada 1 shelter (Chubut province) whilst measuring black pigments. In fig.3.3 the spectrum of an environmental measurement is overlaid with the spectrum recorded from a black pigmented rock art painting, and this highlights the interference of sunlight with the spectral data acquisition. The protective foam became partially detached from the rough surface of the rocks and light seepage reached the objective lens.

Although, in general, the portable *EZRaman-I Dual* Raman analyser performed well in rock art paintings analysis, there were some cases when the characterization of the components was difficult. For yellow pigmented rock art paintings only the alteration products on top of the rock could be identified. For green paintings, measured with both lasers, only in one case (painting Nr. 10, Angostura Blanca, Chubut province) were we able to attribute bands to celadonite $[K[(Al,Fe^{3+}),(Fe^{2+},Mg)](AlSi_3,Si_4)O_{10}(OH_2)]$ or glauconite $[(K,Na)(Fe^{3+},Al,Mg)_2(Si,Al)_4O_{10}(OH)_2]$, but the strong interference of the substrata in the spectra was obvious. High fluorescence emission was observed when measuring with both lasers, sometimes overwhelming completely the Raman signal.

In the case of the black pigments, as shown in fig. 3.4, the attribution of bands to certain specific vibrations was impossible. Due to high fluorescence emission, probably from the substrata, a relative weak broad band assignable to the E_{2g2},E_{2g} (bands at ca. 1650-1540 and 1680-1530 cm^{-1}) vibrational modes is observed, but in the absence of the A_{1g} vibrational mode from 1301 to 1390 cm^{-1} [57] then characterizing the black pigment as carbon-based is impossible. No other bands which in combination may be assigned to a different black material were found. The manganese oxides, with Raman frequencies in the range between 300 cm^{-1} to 700 cm^{-1}, have a weak Raman activity [58] and would have been difficult to be investigated using our portable Raman instrument.

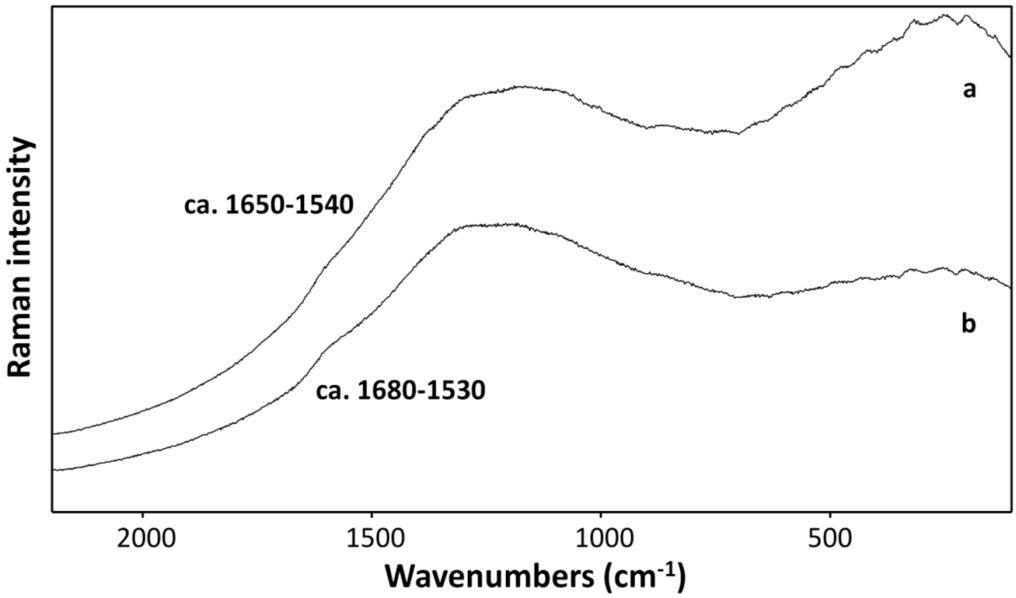

Figure 3.4. *Raman spectra demostrating the problem of the black pigment identification. The spectra are collected (a) from a black rock art painting from the shelter at Alero Las Mellizas, Neuquén province, and (b) from a black rock art painting from the cave at Mirador de Castillo, Río Negro province.*

The problem of the fluorescence is derived partially from the substrata. In all the spectra we collected from the rock surfaces without degradation, broad features have been found between 1100 and 1600 cm^{-1}. These features tend to shift from spectrum to spectrum and cause problems in the identification of components that give rise to Raman bands in that spectral region. A more elaborate study needs to be made before making final conclusions on the nature of these bands and perhaps these are attributable to the fluorescence effects related to the presence of some luminescent chromophores.

3.3.2 Raman spectroscopic identification of pigments and minerals

The portable *EZRaman-I Dual* Raman analyser performed well in the identification of pigments comprising the red and the white features of rock art paintings, the characterization of encrustations and weathering products on the top of the rock surface as well as investigation of the actual rock itself. In some cases, the spectra were noisy with high background which was to be expected from a portable Raman instrument. Baseline correction applied to such spectra could possibly create problems by generating artificial features.

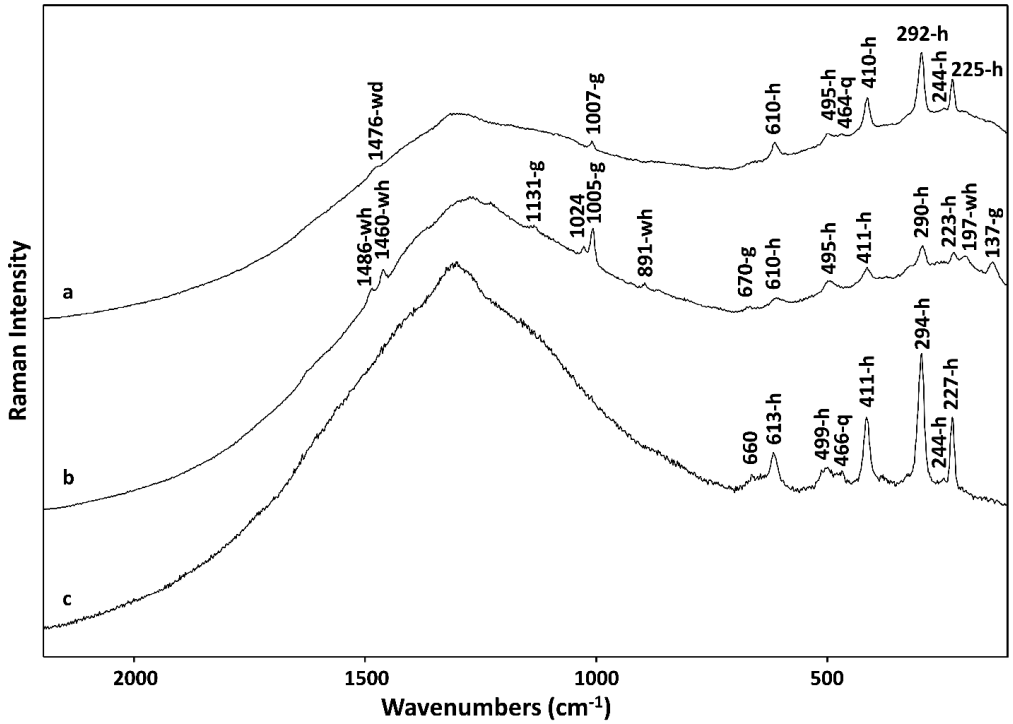

Figure 3.5. *Raman spectra of representative points of: (a) red rock art painting, (b) white-dot rock art painting from the shelter at Alero Las Mellizas, Neuquén province and (c) red rock painting from the shelter at Queutre Inalef, Río Negro province. Labels: wd, weddellite; g, gypsum; h, haematite; q, α-quartz; wh-whewellite.*

In fig. 3.5 spectra collected from red rock art paintings from (a) the shelter at Alero Las Mellizas, Neuquén province and (c) the shelter at Queutre Inalef, Río Negro province are presented. The red chromophore of these two rock art paintings is haematite (Fe_2O_3), which could be identified by the bands at 610, 495, 410, 292, 244 and 225 cm^{-1} [27, 59, 60] for the shelter at Alero Las Mellizas and bands at 613, 499, 411, 294, 224 and 227 cm^{-1} [27, 59, 60] for shelter at Queutre Inalef. Moreover, in the shelter at Alero Las Mellizas a band at 1476 cm^{-1} can be attributed to weddellite ($CaC_2O_4 \cdot 2H_2O$) [61] and bands at 1007 and 464 cm^{-1} assigned to gypsum ($CaSO_4 \cdot 2H_2O$) [62] and α-quartz [63], respectively. The presence of a band at 660 cm^{-1} in the spectrum of the shelter at Queutre Inalef could be due to magnetite (Fe_3O_4) [59, 60, 64]. Magnetite is often associated with thermal treatment of raw minerals (artificial production of haematite through thermal treatment) but also can be formed from microbiological attack on haematite and its oxy-hydroxyoxides and can serve as a decay product [19, 21] of these processes. Moreover, it is present in nature. It is worth mentioning that the assignment of the band at around 660 cm^{-1} is under debate, especially when both haematite and magnetite are present. [65] In 1999, Bersani et al. [66] showed that in the absence of magnetite a band appears in haematite at 660 cm^{-1} related to disorder effects in the crystal lattice and/or the presence of nanocrystals. In the presence of magnetite this peak is enhanced. Among other spectra that were collected from the multicoloured paintings of the shelter at Alero Las Mellizas, that from a white-dot rock art painting was measured (Fig. 3.5 (b)). The white pigment of the painting is identified as gypsum ($CaSO_4 \cdot 2H_2O$) by the bands at 1131, 1005, 670 and 137 cm^{-1} [62]. Haematite (Fe_2O_3) is also present in the white mixture (with bands at 610, 495, 411, 290 and 223 cm^{-1}) [27, 59, 60]. Bands of whewellite ($CaC_2O_4 \cdot H_2O$) were observed at 1486, 1460, 891 and 197 cm^{-1} [27]. The presence of hydrated Ca-oxalates, on the red and white dot rock art paintings of the shelter at Alero Las Mellizas, can be explained biologically and chemically. Ca-oxalate layers are the result of metabolic activity of lichens, fungi or bacteria that colonize superficial Ca-rich substrates. Moreover, oxalates can formed from the degradation of organic media and the alteration of some binders found in the paintings [20, 30, 31]. Special attention should be given to a band at 1024 cm^{-1}. This band is attributed from laboratory thermal studies to metastable soluble anhydrite (AIII). This compound is unstable and rehydrates very quickly [67]. In 2011, Tournié et al. [37], measuring *in situ* San rock art in South Africa, attributed

a band at 1025 cm^{-1} as anhydrite and they discussed the instability of this compound. In the absence of other bands the band at 1024 cm^{-1} can also be attributed to iron (III) sulfate nonahydrate ($Fe_2(SO_4)_3 \cdot 9H_2O$). This chemical formula is shared by two polymorphs with almost identical Raman spectra: coquimbite and paracoquimbite [68]. In environments rich in sulfate aerosols, the formation of $Fe_2(SO_4)_3 \cdot 9H_2O$ is the result of the reaction between iron oxides, in particular haematite, and the soluble sulfate obtained from the formation of gypsum. It is worth mentioning though that the formation of coquimbite and paracoquimbite as decay products is well described for wall paintings and modern mortars [68, 69].

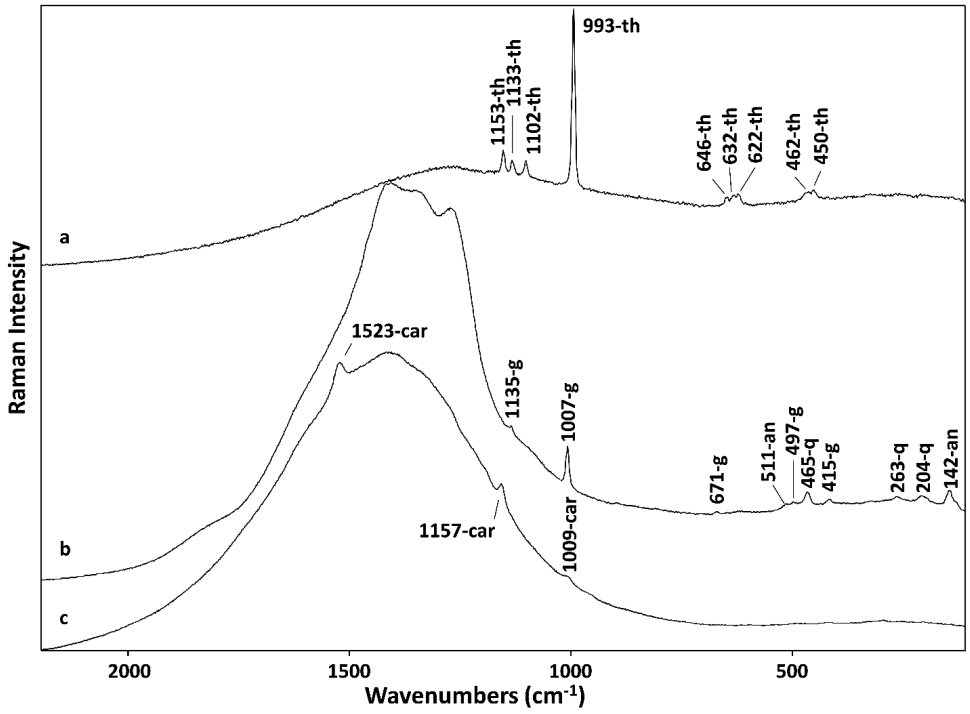

Figure 3.6. *Raman spectra of representative points of: (a) white encrustration near the paintings of Panel 2 in the shelter at Piedra Parada 1, Chubut province, (b) white rock art painting from the shelter at Cueva Olate, Neuquén province and (c) red man horseriding from the shelter at Lago Moreno East, Río Negro province. Labels: th-thernadite; g, gypsum; an, anatase; q, α-quartz; car-carotenoids.*

The Raman spectra from the shelter at Piedra Parada 1, Chubut province and the shelter at Lago Moreno East, Rio Negro province, shown in fig. 3.6 (a) and (c) represent degradation products and compounds resulting from biological activity, respectively. The thenardite (Na_2SO_4) encrustration (bands at 1153, 1133, 1102, 993, 646, 632, 622, 462 and 450 cm^{-1}) [70, 71] was found near the rock art paintings of Panel 2 in the shelter at Piedra Parada 1. The dry environment of the steppe can explain partially the formation of the anhydrous sodium sulfate and can be attributed to the result of attack by atmospheric gases. In the spectrum of the red man horseriding in the painting from the shelter at Lago Moreno East, the bands at 1523, 1157 and 1009 cm^{-1} are attributed to carotenoids [27, 61]. Carotenoids are produced in the metabolism of photosynthetic bacteria or lichens and the precise species of carotenoid is difficult to identify from these the three bands alone.[27] In the white rock art painting from the shelter at Cueva Olate in Neuquén province (Fig. 3.6 (b)) the white pigment is identified as gypsum ($CaSO_4 \bullet 2H_2O$) by the bands at 1135, 1007, 671, 497 and 415 cm^{-1}) [62]. The bands at 511 and 142 cm^{-1} correspond to titanium oxide (anatase) [29] while the bands at 467, 263 and 204 cm^{-1} can be attributed to α-quartz [63].

Working with portable Raman instruments on rock art paintings allows the measurement of all the possible layers that may contribute to the Raman signal of the actual painting and thus one can attribute the bands to the proper compounds in each level. Spectra collected from the rock surfaces, with and without alteration products, revealed the compounds of the substrata and the encrustrations and contribute to the precise identification of the materials of the paintings. Even in cases where certain spectral features and background fluorescence were observed, the molecular fingerprint of the compounds was successfully identified. For the Patagonian sites, being able to create instant libraries of materials found on rocks improved our ability to intergrate the bands and assign them to the correct compound, especially in the cases of mixtures of iron oxides, different groups of silicates, anatase and degradation products such as gypsum ($CaSO_4 \bullet 2H_2O$).

3.3.3 Suggestions for improvement of the portable *EZRaman-I dual* laser Raman spectrometer

The use of portable Raman spectroscopy on the analysis of the rock art materials, accretions and alteration products and substrata on rock art paintings from Patagonia was proven to be successful. In order to overcome difficulties which were encountered during the *in situ* Raman measurement of Patagonian prehistoric rock art several possible improvements are suggested.

A very important factor that needs special attention is the weight of the system. Although the entire Raman system is enclosed in a suitcase weighing ca. 17 kg its transportation was difficult especially when the sites were in remote locations or situated high in the mountains. In order to reduce the total weight of the basic instrument it is suggested that the battery and the computer that are normally fixed inside the suitcase are removed and carried separately. Moreover, a lighter suitcase material would be advantageous, for example one constructed from carbon fibres, titanium or aluminium, to further reduce the total weight of the basic instrument. Additionally, the new suitcase should protect the internal part of the instrument from fine dust penetration and also be waterproof. Instead of carrying the instrument on an exoskeleton, carrying strips are proposed for incorporation into the back of the suitcase in order to facilitate its use as a backpack.

Another aspect that needs to be considered is the lifetime of the batteries. Most of the sites in Patagonia are located far from cities. The shelters in the Chubut province are situated near to or actually in the Piedra Parada Valley, where electrical power in unavailable. As a consequence, the batteries need to have a lifetime of more than 8 h duration to allow for the average working day.

Another problem which occurred whilst measuring in the steppes was the ambient high temperature. When the suitcase is opened, all the metallic parts of the instrument are exposed to heat. Temperature fluctuations may disturb the wavenumber stability, and thus, it is suggested either the metallic components to have a thermostatic cover or that insulator materials are used.

Calibration is very important in order to correctly appreciate the wavenumber stability. Other parameters that can disturb wavenumber stability are temperature fluctuations, vibrations coming from moving the instrument and changing the grating while measuring with different lasers. As some of these were unavoidable when measuring in Patagonia, calibration cannot be entirely assumed to be correct without regular checks being made. Although our instrument was tested for wavenumber stability [38] most studies have been carried out in a laboratory environment. For the Patagonian sites, it is suggested that the operator performs the calibration just before measuring the rock art painting for every single site, even when the sites are closely located. Also, every laser should be calibrated just before use in order to avoid wavenumber shift deviations during the operation of changing the grating. Also, automatic calibration of the spectra before and after the individual runs could reduce the time of post-processing of the data.

Another suggestion for future adoption is the use of a 1064-nm laser in order to decrease the fluorescence background and achieve better results with the consequent limitatiions of noise and background emission. Also the solid state detectors of near IR lasers are more sensitive in the C-H stretching region than charge-coupled device detectors which will assist in the asignmenty of organic moieties. The main problem experienced in the coupling of a 1064-nm laser to an instrument that is designed to operate with 785-nm and 532-nm lasers is that a different geometry, grating and detector is necessary which means that the dimensions and the total weight of the instrument are changed .

Measuring in Patagonia with tripods in order to better focus at the shelters is not possible. Most of the sites are located on sloping terrain or the rocky ground is rough and uneven. Moreover, if three or four sites need to be measured in the same day the carriage of extra positioning equipment is impossible. Positioning of the probehead by hand, although difficult, has been proven successful in measuring rock art paintings. However, It is suggested that it is advisable to perform short measurements when focusing by hand as the focus can tend to fluctuate because of hand tremors. Moreover, in order to reach and focus on paintings that are situated in elevated

positions at the sites an adjustable stick of 2 m in total length with a rotary head capable of operating through 180° is essential.

The plastic tubes with foam that were slid on the objective lens proved excellent for the blocking of the ambient light. The only problem occurred during the last measuring day because the protective foam had been damaged by rough rock surfaces. Additional light blockers should be carried when measuring rock art paintings or possibly to replace soft foam at the edge of the plastic tube with a more durable material.

The portable *EZRaman-I Dual* Raman analyser is not coupled with a microscope and this created a further problem regarding the ability to focus appropriately on the region of interest. The use of a microscope or camera with a high magnification would alleviate this problem and is highly recommended in the future.

3.4 Conclusions

The current research focused on the direct investigation of prehistoric rock art paintings at 17 archaeological sites in the broad Patagonian regions of El Neuquén, Rio Negro and Chubut. The purpose of this work is twofold: to describe possible difficulties occurring during the *in situ* Raman measurements of Patagonian prehistoric rock art and to suggest some possible improvements for future deployment. The portable Raman spectrometer used in the current study was also applied in previous projects, covering a broad range of artefacts, but was never used in the investigation of rock art paintings hitherto. The portable *EZRaman-I Dual* Raman spectrometer successfully characterized the substrata, encrustrations, degradation products, biologically active related compounds and most of the pigments used for rock art painting.

An additional challenge for the current research campaign is that a significant number of rock art paintings from different archaeological sites were investigated in a single expedition, which

was accomplished in a short time, resulting in one of the most comprehensive studies made on the measurement of rock art paintings ever published.

As the important characteristics and possible drawbacks of the EZRaman-I Dual Raman analyser are evaluated and discussed, the suitability of the spectrometer for the analysis of rock art paintings have been explored. In the next chapter, the analysis of the main chromophores, together with the (bio)degradation products found on 16 open air shelters in different environments, in Argentinian part of Patagonia*, will be surveyed.*

3.5 References

[1] C. Bellelli, F. X. Pereyra, M. Carballido, in *Geomaterials in Cultural Heritage,* (Eds: M. Maggetti and B. Messiga), The Geological Society, London, **2006**, pp. 241-255.

[2] C. J.Gradin, C. A. Aschero, A. M. Aguerre, *Relaciones* **1977**, *X*, 201.

[3] C. A. Aschero, *Cuadernos* **1985**, *10*, 291.

[4] C. E. Barbosa, G. E. Rial, *Primeras Jornadas de Arte y Arqueología* **1985**, 1, 21.

[5] C. E. Barbosa, C. J. Gradin, *Relaciones* **1988**, *XVII***,** 143.

[6] M.T. Boschin, M.S. Maier, G.I. Massaferro, *L'anthropologie* **2011**, *115*, 360.

[7] I. N. M. Wainwright, K. Helwig, D. S. Rolandi, C. A. Aschero, C. Gradin, M. M. Podestá, M. Onetto, C. Bellelli, *10° Journées d'etudes de la Section Francaise de l'Institut International de Conservation*, **2002**, 15.

[8] D. Fiore, , M. Maier, S. D. Parera, L. Orquera, E. Piana, *J. Archaeol. Sci.* **2008**, *35*, 3047.

[9] I. N. M. Wainwright, K. Helwig, M. M. Podestá, C. Bellelli, in *Arte en las Rocas,* (Eds: M. M. Podestá, M. de Hoyos), Sociedad Argentina de Antropología, AINA, Buenos Aires, **2000,** pp. 203-206.

[10] C. Vázquez, G. Custo, A. Albornoz, A. Hajduk, A. M. Maury, O. M. Palacios, Pigment characterization by scanning electron microscopy and X-ray diffraction techniques: archaeological site El Trebol, Nahuel Huapi, Rio Negro, Argentina. *Report IAEA/AL,* **2007** *181*, 29.

[11] A. Hajduk, A. Albornoz, M. Lezcano, M., P. Arias Cabral, in *Southbound late Pleistocene peopling of Latin America. Current Research in the Pleistocene,* (Eds: L. Miotti, M. Salemme, N. Flegenheimer, T. Goebel), Texas, Texas A&M University, **2012**, pp. 117- 120.

[12] L. Darchuk, E. A. Stefaniak, C. Vázquez, O. M. Palacios, A. Worobiec, R. Van Grieken, *e-Preservation Sci.* **2009**, *6*, 112.

[13] C. Vázquez, O. M. Palacios, L. Darchuk, L. M. M. Parra, *Powder diffraction* **2010**, *25*, 264.

[14] G. I. Massaferro, G. I Arrigoni, M. T. Boschín, M. M. Fernández, E. A. Crivelli, J. A. Cordero *Bol. Museo Chil. de Arte Precol.* **2012**, *1*, 117.

[15] V. Aldazábal, M. Silveira, G. Custo, M. Ortiz, *Bol. Museo Chil. de Arte Precol.* **2014**, *19,* 95.

[16] M. Maier, D. L. A. de Faria, M. T. Boschín, S. D. Parera, *ARKIVOC* **2005**, *XII*, 311.

[17] M.S. Maier, D. L. A. de Faria, M. T. Boschín, S. D. Parera, M. F. del Castillo Bernal, *Vib. Spectrosc.* **2007**, *44*, 182.

[18] C. Bellelli, P. Marchione. C. Vázquez, in *Arqueología Argentina. Metodologías científicas aplicadas al estudio de los bienes culturales. Datación, caracterización, prospección y conservación*, (Eds: A. Pifferetti, I. Dosztal), **2015**, p. 261-269.

[19] A. Rousaki, C. Bellelli, M. Carballido Calatayud, V. Aldazábal, G. Custo, L. Moens, P. Vandenabeele, C. Vázquez, *J. Raman Spectrosc.* **2015**, *46*, 1016.

[20] H.G.M. Edwards, L. Drummond, J. Russ, *Spectrochim. Acta A* **1998**, *54*, 1849.

[21] H.G.M. Edwards, E.M. Newton, J. Russ, *J. Mol. Struct.* **2000**, *550–551*, 245

[22] H. Gomes, P. Rosina, H. Parviz, T. Solomon, C. Vaccaro, *J. Archaeol. Sci.* **2013**, *40*, 4073.

[23] F. Ospitali, D. C. Smith, M. Lorblanchet, *J. Raman Spectrosc.* **2006**, *37*, 1063.

[24] D. C. Smith, M. Bouchard, M. Lorblanchet, *J. Raman Spectrosc.* **1999**, *30*, 347.

[25] L. Prinsloo, W. Barnard, I. Meiklejohn, K. Hall, *J. Raman Spectrosc.* **2008**, *39*, 646.

[26] L. Prinsloo, A. Tourni**é**, Ph. Colomban, C. Paris, S.T. Bassett, *J. Archaeol. Sci.* **2013**, *40*, 2981.

[27] A. Hernanz, J. M. Gavira-Vallejo, J. F. Ruiz-López, H. G. M. Edwards, *J. Raman Spectrosc.* **2008**, *39*, 972.

[28] A. Hernanz, J. F. Ruiz-López, J. M. Gavira-Vallejo, S. Martin, E. Gavrilenko, *J. Raman Spectrosc.* **2010**, *41*, 1394.

[29] A. Hernanz, J. M. Gavira-Vallejo, J. F. Ruiz-López, S. Martin, A. Maroto-Valiente, R. de Balbín-Behrmann, M. Menéndez, J. J. Alcolea-González, *J. Raman Spectrosc.* **2012**, *43*, 1644.

[30] C. Lofrumento, M. Ricci, L. Bachechi, D. De Feo, E.M. Castellucci, *J. Raman Spectrosc.* **2012**, *43*, 809.

[31] M. Mas, A. Jorge, B. Gavilán, M. Solís, E. Parra, P.-P. Pérez, *J. Archaeol. Sci.* **2013**, *40*, 4635.

[32] A. Zoppi, G. F. Signorini, F. Lucarelli, L. Bachechi, *J. Cult. Herit.* **2002**, *3*, 299.

[33] S. Gialanella, R. Belli, G. Dalmeri, I. Lonardelli, M. Mattarelli, M. Montagna, L. Toniutti, *Archaeometry* **2011**, 53, 950.

[34] M. Iriarte, A. Hernanz, J. F. Ruiz-López, S. Martín, *J. Raman Spectrosc.* **2013**, *44*, 1557.

[35] A. Bonneau, D.G. Pearce, A.M. Pollard, *J. Archaeol. Sci.* **2012**, *39*, 287.

[36] R. A. Goodall, B. David, P. Kershaw, P. M. Fredericks, *J. Archaeol. Sci.* **2009**, *36*, 2617.

[37] A. Tournié, L.C. Prinsloo, C. Paris, Ph. Colomban, B. Smith, *J. Raman Spectrosc.* **2011**, *42*, 399.

[38] D. Lauwers, A. G. Hutado, V. Tanevska, L. Moens, D. Bersani, P. Vandenabeele, *Spectrochim. Acta A* **2014**, *118*, 294.

[39] S. Lahlil, M. Lebon, L. Beck, H. Rousselière, C. Vignaud, I. Reiche, M. Menu, P. Paillet, F. Plassard, *J. Raman Spectrosc.* **2012**, *43*, 1637.

[40] T. R. Ravindran, A. K. Arora, M. Singh, S. B. Ota, *J. Raman Spectrosc.* **2013**, *44*, 108.

[41] M. Olivares, K. Castro, M.S. Corchón, D. Gárate, X. Murelaga, A. Sarmiento, N. Etxebarria, *J. Archaeol. Sci.* **2013**, *40*, 1354.

[42] A. Hernanz, J. F. Ruiz-López, J. M. Madariaga, E. Gavrilenko, M. Maguregui, S. Fdez-Ortiz de Vallejuelo, Ir. Martínez-Arkarazo, R. Alloza-Izquierdo, V. Baldellou-Martínez, R. Viñas-Vallverdu, A. Rubio i Mora, A. Pitarch, A. Giakoumaki, *J. Raman Spectrosc.* **2014**, *45*, 1236.

[43] A. Pitarch, J. F. Ruiz, S. Fdez-Ortiz de Vallejuelo, A. Hernanz, M. Maguregui, J. M. Madariaga, *Anal. Methods* **2014**, *6*, 6641.

[44] P. Vandenabeele, H. G. M. Edwards, J. Jehlička, Chem. Soc. Rev. **2014**, *43*, 2628.

[45] A. Culka, J. Jehlička, L. Strnad, *Spectrochim. Acta A* **2012**, *86*, 347.

[46] A. Culka, H. Kindlová, Petr Drahota, Jan Jehlička, Spectrochim. Acta A-Part A Mol. Biomol. Spectrosc. 2016, 154, 193.

[47] J. Jehlička, A. Culka, Peter Vandenabeele, H. G. M. Edwards, *Spectrochim. Acta Part A Mol. Biomol. Spectrosc.* **2011**, *80*, 36.

[48] Z. Petrová, J. Jehlička, T. Čapoun, R. Hanus, T. Trojek, V. Goliáš, J. Raman Spectrosc. 2012, 43, 1275.

[49] J. Jehlička, A. Culka, M. Baštova, P. Bašta, J. Kuntoš, *Philos. Trans. A Math. Phys. Eng. Sci.* **2016**, *374*, 20160042.

[50] R.L McCreery, *Raman Spectroscopy for Chemical Analysis,* John Wiley & Sons, New York, USA, **2000**.

[51] D. Lauwers, A. Candeias, A. Coccato, J. Mirao, P. Vandenabeele, L. Moens, *Spectrochim. Acta A* **2016**, *15,* 146.

[52] D. Lauwers, V. Cattersel, L. Vandamme, A. Van Eester, K. De Langhe, L. Moens, P. Vandenabeele, *J. Raman Spectrosc.* **2014**, *45,* 1266.

[53] L. Van de Voorde, M. Vandevijvere, B. Vekemans, J. Van Pevenage, J. Caen, P. Vandenabeele, P. Van Espen, L. Vincze, *Spectrochim. Acta B* **2014**, *102,* 28.

[54] L. Van de Voorde, J. Van Pevenage, K. De Langhe, R. De Wolf, B. Vekemans, L.Vincze, P.Vandenabeele, M. Martens, *Spectrochim. Acta B* **2014**, *97,* 1.

[55] J. Jehlička, P. Vandenabeele, *J. Raman Spectrosc.* **2015**, *46*, 927.

[56] C. Baita, P. P. Lottici, E. Salvioli-Mariani, P. Vandenabeele, M. Librenti, F. Antonelli, D. Bersani, *J. Raman Spectrosc.* **2014**, *45*, 114.

[57] A. Coccato, J. Jehlička, L. Moens, P. Vandenabeele, *J. Raman Spectrosc.* **2015**, *46*, 1003.

[58] F. Buciuman, F. Patcas, R. Craciun, D. R. T. Zahn, *Phys. Chem. Chem. Phys.* **1999**, *1*, 185.

[59] D. L. A. de Faria, F. N. Lopes, *Vib. Spectrosc.* **2007**, *45*, 117.

[60] S. Das, M. J. Hendry, *Chemical Geology* **2011**, *290*, 101.

[61] M. Maguregui, U. Knuutinen, I. Martínez-Arkarazo, A. Giakoumaki, K. Castro, J. M. Madariaga, *J. Raman Spectrosc.* **2012**, *43*, 1747.

[62] J. Jehlička, P. Vítek, H. G. M. Edwards, M. D. Hargreaves, T. Čapoun, *J. Raman Spectrosc.* **2009**, *40*, 1082.

[63] I. Martínez-Arkarazo, D. C. Smith, O. Zuloaga, M. A. Olazabal, M. J. Madariaga, *J. Raman Spectrosc.* **2008**, *39*, 1018.

[64] D. A. de Faria, S.V. Silva, M. T. de Oliveira, *J. Raman Spectr.* **1997**, *28*, 873.

[65] D. Bersani, P. P. Lottici, *J. Raman Spectr.* **2016**, *47*, 499.

[66] D. Bersani, P. P. Lottici, A. Montenero, *J. Raman Spectr.* **1999**, *30*, 355.

[67] N. Prieto-Taboada, O. Gómez-Laserna, I. Martízez-Arkarazo, M. Ángeles Olazabal, J. M. Madariaga, *Anal. Chem* **2014**, *86*, 10131.

[68] M. Maguregui, U. Knuutinen, K. Castro, J. M. Madariaga, *J. Raman Spectr.* **2010**, *41*, 1400.

[69] N. Prieto-Taboada, M. Maguregui, I. Martínez-Arkarazo, M. A. Olazabal, G. Arana, J. M. Madariaga, *Anal. Bioanal. Chem* **2011**, *399,* 2949.

[70] A. Hamilton, R. I. Menzies, *J. Raman Spectr.* **2010**, *41*, 1014.

[71] M. L. Frezzotti, F. Tecce, A. Casagli, *J. Geochemical Explor.* **2012**, *112*, 1.

Chapter 4 In-field Raman Spectroscopy of Patagonian Prehistoric Rock Art: Pigments, Alteration Products and Substrata

Based on the paper: A. Rousaki, E. Vargas, C. Vázquez, V. Aldazábal, C. Bellelli, M. Carballido Calatayud, A. Hajduk, O. Palacios, L. Moens, P. Vandenabeele, *Trends Anal. Chem*. **2018**, accepted.

In the previous chapter, the evaluation of the EZRaman-I Dual Raman spectrometer has been extensively described for the first-time analysis under extreme conditions of rock art paintings in Argentinian part of Patagonia*. Several improvements are proposed to maximize the quality of the research output from comprehensive expeditions with limited time availability. The use of the portable Raman spectrometer was proven to be successful for the identification of pigments and minerals found on rock art paintings. In the next chapter, the overall results from this extensive in situ Raman spectroscopic campaign are discussed. This research is based on the analysis of 16 open air shelters located in different environments (forests, ecotones, steppes) in* Argentinian part of Patagonia *(Neuquén, Río Negro and Chubut). The results are interpreted in terms of pigments used by the local people and the identification of substrata. Special attention is given to the formation of alteration products and accretions that were found on the rock art paintings of the shelters and on the surface of the rock walls as these can affect and damage these magnificent works of art.*

The main chromophores (haematite, green earth, gypsum etc.) that were found on the colourful paintings in most of the shelters, were successfully identified. The advantage of using a dual laser system is underlined by the positive characterization of the green earth, glauconite. Many minerals and silicates were found on the coloured areas and also on the rock substrate. (Bio)degradation product crystallization was identified on the paintings, crusts and rock surfaces, and are associated with weathering. In some cases the shelters were so severely degraded that no Raman signal of pigments and/or other components could be retrieved. Layered zones were observed in all the

shelters studied, posing difficulties in the interpretation of the results and introducing several complications for the retrieval of the Raman signal.

4.1 Introduction

Physicochemical analysis of the composition of materials and pigments is currently a standard analytical procedure in archaeology and particularly in rock art studies [1-3]. From its application the analysis of pigments from both rocky supports and excavated samples allows us to answer key archaeological questions related to their technological, stylistic and/or temporal aspects [4-8]. As a consequence, the active and continuous communication between archaeologists, chemists and physicists has promoted interdisciplinary investigations and the generation of working protocols to reach a methodological and interpretive consensus [9].

Patagonia (Argentina) hosts a remarkable number of painted rock art sites which are found quite commonly from the North to the South. The rock art paintings can be found ranging from single, multi- and/or mono-coloured panels to more sophisticated multipanels. The examination of these prehistoric works of art, combined with archaeological studies in the Patagonian field from several archaeological sites, provides rich knowledge of the local hunter-gatherer populations and a deeper understanding of their practices within their environmental systems (forests, ecotones and steppes). Within these different, hostile and remote environments, hunter-gatherer groups demonstrated a great mobility [10-11].

In general, micro-Raman spectroscopy is a powerful tool for the investigation of pigments, degradation products and substrata in rock art paintings [12-15]. Minimal samples can be brought into the laboratory and measured *in vitro* down to a micrometer-scale [16]. In cases where the invasive character of this approach cannot be justified, mobile Raman instrumentation can be employed. In fact, there are several studies in the literature describing the use of portable Raman spectrometers [11, 17-18] in field studies with excellent results reported for the characterization

of pigments, crusts and substrata. Moreover, by bringing such instrumentation onto the site the preservation state of the work art can be monitored directly.

Previous studies in Argentina have focused mainly on the characterization of pigments from different archaeological contexts by means of multiple, non-portable techniques [5, 9, 12, 19-27]. However, most of these studies did not specifically address the degradation processes that affect the rock art motifs and the preservation state of the archaeological sites in general. Moreover, severe degradation and the presence of thick encrustations can encapsulate the actual painting in between layers to the point that it might be not visible anymore. Therefore, we consider it necessary, in addition to the pigment identification, to study also those factors in detail that cause the deterioration of the rock art paintings and which may have important implications when studying the main chromophores used by the hunter-gatherer societies. These factors are usually described macroscopically in the field and afterwards investigated microscopically in the laboratory. In fact, there are few studies dedicated to the *in situ* analysis of degradation and taphonomic processes of rock art pigments and rock supports [28-30].

The current research focusses on the *in situ* investigation of rock art paintings in 16 open air shelters found in the forests and ecotones of Neuquén and Río Negro and the steppe at Chubut. The study includes the identification of pigments and substrata. Great attention is given to the alteration products and accretions that were found on the paintings in the shelters and on the surface of the rock walls, as they can affect and damage the rock art paintings. This work builds on the previous study, as demonstrated in chapter 3, on the evaluation of our portable Raman spectrometer to analyse rock art paintings under extreme conditions in Argentinian part of Patagonia where a more detailed description of the literature and the possibilities of Raman spectroscopy on rock art paintings is given [11].

The information obtained by in-field measurements is of great importance as an initial step prior to the physicochemical characterization of the rock art pigments, since in this way we can identify and differentiate on site between natural processes and the intentional (cultural)

processes. In this sense, the use of portable instruments gives us critical information regarding the different sectors of the site that may be affected by different processes. At the same time, the information retrieved from this kind of analysis allows us to select in a more objective way those motifs that, due to their distinguishable characteristics and/or archaeological interest, should be further investigated, or eventually, conclude if the extraction of samples is necessary for a more comprehensive analysis to be undertaken in the laboratory.

4.2 Experimental

In situ Raman spectroscopy was performed with a portable *EZRaman-I dual* Raman analyser from TSI Inc. [31]. The specifications and the characteristics of the portable Raman instrument can be found in chapter 3, section 3.2.

For measuring the Patagonian rock art paintings the standard objective lens was selected that has a focal length of ca. 7 mm and a circular spot size of 74 ± 2 µm and 88 ± 2 µm for the 785 nm and 532 nm laser, respectively. The laser power was kept low to avoid thermal alteration of the components measured: ca. <30 mW (785 nm) and <8mW (532 nm). To avoid interference of ambient light a plastic tube with a protective foam layer was slid over the standard objective lens. The probehead was manually positioned, perpendicular to and in complete contact with the area selected for examination. For maintaining the focussing during this process, the measurement times and number of accumulations were selected to obtain good spectra with acceptable signal-to-noise (S/N) ratios. Wavelength calibration was performed with sulphur, epsilon-caprolactone (Acros Organics), cyclohexane (Kaiser), polystyrene pellets (Aldrich) and acetonitrile (Panreac) toluene (UCB) (mixed in 50/50 volume %) [32]. Data post-processing was performed by using Thermo Grams/AI 8.0® suite software (Thermo Fischer Scientific).

4.3 Results and discussion

4.3.1 Environments, shelters and rock art painting studied

The portable Raman measurement campaign started in North Patagonia by investigating shelters in Neuquén province and ended in the steppe in Piedra Parada Valley (Chubut province). Different environmental conditions affect the paintings and also environmental pollution can potentially damage the artefacts. In the wet forests, rock art paintings are found high in the mountains in remote places away from busy arterial roads. In the steppes, the shelters are much closer to the road and are accessible to possible visitors [11]. As a consequence these are more vulnerable to vandalism. Moreover, as all sites are in the open air, they can also serve as shelters for animals. This can increase the opportunity for decay and further damage the artefacts.

4.3.1.1 Traful area, Neuquén province

The archaeological sites of Traful are located in forest areas off the northern coast of Lake Traful, Nahuel Huapi National Park, and in the middle and upper valley of the eponymous river in the south of the Neuquén Province. Currently, in general terms the weather is cool, temperate and humid, with an average annual rainfall for the area estimated close to 1,400 mm [33]. The average temperature in the hottest month (January) ranges from 14 to 16 °C and in the coldest month (July) from 2 to 4 °C with frequent snowfalls. The rainfall regime is determined by the humid winds of the Pacific anticyclone and the Andes mountain range, which acts as a natural barrier in its movement towards the east.

From the phytogeographic point of view, the area is located within the subhumid mixed forest of “coihue” (*Nothofagus dombeyi*), “cypress” (*Austrocedrus chilensis*), "ñire" (*Nothofagus antarctica*) and "lenga" (Nothofagus pumilio), corresponding to the eastern part of the Valdivian District, Subantarctic Province [34]. In general, in the northwest of Patagonia, the forest becomes denser towards the west in the subhumid forest of coihue (*Nothofagus dombeyi*), cypress, and

even more "closed" in the humid forests of coihue and cane “coligüe” (*Chusquea culeu*). According to V. Markgraf in 1989 [35], the cypress/coihue-steppe line is found in the 800 mm isohieta and from 2000 mm on, the first elements of the "Valdivian forest" appear.

Archaeological research in the area of the Nahuel Huapi Lake-Traful National Park, Neuquén province, Argentina, began in the 1980s by M. Silveira, in order to discover the human use of this natural forest environment [36].

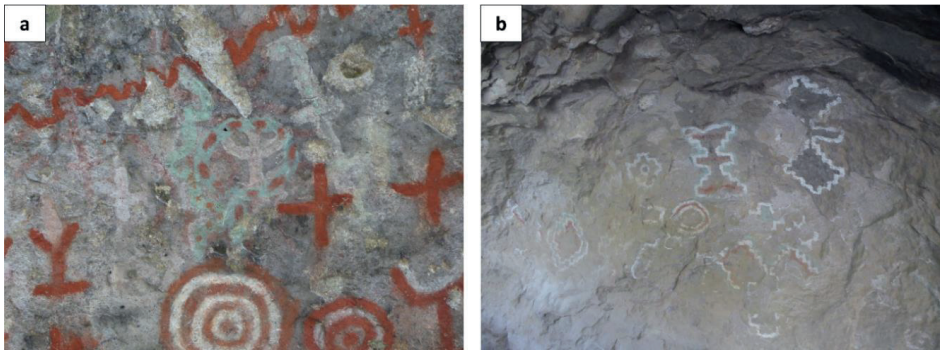

Figure 4.1. *Details from rock art paintings found in (a) the shelter at Alero Las Mellizas (El Neuquén) and (b) the shelter at Cueva Olate (Neuquén).*

During this project, excavations and surveys were conducted at different archaeological sites situated between 300 to 3500 meters away from the northern bank of the Traful Lake and in the middle- and upper-valley of the Traful River. The cultural remains correspond to hunter-gatherer occupations dating from 4000 years BP. The landscape is characterized as an ecotonal environment between the rain forest and the steppe, showing a high diversity and availability of minerals, fauna and plant resources. At Los Cipreses (North of Traful Lake), which has been sampled before, the rock art consists of red and yellow colours with simple geometric shapes [37]. Currently, a high degree of degradation is observed at the aforementioned site. The paintings of the shelter at Alero Las Mellizas are mostly geometric shapes with some figurative motifs comprising animals and humans (Fig. 4.1 (a)) combining red, yellow, orange, white, black and green pigments [38]. On the

south side of the lake, the shelter at Cueva Olate is well preserved and has a special interest as its rock art presents a different painting technique: all the motifs were outlined with a white line and filled in another colour, mostly red, green and black (Fig. 1 (b)). Moreover, the lines are mostly staggered and diamonds, circles and humanoids were designed from the union of two triangles.

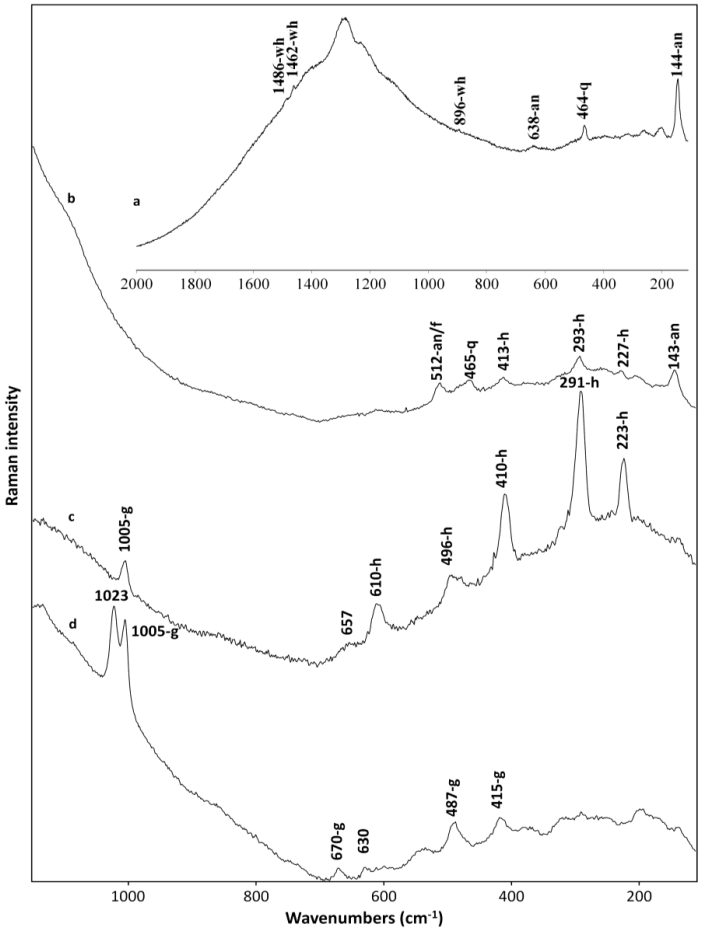

Figure 4.2. *Raman spectra of representative points of: (a) white rock art painting (b) red rock art painting from the shelter at Cueva Olate, Neuquén province and (c) red rock art painting (d) green rock art painting from the shelter at Alero Las Mellizas, Neuquén province. Labels: wh, whewellite; an, anatase; q, α-quartz; f, feldspar; h, haematite; g, gypsum.*

On a white rock art painting of the shelter at Cueva Olate Raman bands attributed to (Fig. 4.2 (a)) whewellite ($CaC_2O_4 \cdot H_2O$) [17, 39-41], α-quartz [42-43] and anatase (TiO_2) [44] are identified, where on a red rock art painting (Fig. 4.2 (b)) the main chromophore corresponds to haematite (α-Fe_2O_3) [39, 45]. Moreover α-quartz [42-43] and anatase [44] are also present in the red pigment mixture. The band at 512 cm^{-1} (Fig. 4.2 (b)) can also be attributed to the strongest Raman band, I_a, of potassium-rich alkali feldspar (K-feldspar) [46]. In addition to the Raman spectra, the general analysis of the site revealed the presence of gypsum ($CaSO_4 \bullet 2H_2O$) mainly on the white rock art paintings but also on some of the red ones. For the green and black rock art paintings no information about the main chromophore is obtained from portable Raman spectroscopy except from mixtures of components that were already identified on other coloured areas. A weak signal of whewellite was also observed on the rock surface of the shelter.

Bands of gypsum [47-48] and haematite [39, 45] (Fig. 4.2 (c)) are identified on a red rock art painting from the shelter at Alero Las Mellizas. It is worth mentioning that some bands with intensity differences of haematite and gypsum are overlapping and the overall Raman signal for these wavenumbers is affected by the presence of both compounds in the mixture. The presence of a band at 657 cm^{-1} corresponds to distortion of the degree of crystallinity of the haematite matrix [45]. Gypsum [47-48] was identified on a green rock art painting (Fig. 4.2 (d)) but also on all the coloured (white, red, yellow, black) figures measured and on the rock surface. Probably, gypsum is the main chromophore of the white paintings although it can also be related to a post-degradation process or accretion formed on top of the rock wall affecting the figures and motifs. More studies should be carried out in order to positively attribute its presence as a pigment. Special attention should be given to the vibrations arising at 1023 and 630 cm^{-1} (Fig. 4.2 (d)) as these can be attributed to more than one sulfate species. The band at ca. 1024 cm^{-1} was observed on spectra collected from red, green and white (in admixture with red) rock art paintings. Calcium oxalates in the form of whewellite and weddellite ($CaC_2O_4 \cdot 2H_2O$) and α-quartz are also present mostly on the coloured figurative motifs of the shelter.

4.3.1.2 Limay river, Nahuel Huapi lake, Gutierrez lake and Mascardi lake areas, Río Negro province

In the area containing the upper basin of the Limay river and large lakes such as Nahuel Huapi, Gutiérrez, and Mascardi, a total of 8 sites with rupestrian paintings were analyzed. This area covers an extensive region in the Province of Rio Negro, with different environments ranging from the pasture steppe, passing through an intermediate or ecotone area, to an area full of native Andean Patagonian forest. In this area the forest environment has very similar characteristics as those from the Traful area described above. In contrast to this, the Limay River valley, located about 60 km east of the Andes mountain range, is already in a typical herbaceous steppe environment composed of "sweet coirón" (*Festuca pallecens*), various *Stipa* species and small isolated bushes. Towards the east the "neneo" (*Molinum spinosum*) becomes more frequent. The annual average precipitations are inferior to those experienced in the forest and ecotone with an average of 600 to 800 mm per year [33].

Archaeological evidence from this area accounts for human occupations of hunter-gatherer groups from ca. 10600 years BP until post-conquest periods [49]. These groups would have had access to a wide variety of resources in a relatively short distance of about 30 km. In this sense, mobility and subsistence patterns have been proven by archaeological evidence to be focused on the supply and use of these resources from different environments [50].

The archaeological site at Alero Maqui (Fig. 4.3 (a)) is located ca. 55 km to the south from the source of the Limay Superior River. This small shelter is located at the base of a high wall formed by tuffs and is surrounded by vegetation which is characteristic for the ecotone steppe forest. The site presents a total of 28 non-figurative motifs of geometric shapes, simple as well as compound. One of its most remarkable features is the presence of different colours that are combined in bichromatic and polychromatic paintings: red, yellow, white and green [51]. The physicochemical studies previously carried out on the different pigments of the motifs showed the presence of haematite, limonite, gypsum and muscovite [52]. Rocks near the site were analyzed and identified

as possible sources of raw materials for the preparation of the paintings, except for the green colour [52].

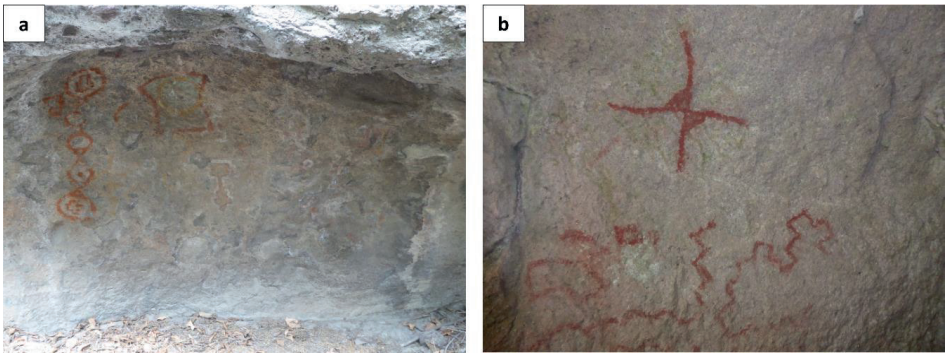

Figure 4.3. *(a) Overview of the rock art painting from the shelter at Alero Maqui (Río Negro) and (b) red detail from the painting found in the shelter at Queutre Inalef (Río Negro).*

Another set of analyzed sites are very close to each other, located in the forest lake environment about 20 km west of the city of San Carlos de Bariloche, and near the El Trébol lagoon, Lake Nahuel Huapi and Lake Moreno. The site at El Trébol is a wide shelter of Toba rock near the lagoon of the same name and records an extensive chronology of human occupation that began some ca. 10600 BP [49]. As for their rock paintings, a total of 28 motifs have been identified mainly in red and yellow, where simple and complex non-figurative designs predominate and some anthropo-zoomorphic designs stand out [53-54]. Preliminary chemical analyses of the rock pigments and pigments from the stratigraphy of the site confirmed the presence of akaganeite in both contexts for the red and albite and gypsum for the yellow motifs [55-56]. Finally, the analysis of the support rock tend to support that the pigments used for the paintings may have been obtained from the same shelter [55]. The sites at Campanario I and II, are located about 1000 m from the previous site and in this case also their paintings are in red and present geometric designs similar to those observed in other sites of the area [57]. In the Lake Moreno, ca. 2.5 km from Nahuel Huapi Lake, the site that we have called Lago Moreno East is located on the east coast and also has rock

paintings of similar characteristics made in red and also with figurative designs similar to those of the site at El Trébol [53].

The third set of sites is located further south in the middle of the Patagonian Andean forest and near the Gutiérrez, Mascardi and Guillelmo Lakes. The site at Queutre Inalef (Fig. 4.3 (b)), located 1 km from Lake Gutierrez, is a large isolated rock block of granite origin which registers a total of 60 motifs made in shades of red with simple as well as complex geometric designs [58]. On the other hand, the site that we call Lake Guillelmo (near the lake of the same name) also presents similar characteristics in the designs which are all painted with red colour, although it also presents other types of motifs, mainly quadruple zoomorphs [58]. Finally, the site at Los Rápidos is very close to Lake Mascardi and to the springs of the Upper Manso River, in the middle of the forest. It is a small cave with paintings which are also red and with mainly geometric motifs.

In situ Raman analysis carried out on the shelter at Alero Maqui revealed severe degradation to all the coloured features found on its rock wall. Gypsum [47-48] was identified on the crust found on top of the rock (Fig. 4.4 (a)) and on a macroscopically free crust area of the rock surface as well as on red (Fig. 4.4 (b)), yellow, green and white rock art paintings. Gypsum is the main component found on the white motifs, although the spectra might contain also contributions from the degradation crust. The calcite ($CaCO_3$) signal [59-60] was more evident on the red (Fig. 4.4 (b)), yellow, green pigments and weaker in the white areas. Weddellite was also observed in the case of a white painting. Fluorescence caused by the encrustrations in the shelter at Alero Maqui completely blocked or overwhelmed the Raman signal in such a way that the identification of the main chromophores was impossible. Only, calcite was identified on the red motifs of Guillelmo Lake while on the rock surface albite ($NaAlSi_3O_8$) [46, 61] (Fig. 4.4 (c)) is present. Haematite [39, 45] along with α-quartz [42-43] (Fig. 4.4 (d)) and calcite [59-60] (Fig. 4.4 (e)), were observed on a red rock painting from the shelter at Los Rapidos and the white crust from the shelter at Lago Moreno East, respectively. For the latter, haematite and carotenoids can be found on the red figures as well as weak signals of albite in the rock surface. Calcite and gypsum were commonly identified on different coloured areas of the shelter at El Trébol with gypsum found on a crust on

the rock. The red pigment used is haematite [39, 45] (Fig. 4.4 (f)). Furthermore, anatase [44] and α-quartz [42-43] are present on both the rock surface and pigmented areas (Fig. 4.4 (g)-(h)).

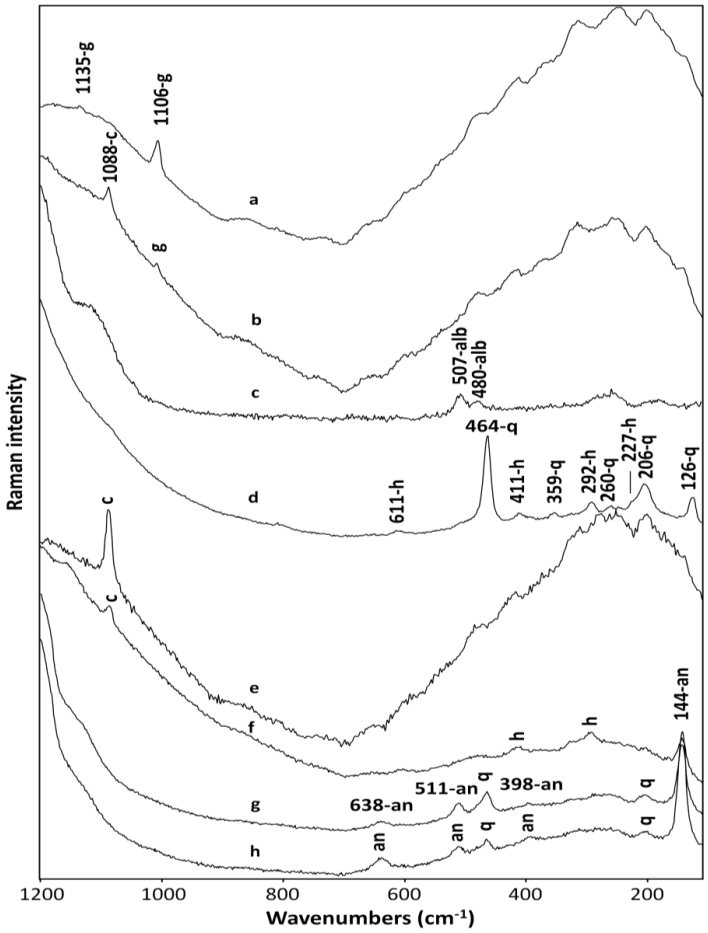

Figure 4.4. *Raman spectra of representative points of: (a) crust on top of the rock surface and (b) red rock art painting from the shelter at Alero Maqui; (c) rock support from the shelter at Guillelmo Lake; (d) red rock art painting from the shelter at Los Rápidos; (e) white crust found on the rock surface from the shelter at Lago Moreno East; (f)-(h) red rock art painting, rock support and yellow rock art painting, respectively, from the shelter at El Trébol, all located in the Río Negro province. Labels: g, gypsum; c-calcite; alb-albite; q, α-quartz; h, haematite; an, anatase.*

The main red chromophore found in the shelters at Queutre Inalef, Cerro Campanario and Cerro Campanario 2 is haematite. Some other components that were identified are α-quartz and calcite for the first shelter and α-quartz only for the other two. α-quartz is the main phase found on the rock surface.

4.3.1.3 Lower Manso River area, Río Negro province

The lower Manso area is located in a glacially modified landscape ranging between 1700 and 550 metres above sea level (at the bottom of the Manso River valley). Climatic and phytogeographic characteristics are similar to those found at the Traful, Nahuel Huapi Lake, Gutierrez Lake and Mascardi Lake areas described above. On slopes and riverbanks, mixed forests of deciduous *Nothofagus* with grassland patches predominate. The climate is moderately continental cold with high annual temperature variance. Precipitation is scarce in summer (700 mm) but in fall-winter it can reach 2000 mm/m^2 at the western part of the valley, in the Andes range.

21 rock art sites are known at the lower Manso and Foyel river valleys. The oldest human occupation was dated at 8200 years BP in a site where only few bone and stone tools were found. At this time the forest inhabitants were hunter-gatherers and their staple diet was an autochthonous deer ("huemul") and other smaller forest species. At ca. 1600 years BP the archaeological record increased and from 1200 years BP onwards rock art sites are recorded.

Two archaeological sites are discussed in the current study, Campamento Argentino and Paredón Lanfré. The first one is a small rock shelter that is 6 metres high and 2.5 metres wide. Human occupation corresponds to hunter-gatherer groups, dated at 570 and 230 years BP. Rock art is very scarce: only two red semi-circles have been identified [62]. Paredón Lanfré (Fig. 4. 5 (a)-(b)) is a rocky wall and shelter where hunter-gatherer occupations are dated between 1500 to 500 BP.

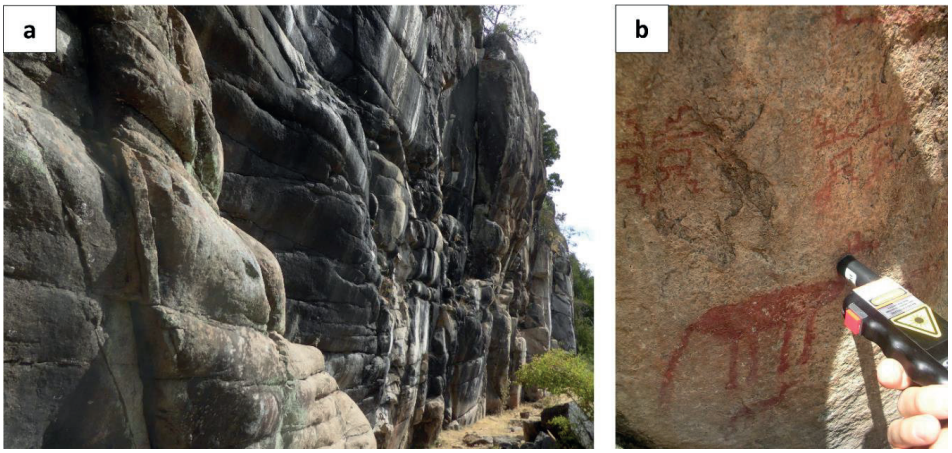

Figure 4.5. *(a) A complete view of the multipanel wall of the shelter at Paredón Lanfré, (Río Negro) and (b) measurment of a horse (Motif 28) in one of its panels. Initially the figure was a guanaco but when the local population started riding horses, the tail and hooves were added in order to resemble a horse.*

The numerous paintings are arranged along a 42 metres multipanel wall (Fig. 4.5 (a)). Most motifs are geometric: rectilinear, stepped, crenellated, curvilinear lines, zig zags etc. are combined in different ways, shaping crosses, suns, hourglasses, concentric circles, framed motifs, etc. There are also some figurative zoomorphic motifs representing two "guanacos" (*Lama guanicoe*) recycled as horses by adding tails and hooves (Fig. 4.5 (b)), along with anthropomorphic figures. Red colour predominates in all the tonalities. Yellow and green were also used to a lesser extent [63]. Paintings of both sites were made on granite rock, therefore, microexfoliation is facilitated. Also, the high humidity encourages the growth of lichens and fungi which are most likely responsible for the formation of calcium oxalate on paints [26].

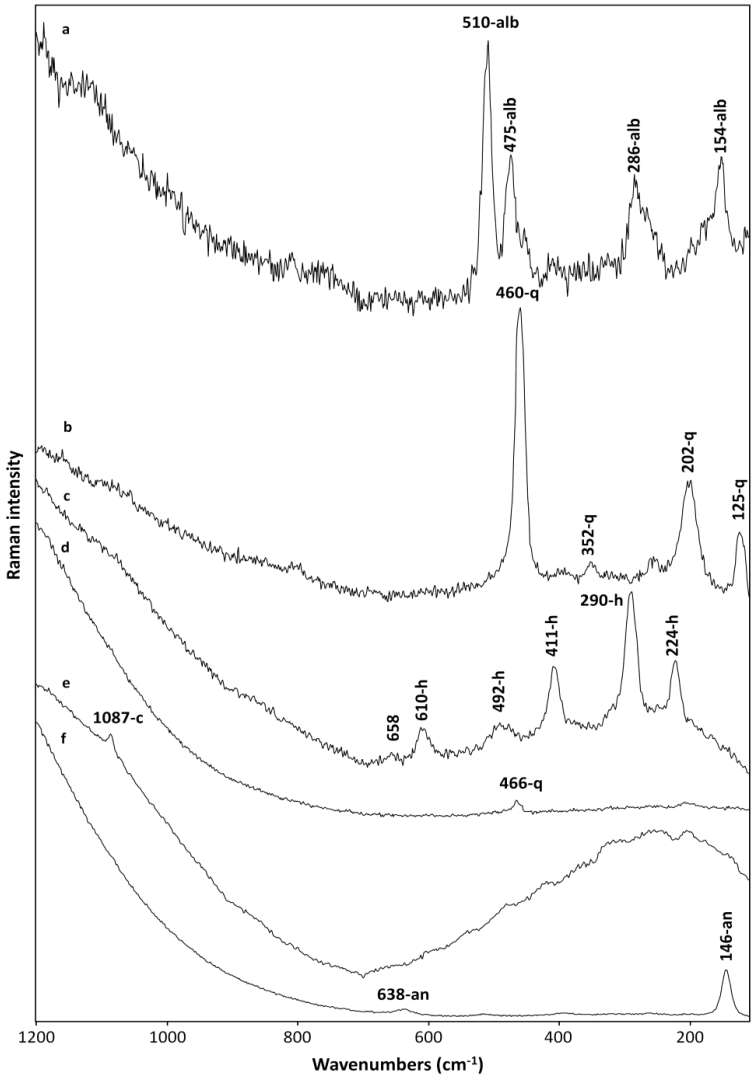

Figure 4.6. *Raman spectra of representative points of: (a)-(b) rock support near paintings Nr. 58 and Nr. 51, respectively and (c) Nr. 28a, red guanaco painting from the shelter at Paredón Lanfré; (d) Nr. 4, red rock art painting and (e)-(f) natural white crust and rock surface with a patina, respectively, near painting Nr.1 from the shelter at Campamento Argentino, all located in the lower Manso River area, Río Negro province. Labels: alb-albite; q, α-quartz; h, haematite; c-calcite; an, anatase.*

In fig. 4.6 spectra collected from rock supports near paintings 58 and 51 (a)-(b) and 28a (red guanaco painting (c), from the shelter at Paredón Lanfré, are presented. Albite [46, 61] and α-quartz [42-43] can be found on the rock surfaces but also inside coloured figures while haematite [39, 45] is the main chromophore of all the red paintings. In the case of the red guanaco painting the band at 658 cm^{-1} corresponds to iron oxide with a low degree of crystallinity [45]. For the yellow and green paintings no coloured components were identified due to fluorescence and the strong Raman signal of the substrate.

The wall of the shelter at Campamento Argentino is severely degraded. Even the main chromophore of the red paintings could not be identified due to superimposed crusts of calcite [59-60] found on the natural white crust of the rock (Fig. 4.6 (e)). In some other cases, only the dominant band of α-quartz [42-43] could be identified in the red areas (Fig. 4.6 (d)). In another area of the wall where a patina/crust was macroscopically observed the presence of anatase [44] was verified from its Raman spectrum (Fig. 4.6 (f)). Moreover, a weak Raman signal of feldspar was also observed on the rock surface.

4.3.1.4 Piedra Parada area, Chubut province

Piedra Parada area is located at the Chubut River Basin, one of the five largest rivers in Patagonia, which has a source in the foothills of the Andes and flows to the Atlantic Ocean. Piedra Parada area is located in its middle course at 400-500 metres above sea level. The river modelled the landscape over volcanic ancient rocks dated between 57 - 45 million years ago [64]. The region is arid (138 mm/m^2 annual precipitation) with the main precipitation occurring in winter (as snow). The predominant vegetation is a shrub steppe. Temperature ranges between ca. 37º C in January to 3º C in July. In the last 100 years overgrazing has provoked desertification. An important climatic characteristic in Patagonia is the strong western winds (Westerlies) occurring especially in summer.

The area was populated by hunter-gatherers from 5000 years ago. There is evidence of this first occupation found in only one rock shelter. From 3000 years BP to 450 BP, changes in settlement patterns and an increase in demography is detected. 36 rock art sites were detected and analysed. A stylistic sequence was elaborated: a) an initial period (prior to 2500 years BP) characterized by simple geometric motifs and stencil hand prints; b) a second period including geometrical engravings and paintings (around 1300 years BP); and c) a final period when the so called “Grecas” style appears (around 500 years BP) [65].

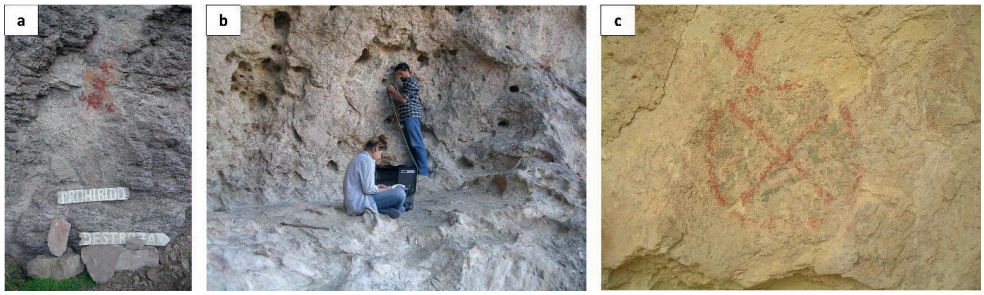

Figure 4.7. *(a) Figure of yellow and red flowers from the shelter at Campo Moncada 1 (Chubut), (b) Raman portable instrument set up placed in the shelter at Piedra Parada 1 (Chubut) and (c) a red and green figure (Nr.10) from the shelter at Angostura Blanca (Chubut).*

Piedra Parada 1, Angostura Blanca, Campo Cerda 1 and Campo Moncada 1 are archaeological sites situated in the Piedra Parada Valley. All of them are rock shelters located in volcanic formations along both margins of the Chubut River. Piedra Parada 1 (Fig. 4.7 (b)) is the only one that shows stencil hand prints in yellow, white and green, and the use of black colour in other geometric motifs. Also, there are dotted lines and straight and curved lines in green, black, red and yellow. All these motifs are characteristics of an earlier period. The other three rock art sites show some of the most frequent motifs of the geometric ”Grecas” style, as irregular lines, crosses, crenellated designs, guards, etc. (Fig. 4.7 (a)-(c)). In the latter period, the motifs are less polychromatic than those found in the Piedra Parada 1 rock art; because the red colour predominates, the other colours such as white, green and yellow are less frequently found [66].

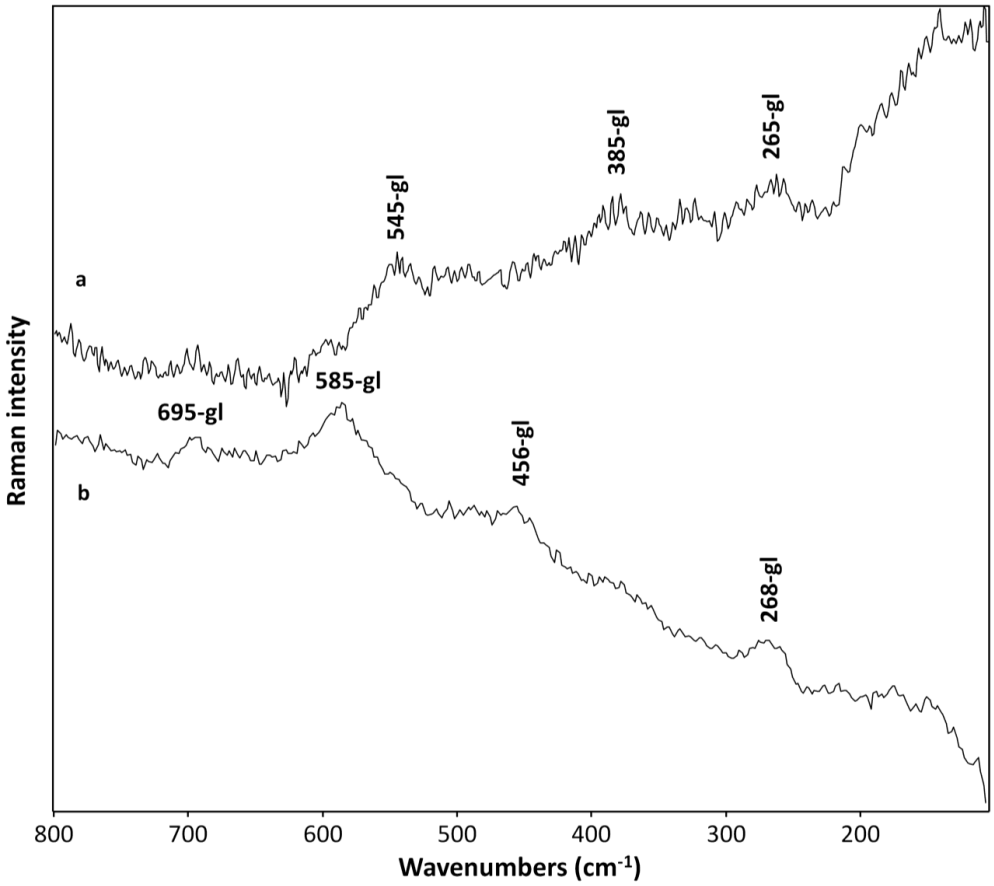

Figure 4.8. *Raman spectra of representative points of Nr. 10 green rock art painting from the shelter at Angostura Blanca, Chubut province measured (a) with the 785 nm laser and (b) with the 532 nm laser, revealing the characteristic bands of glauconite (gl).*

Glauconite [$(K,Na)(Fe^{3+},Al,Mg)_2(Si,Al)_4O_{10}(OH)_2$] (Fig. 4.8) is the only green pigment identified in the case of the Nr. 10 green rock art painting from the shelter at Angostura Blanca (Fig. 4.7 (c)). The spectra, although rather noisy, indicate the presence of a green earth. Furthermore, taking into account the resonance behaviour and the position of the diagnostic bands of glauconite [67], rather than celadonite [$K[(Al,Fe^{3+}),(Fe^{2+},Mg)](AlSi_3,Si_4)O_{10}(OH_2)_2$], is more likely to be present. In general, green earths are not very good Raman scatterers and as a consequence, few *in situ* Raman

spectra of this pigment have been reported. Due to this resonance Raman effect, band shifts are observed when comparing the spectra recorded with red (785 nm) and green (532 nm) laser excitation. In previous studies, made in the Chubut province and in the shelter at Campo Moncada 1, it is clear that green earth was the main component of the green samples [26].

Haematite [39, 45] is the iron oxide found on all the red rock art paintings of the 4 shelters measured in the Piedra Parada Valley with representative spectra presented in fig. 4.9 (a) (i) (m). Microcline ($KAlSi_3O_8$) [46, 61] was identified on the red rock art painting Nr. 11 (Fig. 4.9 (a)) and the rock surface (Fig. 4.9 (b)) of the shelter at Angostura Blanca and also in different panels of the shelter at Piedra Parada Valley 1. Albite was also present in spectra collected from a red rock art painting from the shelter at Angostura Blanca. Gypsum [47-48] is one of the major components found on the paintings and the rock surfaces and rock art paintings of the shelters at Piedra Parada 1, Campo Cerda 1 and Campo Moncada 1 (Fig. 4.9 (c)-(f), (i)-(m). Its presence in the shelter at Angostura Blanca needs further investigation as a weak signal was found in only in two points (in admixture with K-feldspars). On the PP1_10 black rock art painting of panel 6 (Piedra Parada 1) (Fig. 4.9 (d)) anhydrite II/natural anhydrite was also identified [48]. Gypsum is the main white component that was detected in the white negatives of hands of panel 2 (Piedra Parada 1) (Fig. 4.9 (h)). A different composition was observed for the case of Nr. 15, a white negative of a hand in panel 1 (Piedra Parada 1). The phyllosilicate, muscovite [$KAl_2(AlSi_3O1_0)(F,OH)_2$] [39, 42], was positively identified together with α-quartz [42-43] and anatase [44] (although the presence of a feldspar cannot fully be excluded here) (Fig. 4.9 (g)). On the yellow negative of a hand found in panel 2 of the shelter at Piedra Parada 1, microcline was identified (although gypsum might also be present here). Calcium oxalate, in the form of whewhellite [17, 39-41], was also present on a red rock art painting PP1_6 of panel 5 of the shelter at Piedra Parada 1 and in a yellow floral rock art painting Nr. 17 at Campo Moncada 1 (Fig. 4.9 (e) and (j), respectively). In general, weak Raman bands of calcium oxalates were also observed in several cases.

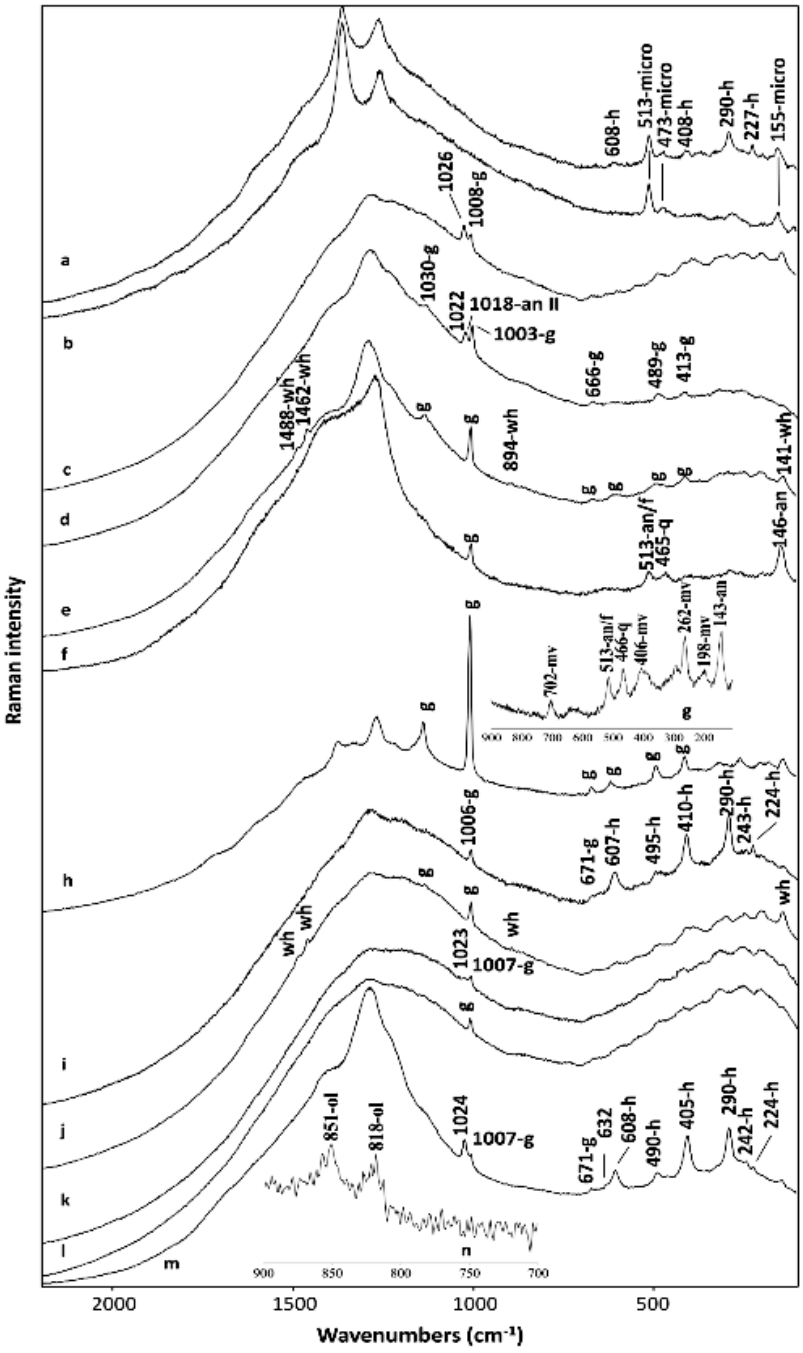
Raman intensity
Wavenumbers (cm⁻¹)
2000
1500
1000
500
a
b
c
d
e
f
g
h
i
j
k
l
m
n
608-h
513-micro
473-micro
408-h
290-h
227-h
155-micro
1026
1008-g
1030-g
1022
1018-an II
1003-g
666-g
489-g
413-g
1488-wh
1462-wh
894-wh
141-wh
513-an/f
465-q
146-an
702-mv
513-an/f
466-q
406-mv
262-mv
198-mv
143-an
1006-g
671-g
607-h
495-h
410-h
290-h
243-h
224-h
wh
1023
1007-g
851-ol
818-ol
1024
671-g
632
608-h
490-h
405-h
290-h
242-h
224-h

Figure 4.9 (previous page). *Raman spectra of representative points of: (a) Nr. 11 red rock art painting and (b) rock support, from the shelter at Angostura Blanca; (c) PP1_9 yellow rock art painting of panel 5, (d) PP1_10 black rock art painting of panel 6, (e) PP1_6 red rock art painting of panel 5, (f) rock support of panel 2, (g) Nr. 15 white negative of a hand of panel 1, (h) PP1_2 white negative of a hand of panel 2, from the shelter at Piedra Parada 1; (i) Nr. 20 dark red rock art painting, (j) Nr. 17 yellow floral rock art painting, (k) CM1_3 green rock art painting, (l) rock surface, from the shelter at Campo Moncada 1; (m) M2 red rock art painting and (n) rock surface from the shelter at Campo Cerda 1, all located in Chubut province. Labels: h, haematite; micro, microcline; g, gypsum; an II, anhydrite II, wh, whewellite; an, anatase; f, feldspar; q, α-quartz; mv, muscovite; ol, olivine.*

The orthosilicate olivine $[(Fe,Mg)_2SiO_4]$, [68] is one of the components measured on the rock surface of the shelter at Campo Cerda 1 (Fig. 4.9 (n)). α-quartz was also identified in a white pigmented area of the shelter at Campo Cerda 1. As in the case of the shelter at Alero Las Mellizas, a band at ca. 1024 cm^{-1} is observed (Fig. 4.9 (c)-(d), (k), (m)) in combination with a band at 632 cm^{-1} (Fig. 4.9 (m)) in 3 different shelters and different colouring hues at Piedra Parada Valley, namely: blue green, green, yellow, black in the shelter at Piedra Parada Valley 1; green in the shelter at Campo Moncada 1; red in the shelter at Campo Cerda 1. On a white crust of panel 2 in the shelter at Piedra Parada 1 thenardite (Na_2SO_4) was also detected.

4.3.2 Comparison between the different archaeological sites

An overview of the shelters that were analysed along with the major components that were positively identified by *in situ* Raman spectroscopy is presented in Table 4.1. In the next paragraphs, we will focus on the analysis of chromophores, possible encrustations and the source of the oxalates.

In general, the main chromophore of the red rock paintings is haematite. In some cases the shelters were so severely altered and degraded that no signal from haematite could be retrieved.

Bands at 657 cm^{-1} (red rock art painting from the shelter at Alero Las Mellizas), 658 cm^{-1} (Nr. 28a red guanaco from the shelter at Paredón Lanfré) and 660 cm^{-1} (red rock art painting from the shelter at Queutre Inalef) can be attributed to an IR-active longitudinal (LO) mode which is symmetry forbidden in Raman spectra and is appearing due to a low degree of crystallinity associated with disordered structures [43, 45, 69-71]. However, in the literature it is also mentioned that this band can be assigned to traces of magnetite contributing to the haematite spectra, although this should be considered with caution [72-73]. Consequently, bands arising at these wavenumbers have been often debated [74-75] especially when magnetite and haematite are present together.

For most of the yellow, green and black paintings no information from the main colourant could be obtained. Gypsum and calcite are commonly found from severe degradation on most of the shelters measured. Gypsum was more frequently identified at the provinces of Neuquén and Chubut, while at the Río Negro and lower Rio Manso (Río Negro) sites calcite was present. Both degradation factors are found on pigmented as well as nonpigmented areas (crusts). As gypsum was also identified on the white rock art paintings, the results should be interpreted with caution as it is also a major decay product of the rock surfaces. The gypsum accretion should have an impact on the actual Raman signal of the white chromophore, even if gypsum may seem to be a logical selection for a white pigment. An archaeological question arises if gypsum was introduced in other coloured mixtures as an extender or to change the hue. This question cannot be answered with portable Raman instrumentation alone. The only observation was that in the cases where no gypsum was identified in the crusts, it was also not present in the coloured mixtures. It should also be remarked that it is believed that in some cases, local hunter-gatherer groups are thought to paint on already degraded surfaces, that acted as a homogeneous lighter background (compared to the darker rock wall) to create their synthesis on.

The most important challenge relating to the correct attribution of the Raman bands to the exact compound comes from the vibrations arising at ca. 1022-1026 cm^{-1} found on the shelters at Alero Las Mellizas (along with a band at 630 cm^{-1}), in Neuquén province, and the shelters at Piedra

Parada 1, Campo Moncada 1, Campo Cerda 1 (along with a band at 632 cm^{-1}) located in the Piedra Parada valley. On reviewing the analytical literature, there is an interesting outcome: Prinsloo et al. [69] in their studies in 2008 found a red pigment on a shard from San rock art (in South Africa) referring to a band at 1022 cm^{-1} assigned as anhydrite. Tournié et al. [17], in 2011, measuring a yellow figure in San rock art in a site in South Africa assigned also a band at 1025 cm^{-1} as anhydrite ($CaSO_4$). Moreover, as pointed out in the literature for bassanite ($CaSO_4 \cdot 0.5(H_2O)$) and natural anhydrite, chemical transitions occur between gypsum and these two compounds and more research should be conducted to verify the source of this vibration.

Iriarte et al. [76], in 2013, when studying violet microparticles of a bluish-black pigment from the shelter at Abrigo Remacha (Spain), assigned the bands at 1170, 1027 (vvs), 676, 634 and 493 cm^{-1} to paracoquimbite [$(Fe_2(SO4)_3 \cdot 9H_2O)$]. Calcite, α-quartz, carbon black and Ca-oxalates were also found in the mixture. Pitarch et al. [41], in 2014, when analysing blackish pictographs from the Los Chaparros shelter (Spain) attributed a band at 1027 cm^{-1} to gypsum (along with other bands of calcium sulfate dihydrate). Hernanz et al. [61], in 2016, measuring hand stencils from the Yabrai Mountain (China) assigned a band at ca. 1028 cm^{-1}, found on rock surfaces and red paintings, as anhydrite III and gypsum and anhydrite II were also present.

The band at ca. 1022-1026 cm^{-1} along with those at 630 and 632 cm^{-1} found in the Patagonian shelters can be attributed to one of the five phases of the $CaSO_4/H_2O$ system [48]. This is likely to be soluble anhydrite, γ-$CaSO_4$/anhydrite III, a compound with metastable thermodynamic stability. The Raman spectra of this compound consists of bands at 1167, 1025, 673, 630, 490 and 420 cm^{-1} [48]. Moreover, it is suggested that microconditions in the sample under the influence of the laser power can promote the transformation of gypsum to anhydrite III [48]. Hence, when performing *in situ* Raman measurements in the Patagonian field the laser power density was kept low in order to minimise any transformation of the matrices.

On the other hand, a band at ca. 1025 cm^{-1} can also be attributed to the iron (III) sulfate nonahydrate, (para)coquimbite. Maguregui et al. [77] in 2010 described a three-step decay

pathway in the formation of iron sulfate as a result of atmospheric SO_2 attack on the walls of a Pompeiian house. For such a reaction, haematite and calcite should be involved, in the presence of sulphur pollutants, resulting in the formation of (para)coquimbite and gypsum.

For the Patagonian shelters, the aforementioned Raman band was observed in spectra collected from the red, green and white (in admixture with red) rock art paintings from the shelter at Alero Las Mellizas, Neuquén province, and it also appeared in the Piedra Parada Valley on blue green, green, yellow and black rock art paintings of the shelter in Piedra Parada 1, on a green rock art painting of the shelter in Campo Moncada 1 and on a red rock art painting of the shelter in Campo Cerda 1. In the red haematitic figures and motifs no calcite was detected due to a chemical reaction, hence the interpretation as (para)coquimbite cannot be promoted. In general, no calcite was detected in the shelters where this band appears. However, while investigating the wall of the shelter at Campo Cerda 1, we realised that calcite was present in a hidden way in a natural dual layered encrustation on top of the rock. Calcite and gypsum were both measured within a superficial layer situated on top of the rock surface whereas measuring the surface of this layer only gypsum was found (Table 4.1). If we assume that the band at 1025 cm^{-1} is assigned to (para)coquimbite then other hypotheses should be addressed. If it is a matter of origin and natural sources in Patagonia, Argentina, then it is necessary to examine possible sources of these deposits, related to the distance from the archaeological sites. In general, (para)coquimbite can also be formed by the flow of acid water on ferric sulfates [76] or by the evaporation of acid sulfate pools/brines as a consequence of the oxidation of pyrites [78].

It is noteworthy that some spectra from the Patagonian rock art sites contained a band at ca. 1022-1026 cm^{-1} which seems to correspond to that of anhydrite III as identified by Hernanz in the red paintings of Yabrai Mountain (China) [61]. In our observations, this band was always identified in zones where gypsum was observed.

Though not completely conclusive, Raman spectroscopy has identified the vibrational mode of the sulfate anion (ca. 1022-1026 cm^{-1}) but the attribution to the correct compound needs further

research. The identification via Raman spectroscopy is more difficult than initially thought, especially for mixtures of gypsum and iron oxides, and moreover some anhydrite III and (para)coquimbite bands are overlapping in wavenumber. The sulfate vibration band was found to occur in various colours on the pigmented areas of shelters that are located in different provinces. More research should be conducted, including other analytical techniques that reveal the molecular/crystalline structures, in order to verify the presence of anhydrite III and to further investigate possible formation pathways in the case of (para)coquimbite in the Patagonian environments.

Calcium oxalates, in the form of whewellite and weddellite, were identified by their strong Raman bands in the shelters of the Neuquén province, in the shelter at Alero Maqui, in Río Negro province, and the shelters at Piedra Parada 1 and Campo Moncada 1, in Chubut province. Oxalic acid production arising from the metabolic acivity of fungi, lichens or bacteria attacks the Ca-based substratum and provides a biological explanation of the deposition of the hydrated calcium oxalates [8, 39, 70] detected in the spectra. Furthermore, another chemical explanation for the formation of such compounds is the decay of organic media and/or binders, containing oxalic acid or calcium oxalates [8, 70]. Lofrumento et al. [70], in 2012, when investigating Ethiopian prehistoric rock painting, suggested the use of a binder as the source of Ca-oxalate by comparing using a Raman mapping image the concentration on a haematite area on a red fragment. The Ca-oxalate appeared inhomogeneous and scattered. Another hypothesis for the presence of oxalates inside rock art mixtures [70, 79] was suggested as the intentional incorporation of Ca-oxalate by the artist for the composition of the pigment itself.

Although lichen activity was very obvious in some shelters, Ca-oxalates were found mainly on pigmented zones rather than on top of crusts and rock surfaces. When oxalates were found on the crusts, the Raman signal was very weak. Although, this tends to support the thesis of intentional admixture of oxalates and/or the decay of organic binders, this should not be considered as fully conclusive. In the sites measured, lichen activity could be macroscopically confirmed and due to limited measurement time, the number of measurement points was somehow restricted

compared with the extent of the sites of the rock art panels investigated. A more elaborate study, including the analysis of cross-sections of the poaintings and rock surfaces, could further clarify this issue.

From the two calcium oxalates the dehydrated form, weddelite, is the most unstable and in ambient conditions transforms into whewellite [81, 82]. Its presence on the Patagonian rock art paintings can be justified via other possible pathways that block or slow the transformation. In 2000, McAlister et al. [83] when instigating the presence of weddellite in street sediments from Niterói, Brazil stated that under certain temperature and humidity, heavy metals and other low and high molecular weight compounds are responsible of its stability.

The presence of Ca-oxalates, on crust surfaces can be of importance for dating the pictorial layers. As described by Hernanz et al. [59], in 2014, if thick Ca-oxalate crusts are present on top of the motif/figure an "*ante quem"* date, by radiocarbon dating, can be established for the rock art paintings. Moreover, if the pictorial layer is encapsulated or sandwiched in between Ca-oxalate layers, an "*ante quem* and *post quem* radiocarbon dating" of the event can be determined [39-40, 59, 84]. For the case of the shelters in Patagonia, we propose perpendicular sampling of the pigmented and nonpigmented areas of the sites be carried out where Ca-oxalates are found to evaluate the homogeneity of the crusts for potential radiocarbon analysis.

Table 4.1. An overview of archaeological sites that were analysed along with the major components that were positively identified by *in situ* Raman spectroscopy.

Province	Shelter	Colours measured	# motifs measured	Haematite [39, 45]	Gypsum [47-48]	Calcite [59-60]	α-quartz [42-43]	Ca-oxalates [17, 39-41]	Titanium dioxide [44]	Anhydrite III [48]	Feldspars [42, 46, 61]	Other
Neuquén	Cueva Olate	Red, white, green, black	3	x	x		x	X	x		x?	
	Alero Las Mellizas	Red, white, green, black, yellow	12	x	x		x	X		x		
Río Negro	Alero Maqui	Red, white, green, yellow	3		x	x		X				
	Queutre Inalef	Red	5	x		x	x					
	Guillelmo Lake	Red	1			x					X	
	Los Rápidos	Red	1	x			x					
	Cerro Campanario	Red	1	x			x					
	Cerro Campanario 2	Red	1	x			x					
	Lago Moreno East	Red	2	x		x					X	Carotenoids
	El Trébol	Red, yellow	5	x	x	x	x		x			
Río Negro (Rio Manso)	Paredón Lanfré	Red, yellow, green	10	x			x				X	
	Campamento Argentino	Red	3			x	x		x		x?	
Chubut	Angostura Blanca	Red, green	4	x	x?						X	Green earth
	Piedra Parada 1	Red, white, green, black	14	x	x		x	X	x	x	X	Anhydrite II, muscovite, thenardite
	Campo Moncada 1	Red, white, green, yellow	8	x	x			x		x		
	Campo Cerda 1	Red, white, orange, yellow	11	x	x	(x)*	x			x		Olivine

4.4 Conclusions

In situ Raman spectroscopy was performed on 16 open air shelters, in Argentinian part of Patagonia, in the provinces of Neuquén and Río Negro and Chubut. The purpose of the current study is the identification of pigments and substrata. The main focus of the research was the positive identification of alteration products and encrustations found on the rock art paintings of the shelters and on the surface of the rock walls. Apart from the pigment identification, compounds attributed to decay mechanisms and weathering of the shelters were discussed. Although in some cases the results were not completely conclusive, portable Raman spectroscopy shed light on the main chromophores used and characterized the substrata and alteration products in a non-invasive way. The results demonstrated in this chapter do not reflect the whole variety of components that can be found on the walls of the shelters due to restrictions of the portable instrumentation and due to the limited measurement time available.

The information obtained from on-site measurements is of great importance regarding the preservation state of these important works of art. The results retrieved from this analysis allow the selection of rock art paintings that, because of their degradation state and/or archaeological interest, should be further investigated, by extraction of samples for laboratory analysis, possibly with multiple analytical techniques. The documentation and physicochemical characterization of the Patagonian rock art paintings is a priority in this exercise as these art works made by hunter-gatherer populations are doomed to be consumed by nature and/or human activity.

When studying rock art, the importance of performing non-invasive analysis is highlighted throughout this chapter. In the cases that the artefact cannot be sampled, portable Raman spectrometers can be employed, yielding clear results on the characterization of the different components. As Raman spectroscopy uses visible light, information is obtained from the surface layer (where the visible radiation penetrates and, thus, deeper layers cannot be reached. The latter was an important problem when analysing Patagonian rock art. In many cases micrometre-thick,

superimposed, non-transparent, degradation crusts were observed on the pigmented surfaces, blocking the Raman signal and significantly influencing the quality of the spectra obtained.

From the literature we expect that microspatially offset Raman spectroscopy (micro-SORS) could be used to probe zones covered by a non-transparent (turbid) layer. In the following chapter, we will develop a novel approach, namely fibre-optics micro-spatially offset Raman spectroscopy (fibre-optics micro-SORS). The applicability of the technique is tested by using a prototype fibre-optics micro-SORS sensor prototype on different layered compounds with a range of thicknesses.

4.5 References

[1] M. W. Rowe, in *Handbook of Rock Art Research* (Ed: D. S. Whitley), AltaMira Press, Walnut Creek, California, **2001**, pp. 190–220.

[2] G. D. Smith, R. J. H. Clark, J. Archaeol. Sci. **2004**, *31*, 1137.

[3] R. C. Bednarik, D. Fiore, M. Basile, G. Kumar, T. Huisheng, *Palaeoart and Materiality: The Scientific Study of Rock Art*, Archaeopress Publishing Ltd, Oxford, **2016**.

[4] E. Chalmin, M. Menu, C. Vigneaud, *Meas. Sci. Technol.* **2003**, *14*, 1590.

[5] D. Fiore, M. Maier, S. D. Parera, L. Orquera, E. Piana, *J. Archaeol. Sci.* **2008***, 35*, 3047.

[6] M. Tascon, N. Mastrangelo, L. Gheco, M. Gastaldi, M. Quesada, F. Marte, *Microchem. J.* **2016***, 129,* 297.

[7] A. Bonneau, D. G. Pearce, A. M. Pollard, *J. Archaeol. Sci.* **2012***, 39,* 87.

[8] M. Mas, A. García, G. Beatriz, S. Mónica, P. Enrique, P-P. Perez, *J. Archaeol. Sci.* **2013**, *40*, 4635.

[9] E. Tomasini, M. Basile, M. Maier, N. Ratto, in *Palaeoart and Materiality, The Scientific Study of Rock Art*, (Eds: R. G. Bednarik, D. Fiore, M. Basile, G. Kumar, T. Huisheng) Archaeopress Publishing Ltd, Oxford, **2016**, pp. 1-13.

[10] C. Bellelli, F. X. Pereyra, M. Carballido, in *Geomaterials in Cultural Heritage,* (Eds. M. Maggetti, B. Messiga), The Geological Society, London, **2006**, pp. 241-255.

[11] A. Rousaki, C. Vázquez, V. Aldazábal , C. Bellelli, M. Carballido Calatayud, A. Hajduk, E. Vargas, O. Palacios, P. Vandenabeele, L. Moens, *J. Raman Spectrosc.* **2017***, 48,* 1459.

[12] A. Rousaki, C. Bellelli, M. Carballido Calatayud, V. Aldazábal,G. Custo, L. Moens, P. Vandenabeele, C. Vázquez, *J. Raman Spectrosc.* **2015**, 1016.

[13] H. G. M. Edwards, E. M. Newton, J. Russ, *J. Mol. Struct.* **2000**, *550–551,* 245.

[14] H. Gomes, P. Rosina, H. Parviz, T. Solomon, C. Vaccaro, *J. Archaeol. Sci.* **2013***, 40*, 4073.

[15] F. Ospitali, D. C. Smith, M. Lorblanchet, *J. Raman, Spectrosc.* **2006***, 37,* 1063.

[16] P. Vandenabeele, L Moens, *J. Raman Spectrosc.* **2012***, 43*, 1545.

[17] A. Tournié, L. C. Prinsloo, C. Paris, P. Colomban, B. Smith, *J. Raman Spectrosc.* **2011***, 42,* 399.

[18] S. Lahlil, M. Lebon, L. Beck, H. Rousselière, C. Vignaud, I. Reiche, M. Menu, P. Paillet, F. Plassard, *J. Raman Spectrosc.* **2012**, *43*, 1637.

[19] M. T. Boschin, A. M. Seldes, M. Maier, R. M. Casamiquela, R. E. Ledesma, G. E. Abad, *Zephyrvs* **2002**, *55*, 183.

[20] C. Vázquez, M. Maier, S. D. Parera, H. Yacobaccio, P. Solá, *Anal. Bioanal. Chem.* **2008***, 391,* 1381.

[21] N. M. Carden, R. V. Blanco, D. G. Poiré, C. I. Genazzini, L. A. Magnin, P. J. García, *Relac. Soc. Argent. Antropol.* **2014***, 39*, 483-508.

[22] A. M. Iñiguez, C. J. Gradin, *Relaciones* **1978***, 11*, 121.

[23] C.E. Barbosa, G. E Rial, *Primeras Jornadas de Arte y Arqueología* **1985**, *1*, 21.

[24] C. E. Barbosa, C. J. Gradin, *Relaciones* **1988***, 17*, 143.

[25] J. B. Belardi, A. Súnico, D.N. Puebla, *An. Inst. Patagon.* **2000**, *28*, 291.

[26] I. N. M. Wainwright, K. Helwig, M. M. Podestá, C. Bellelli, in *Arte en las Rocas, Sociedad Argentina de Antropología*, (Eds: M. M. Podestá, M. de Hoyos), AINA, Buenos Aires, **2000**, pp. 203-206.

[27] I. N. M. Wainwright, K. Helwig, D. S. Rolandi, C. A. Aschero, C. Gradin, M. M. Podestá, M. Onetto, C. Bellelli, *Identification of pigments from rock painting sites in Argentina*, 10°

Journées d'etudes de la Section Francaise de l'Institut International de Conservation, Paris, **2002**, pp. 15-24.

[28] J. Huntley, *Aust. Archaeol.* **2012**, *75*, 78.

[29] F. Gázquez, F. Rull, A. Sanz-Arranz, J. Medina, J. M. Calaforra, C. de las Heras, J. A. Lasheras, *Spectrochim. Acta A* **2017***, 172*, 48.

[30] J. Huntley, C. F. Galamban, in *Palaeoart and Materiality, The Scientific Study of Rock Art,* (Eds: R. G. Bednarik, D. Fiore, M. Basile, G. Kumar, T. Huisheng), Archaeopress Publishing Ltd, Oxford, **2016**, pp. 41-57.

[31] D. Lauwers, A. G. Hutado, V. Tanevska, L. Moens, D. Bersani, P. Vandenabeele, *Spectrochim. Acta A* **2014***, 118*, 294.

[32] D. Hutsebaut, P. Vandenabeele, L. Moens, *Analyst* **2005**, *130*, 1204.

[33] V. Barros, V.H. Cordón, C.L. Moyano, R.J. Mendez, J.C. Forquera, O. Pizzio, *Cartas de precipitación de la zona oeste de las provincias de Río Negro y Neuquén*, Primera Contribución, Centro Nacional Patagónico (CONICET)-Universidad Nacional del Comahue Dirección de Bosques y Praderas (Río Negro) - Secretaría de Estado del Copade (Neuquén) - Departamento Provincial de Aguas (Río Negro), **1983**.

[34] A. L. Cabrera, in *Enciclopedia Argentina de Agricultura y Jardinería*, (Ed: W. F. Kugler), Segunda Ed., Tomo II, Fascículo 1, ACME S.A.C.I., Buenos Aires, **1976**, pp. 1-85.

[35] V. Markgraf, *Quat. Sci. Rev.* **1989***, 8*, 1.

[36] M. J. Silveira, L. López, V. Aldazábal, *Anuario de Arqueología* **2013***, 5*, 85.

[37] M. J. Silveira, in *Arqueología Solo Patagonia, Ponencias de las Segundas Jornadas de Arqueología de la Patagonia*, (Ed: J. G. Otero), CENPAT-CONICET, Puerto Madryn, Argentina, **1996**, pp. 107–118.

[38] M. J. Silveira, L. G. López, V. Aldazabal, *Comechingonia Virtual.* **2014**, *8*, 157.

[39] A. Hernanz, J. M. Gavira-Vallejo, J. F. Ruiz-López, H. G. M. Edwards, J*. Raman Spectrosc.* **2008**, *39*, 972.

[40] A. Hernanz, J. F. Ruiz-López, J. M. Gavira-Vallejo, S. Martin, E. Gavrilenko, *J. Raman Spectrosc.* **2010**, *41*, 1394.

[41] A. Pitarch, J. F. Ruiz, S. Fdez-Ortiz de Vallejuelo, A. Hernanz, M. Maguregui, J. M. Madariaga, *Anal. Methods* **2014***, 6*, 6641.

[42] M. L. Frezzotti, F. Tecce, A. Casagli, *J. Geochemical Explor.* **2012***, 112*, 1.

[43] A. Hernanz, J. M. Gavira-Vallejo, J. F. Ruiz-López, S. Martin, A. Maroto-Valiente, R. de Balbín-Behrmann, M. Menéndez, J. J. Alcolea-González, *J. Raman Spectrosc.* **2012***, 43*, 1644.

[44] U. Balachandran, N.G. Eror, *J. Solid State Chem.* **1982***, 42*, 276.

[45] D. L. A. de Faria, F. N. Lopes, *Vib. Spectrosc.* **2007***, 45*, 117.

[46] J. J. Freeman, A.Wang, K. E. Kuebler, B. L. Jolliff, L. A. Haskin, *Can. Mineral.* **2008**, *46*, 1477.

[47] J. Jehlička, P. Vítek, H. G. M. Edwards, M. D. Hargreaves, T. Čapoun, *J. Raman Spectrosc.* **2009***, 40,* 1082.

[48] N. Prieto-Taboada, O. Gomez-Laserna, I. Martizez-Arkarazo, M. Angeles Olazabal, J. M. Madariaga, *Anal. Chem* **2014***, 86*, 10131.

[49] A. Hajduk, A. M. Albornoz, M. Lezcano, P. Arias, in *Southbound Late Pleistocene Peopling of Latin America, Special Edition of Current Research in the Pleistocene*, (Eds: L. Miotti, M. Salemme, N. Flegenheimer, T. Goebel), Center for the Study of the First Americans, Department of Anthropology, Texas A&M University, **2012**, pp.117-120.

[50] M. J. Lezcano, A. Hajduk, A. M. Albornoz, in *Zooarqueología a Principios del Siglo XXI: Aportes Teóricos, Metodológicos y Casos de Estudio*, (Eds: M. De Nigris, P. M. Fernández, M. Giardina, A. F. Gil, M. A. Gutiérrez, A. Izeta, G. Neme, H. D. Yacobaccio), Ediciones del Espinillo, Argentina, **2010**, pp. 243-257.

[51] A. Hajduk, A. M. Albornoz, in *Soplando en el Viento*, (Eds: J. B. Belardi, P M. Fernández, R. A. Goñi, A. G. Guráieb, M. De Nigris), Neuquén-Buenos Aires, Universidad Nacional del Comahue-inapl, **1999**, pp. 371-391.

[52] C. Vázquez, A. M Albornoz, A. Hajduk, S. A. Maury, S. Boeykens, in *Patrimonio Cultural: la Gestión, el Arte, la Arqueología y las Ciencias exactas aplicadas*, (Eds: O. Palacios, C. Vazquez), Editorial Talleres Gráficos Centro Atómico Constituyentes, CONEA, Argentina, **2010**, pp. 225-232.

[53] A. M. Albornoz, A. Hajduk, *Ladran sancho' jinetes y caballos en el arte rupestre en la arqueología y la etnohistoria del área del Nahuel Huapi*, XII Jornadas Interescuelas,

Departamento de Historia, Eje Nº 12, Representaciones Intelectuales y Culturales, Mesa 12.5, Las Manifestaciones del Simbolismo Prehistórico: Arte Rupestre y Arte Mobiliar, Publicado en CD con referato, Puede Consultarse el Trabajo, http://es.scribd.com/doc/129690568/Albornoz-y-Hajduk-2009-Caballos-en-El-Arte-Rupestre, 2009 (accessed 1 November 1017).

[54] A. M. Albornoz, in, Arqueología Solo Patagonia: Ponencias de las Segundas Jornadas de Arqueología de la Patagonia, (Ed: J. G. Otero), CENPAT Madryn, **1996**, p.p 123-130.

[55] A. M. Albornoz, A. Hajduk, S. P. Fornels, A. Caneiro, C. Vázquez, in *Patrimonio Cultural: la Gestión, el Arte, la Arqueología y las Ciencias Exactas Aplicadas,* (Eds: C. Vázquez, O. Palacios), Editorial Talleres Gráficos Centro Atómico Constituyentes, CNEA, **2008**, pp. 175-194.

[56] C. Vázquez, A. Caneiro, S. P. Fornells, A. M. Albornoz, A. Hajduk, *Avances en Técnicas de Rayos X* **2008***, 14*, 271.

[57] A. M. Albornoz, E. Cúneo, in *En Arte en Las Rocas. Arte Rupestre, Menhires y Piedras de Colores en Argentina*, (Eds: M. M. Podestá, M. de Hoyos), Sociedad Argentina de Antropología y Asociación Amigos del Instituto Nacional de Antropología, Buenos Aires, **2000**, pp. 163-174.

[58] A. M. Albornoz, L. C. Teira Mayolín, *Documentación de yacimientos con arte rupestre del entorno del Parque Nacional Nahuel Huapi, III Jornadas de Historia de la Patagonia*, Universidad Nacional del Comahue, CONICET, Agencia Nacional de Promoción Científica y Tecnológica, Editadas en CD con referato: Historia de la Patagonia: 3eras Jornadas; 1era Ed Neuquén, Universidad Nacional del Comahue, **2008**.

[59] A. Hernanz, J. F. Ruiz-López, J. M. Madariaga, E. Gavrilenko, M. Maguregui, S. Fdez-Ortiz de Vallejuelo, Ir. Martínez-Arkarazo, R. Alloza-Izquierdo, V. Baldellou-Martínez, R. Viñas-Vallverdu, A. Rubio i Mora, A. Pitarch, A. Giakoumaki, *J. Raman Spectrosc.* **2014***, 45*, 1236.

[60] H. G.M. Edwards, S. E. Jorge Villar, J. Jehlick, Tasnim Munshi, *Spectrochim. Acta A* **2005,** *61*, 2273.

[61] A. Hernanz, J. Chang, M. Iriarte, J. M. Gavira-Vallejo, R. de Balbín-Behrmann, P. Bueno-Ramírez, A. Maroto-Valiente, *Appl. Phys. A* **2016***, 122*, 699.

[62] P.M. Fernández, M. Carballido Calatayud, C. Bellelli, M.G. Fernández, *Libro de Resúmenes, X Jornadas de Arqueología de la Patagonia*, IDEAUS-CONICET, Puerto Madryn, **2017**, pp. 91.

[63] M. M. Podestá, A. M. Albornoz, *El arte rupestre del sitio Paredón Lanfré dentro del contexto arqueológico del valle del río Manso inferior (Pcia. de Río Negro), Tras las huellas de la materialidad,* XVI Congreso Nacional de Arqueología Argentina, Tomo III, Editorial Universidad Nacional de Jujuy, **2007**, pp. 429-434.

[64] E. Aragón, M. Mazzoni, *Rev. Asoc. Geol. Argent.* **1997***, 52*, 243.

[65] M. Onetto, in *El Arte Rupestre en la Arqueología Contemporánea*, (Eds: M. M. Podestá, M. I. Hernández Llosas, S. F. Renard de Coquet), Buenos Aires, **1991**, pp. 123-131.

[66] C. Aschero, C. Bellelli, A. Fisher, L. Nacuzzi, M. Onetto, C. Pérez de Micou, *Arqueología del Chubut, El Valle de Piedra Parada, Dirección Provincial de Cultura del Chubut*, Rawson, **1983**.

[67] F. Ospitali, D. Bersani, G. Di Lonardo, P. P. Lottici, *J. Raman Spectrosc.* **2008***, 39*, 1066.

[68] H. G. M Edwards, D. W. Farwell, M. MGrady, D. D Wynn-Williams, I. P. Wright, *Planet. Space Sci.* **1999**, *47*, 353-362.

[69] L. Prinsloo, W. Barnard, I. Meiklejohn, K. Hall, *J. Raman Spectrosc.* **2008**, *39*, 646.

[70] C. Lofrumento, M. Ricci, L. Bachechi, D. De Feo, E. M. Castellucci, *J. Raman Spectrosc.* **2012***, 43*, 809.

[71] D. Bersani, P. P. Lottici, A. Montenero, *J. Raman Spectr.* **1999***, 30*, 355.

[72] D. A. de Faria, S.V. Silva, M. T. de Oliveira, *J. Raman Spectr.* **1997***, 28*, 873.

[73] F. Bordignon, P. Postorino, P. Dore, G. F. Guidi, G. Trojsi, V. Bellelli, *Archaeometry* **2007***, 49*, 87.

[74] I. Aliatis, D. Bersani, E. Campani, A. Casoli, P. P. Lottici, S. Mantovan, I.-G. Marino, *J. Raman Spectrosc.* **2010***, 41,* 1537.

[75] D. Bersani, P. P. Lottici, *J. Raman Spectr.* **2016***, 47*, 499.

[76] M. Iriarte, A. Hernanz, J. F. Ruiz-López, Santiago Martín, *J. Raman Spectrosc.* **2013***, 44*, 1557.

[77] M. Maguregui, U. Knuutinen, K. Castro, J. M. Madariaga, *J. Raman Spectr.* **2010***, 41*, 1400.

[78] D. C. Fernández-Remolara, R. V. Morris, J. E. Gruener, R. Amilsa, A. H. Knoll, *Earth Planet. Sci. Lett.* **2005***, 240*, 149.

[79] R. E. M. Hedges, C. B. Ramsey, G. J. Van Klinken, P. B. Pettitt, C.Nielsen-Marsh, A. Etchegoyen, J. O. Fernandez Niello, M. T. Boschin, A. M. Llamazares, *Radiocarbon* **1998***, 40*, 35.

[81] C. Conti, L. Brambilla, C. Colombo, D. Dellasega, G. D. Gatta, M. Realini, G. Zerbi, *Phys. Chem. Chem. Phys.* **2010**, *12*, 14560.

[82] C. Conti, M. Casati, C. Colombo, M. Realini, L. Brambilla, G. Zerbi, *Spectrochim. Acta A* **2014**, *128*, 413.

[83] J. J. McAlister, B. J. Smith, J. A. Baptista Neto, *Environ. Geochem. Hlth.* **2000**, *22*, 195.

[84] J. F. Ruiz, A. Hernanz, R-A. Armitage, M. W. Rowe, R. Viñas, J. M. Gavira-Vallejo, A. Rubio, *J. Archaeol. Sci.* **2012***, 39*, 2655.

γ

Chapter 5 Development of a *fibre-optics* microspatially offset Raman spectroscopy sensor for probing layered materials

Based on the paper: P. Vandenabeele, C. Conti, A. Rousaki, L. Moens, M. Realini, P. Matousek, *Anal. Chem.* **2017,** *89,* 9218.

Rock art paintings are one of the most ancient forms of human expression. Studies on rock art are revealing the local "palette" of the native population and, if possible, the technology used. In section β (chapter 3 and 4), the importance of using a molecular non-invasive, non-destructive technique is underlined. Raman spectroscopy has proven to be a guide technique in a decision making protocol. Based on these results, it can be decided whether further analysis, involving sampling, is required.

When investigating rock art paintings, a practical difficulty is the focusing on the pigment layers that are often covered by a non-transparent crust. Although the use of different lasers in the near IR region can contribute to larger penetration depths (compared to visible lasers), non-invasive stratigraphic analyisis by using commercial Raman spectrometers is not available.

Therefore, a new approach is proposed for the non-invasive stratigraphic analysis of layers that are covered by a turbid (non-transparent) micrometre-thick layer, namely microspatially offset Raman spectroscopy (micro-SORS). The technique as such, together with its different modes, has been introduced in chapter 2 (2.2.1). In chapter 5, the proof-of-concept of fibre-optics microspatially offset Raman spectroscopy (fibre-optics micro-SORS) is illustrated as an alternalive approach to microspatially offset Raman spectroscopy (micro-SORS) as found in literature.

In general, microspatially offset Raman spectroscopy (micro-SORS) has been proposed as a valuable approach to sample molecular information from stratified structures. When large magnifications and thus short working distances are involved the approach is not straightforward, as spatial constraints exist to position the laser beam and the objective lens (in the case of external beam delivery) or, with internal beam delivery, the maximum achievable spatial offset is restricted. To overcome these limitations, a prototype of a new micro-SORS sensor, which uses bare glass fibres to transfer the laser radiation to the sample, and to collect the Raman signal from a spatially offset zone to the Raman spectrometer, is demonstrated. The concept also renders itself amenable to remote delivery and to the miniaturisation of a probe head which could be beneficial for special applications, e.g. where access to sample areas is restricted.

5.1 Introduction

Raman spectroscopy is a well appreciated spectroscopic technique, that has been shown to be a helpful diagnostic tool in many research fields, including among others geology [1, 2], microbiology [3, 4], medicine [5, 6], cultural heritage research [7, 8], forensics [9, 10] and polymer sciences [11, 12]. The technique has, indeed, many favourable characteristics, such as its non-destructive nature, the possibility for *in situ* analysis [13, 14] and the relatively easy interpretation of the spectra by comparing the spectra against a reference database. Molecular spectra of inorganic as well as of organic materials can be identified and when using a microscope system a small spectral footprint (down to ca. 1 µm) can be achieved.

Raman spectroscopy is often combined with complementary techniques, such as X-ray fluorescence [15, 16]: thus, the molecular information can be combined with the elemental composition. However, when interpreting the results from multiple techniques, one should be aware of the different spatial resolution of the analytical methods: different lateral as well as axial resolution should be taken into account when interpreting the results. For example, X-rays can

penetrate relatively deeply into many materials, and if layered structures are present, it is often not straightforward to distinguish between the different layers by using standard laboratory spectrometers. On the contrary, Raman spectroscopy is often limited to the top layers if they are not transparent to the laser radiation. However, a possible approach to obtain molecular information from deeper layers, which may be covered by a turbid layer, is spatially offset Raman spectroscopy (SORS) [17]. This approach was successfully demonstrated for the analysis of liquids in sealed non-transparent containers [18], bone tissue inside a body [19], or cancer research [20].

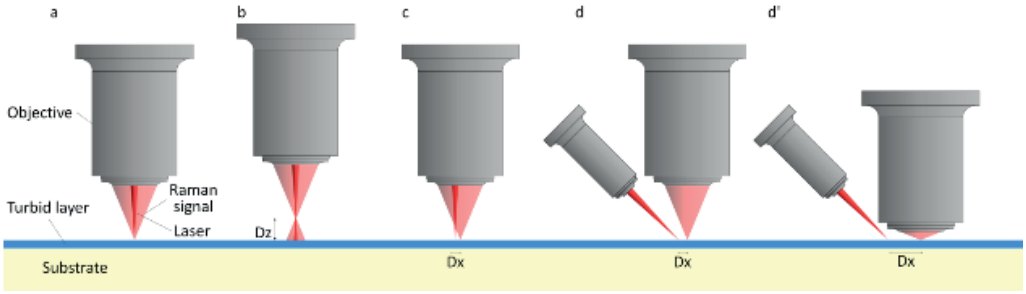

Figure 5.1. *Comparison of (a) the conventional Raman microscopy configuration (in reflection mode) with (b) defocusing micro-SORS, (c) internal beam delivery full micro-SORS and (d) external beam delivery full micro-SORS. When the working distance is small, there are practical constraints to perform external beam delivery full micro-SORS experiments (d').*

In contrast to standard Raman spectroscopy in reflective (backscattering) mode (Fig. 5.1 (a)), in SORS experiments a certain zone of the turbid object is irradiated with a laser, while the Raman signal is collected from a slightly different, spatially offset, zone. As a consequence, the information that is obtained originates from deeper layers lying under a turbid (opaque) top layer. If small details or thin layers have to be studied, one has to rely on a micro-SORS variant [21, 22]. Two main micro-SORS approaches have been proposed: (i) *defocusing* micro-SORS and (ii) full micro-SORS. During *defocusing* micro-SORS the object is positioned out of focus over a defocusing distance Δz, to enlarge the areas of laser illumination and Raman signal collection (Fig. 5.1 (b)). The advantage of this approach is its relatively simple setup: the spectra can be recorded by using a commercial Raman microscope. By using *full* micro-SORS (Fig. 5.1 (c), (d)), the laser is focused in a spot at a

distance Δx from the Raman collection zone on the sample surface. The latter approach has more practical constraints but it yields a better contrast improvement between the different layers and larger penetration depths. Recently, a prototype of a full micro-SORS probehead has been developed and tested for art analysis [23].

Despite the relatively straightforward nature of a full micro-SORS arrangement , there are some practical issues with its implementation, especially when high magnification microscope objectives with a short working distance are required. As a consequence, even when using long working distance objectives, with an externally delivered laser beam, there is insufficient space to focus the laser beam on a spot near to the Raman collection spot (Fig. 5.1 (d')). Alternatively, with an internally delivered laser beam (Fig. 5.1 (c)), the spatial offset can also be set by the internal imaging optics of the microscope although the range of spatial offsets deployable in this arrangement is restricted by the field of view of the microscope. [24, 25].

To overcome these problems, a novel approach is proposed, which allows one to use a small laser spot and sample the Raman signal for relatively short distances Δx from the laser and with no restrictions on the setting of larger offsets. In this setup, optical fibres are brought in contact with the surface to transfer the laser radiation to the object and to collect the Raman signal from the object and transfer it to the spectrometer.

5.2 Experimental section

Micro-SORS Raman spectra were obtained by using a *Kaiser System Hololab 5000R* modular Raman microspectrometer (f/1.8) (KOSI, Ecully, France). The instrument is equipped with a Leica microscope, with a range of objectives and an automated XY stage.

A 785 nm diode laser (Toptica Photonics AG, Martinsried/Munich, Germany) was used as the excitation source and the excitation fibre (length = 0.5 m) was directly coupled to the laser (no laser line filter was used before coupling). The laser power on the sample was reduced to

ca. 20 mW. The collection fibre (length = 0.5 m) was coupled directly to the filter and spectrometer part of the Kaiser system, omitting the standard Raman microscope and probehead. Detection was performed by a back-illuminated deep depletion Pelletier cooled (−70 °C) CCD detector (Andor, Belfast, Northern Ireland). The Raman signal was collected in the spectral range between 150 cm^{-1} and 3500 cm^{-1}. The spectral acquisition time was varied, depending on the sample, and the spectral resolution was ca. 4 cm^{-1}. For comparison, reference spectra were recorded on the same spectrometer but by using the Leica microscope attachment equipped with a 10x objective. Spectra were recorded using the Kaiser Hologram's software, exported in the Galactic SPC format and processed in Matlab. All reported Raman spectra are not baseline corrected, nor corrected for blank or dark signal.

For these experiments, two 62.5 µm diameter multimode low-OH glassfibres (Fisfiber, Oriskany, NY, USA) were used and stripped to the bare fibre. These fibres were implemented in the experimental set up described below and connected with an FC/PC coupler to the laser and spectrometer, respectively. In the experimental set up the fibres were mounted on a Thorlabs micrometer stage system to allow for controlled movement of the fibres with respect to each other.

For these proof-of-concept experiments, a series of samples was selected which allowed the evaluation of the performance of *fibre-optics* micro-SORS with different compounds and thickness of the top layer (ranging from 50 µm to 500 µm with the latter being at the border between micro-SORS and SORS). A mock-up sample was created, consisting of well-known, homogeneous materials that are reasonable Raman scatterers. For this reason, a sandwich was made consisting of Teflon (thickness: 600 µm, on top of an aluminium plate) covered with one or two layers of non-transparent white PVC tape (thickness: ca. 150 µm). Both materials are commonly available in local hardware stores: Teflon is commonly used for plumbing, PVC tape as an electrical insulator. As a second example , an inorganic powder in a polystyrene container (thickness: ca. 500 µm) was selected. For this experiment, K_2CO_3 (99.99% pure, Sigma Aldrich) was used. The third sample consisted of an organic liquid (nitrobenzene, p.a., Sigma Aldrich) in a polystyrene vessel (thickness:

ca. 500 µm). The fourth sample has been selected in order to demonstrate the system's capability to detect layers with a thickness less than 100 µm: this was an artificially prepared two-layer system simulating the application of a spray paint coating on stone, namely, a PY151 acrylic spray colourant was spread with a thickness of 50 µm on a marble (calcite) stone (1 cm thick) ($CaCO_3$).

5.3 Results and discussion

5.3.1 Assembly of the *fibre-optics* micro-SORS sensor

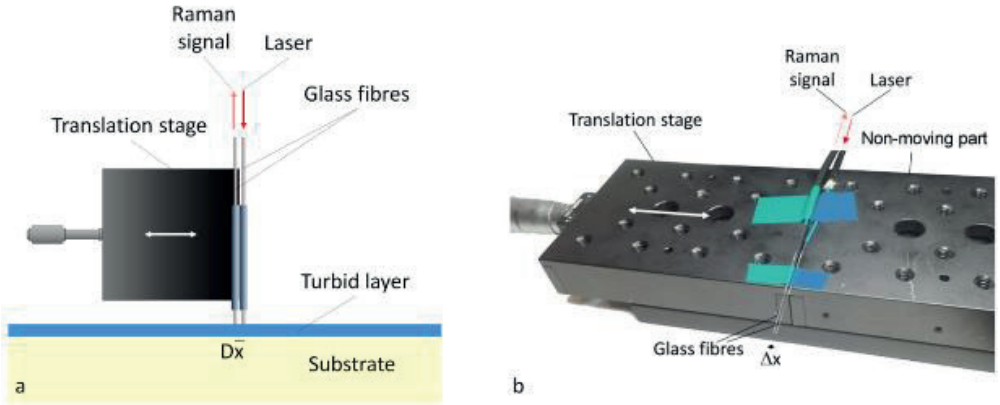

Figure 5.2. *Experimental set-up of the fibre-optics micro-SORS sensor. (a): Schematic drawing of the different components; (b): picture of the sensor prototype that was used in these experiments.*

For these experiments a prototype of a *fibre-optics* micro-SORS sensor was designed (Fig. 5.2). To facilitate this, a 62.5 µm (low OH) multimode glass fibre was cut in two with Kevlar scissors. The plastic sleeve (mantle as well as filling fibres) was removed over a distance of ca. 5 cm using a stripping tool. As it was desirable to mount the fibres adjacent and parallel next to each other, and as it was necessary to control the distance between the fibres accurately and to maintain their positioning stability, one of the fibres was taped to the edge of a translation stage whilst the other one was mounted on the edge of a small breadboard that was level with the translation stage.

Thus, both fibres were assured parallel with an adjustable inter-fibre distance. As bare fibres are very brittle and flexible, the fibres were mounted on two needles with a diameter of 0.6 mm. Thus, it was possible to make the set-up more resistant to mechanical damage and minimise the bending of the fibres. The fibers were connected to the laser and the spectrometer using a TC/PC connector. The excitation fibre was stationary and the collection fibre was mounted on the travelling stage.

5.3.2 Testing and application of the *fibre-optics* micro-SORS sensor

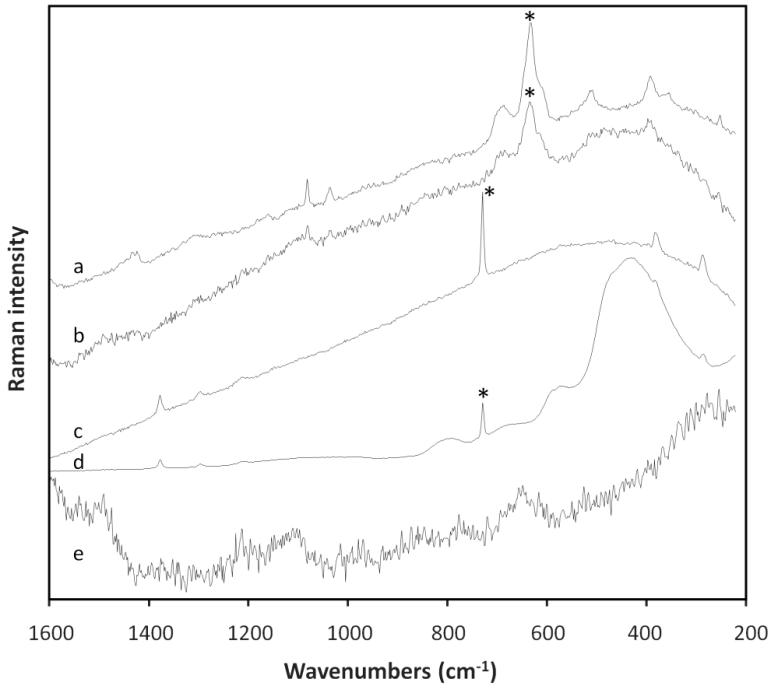

Figure 5.3. *(a) Micro-Raman spectrum of PVC tape; (b) fibre-optics Raman spectrum of PVC tape; (c) micro-Raman spectrum of Teflon; (d) fibre-optics Raman spectrum of Teflon; (e) blank fibre-optics Raman spectrum. The Raman bands that are used for the fibre-optics micro-SORS experiments are marked.*

The prototype of the *fibre-optics* micro-SORS sensor was tested by analysing a mock-up sample that consisted of white PVC tape mounted on a Teflon carrier. Reference Raman spectra of the pure (bulk) materials were recorded by Raman microscopy (Fig. 5.3 (a), (c)) and compared with the fibre-optics Raman spectra of these bulk materials (Δx = 0 µm, Fig. 5.3 (b), (d)). It can be seen that the Raman spectra that were obtained with the prototype were highly similar; although in the case of Teflon, a different background signal is observed due to the strong Raman signature of silica fibre acquired through the use of unfiltered fibres. The spectral background as recorded with the fibre-optics Raman sensor was influenced by the contact of both fibres with the sample as it varied with the amount of scattered radiation received from the input fibre into the collection fibre. In this context, a spectrum was recorded (Fig. 5.3 (e)) with the fibre-optics sensor without the presence of a sample. As such, a blank spectrum was recorded, revealing that the fibre signal can indeed interfere with the Raman signal obtained. In the current measurements, the influence of the fibre was found to be minimal but in future applications, in order to improve the sensitivity of the approach a different strategy is required to reduce this effect either by introducing micro-filters at the tips of the fibre and/or by mathematically correcting for these signals.

On the basis of the spectra observed for the bulk samples (Fig. 5.3 (a)-(d)), the two most prominent Raman bands were selected for the micro-SORS experiments. It was confirmed that these bands did not overlap significantly with the Raman features generated from the other sources. The Raman bands positioned at 635 and 730 cm^{-1} were selected for PVC and Teflon, respectively. Two test samples were constructed, where a single and a double layer of PVC tape was placed on top of the Teflon. The *fibre-optics* micro-SORS sensor was used to record spectra with increasing distances between the excitation and collection fibre, ranging from 0 to 1500 µm, in step sizes of 125 µm. The ratio of the net Raman intensities (employing a linear baseline correction of the Raman band base to reduce the influence of fluorescence emission) of the Teflon/PVC Raman bands was plotted as a function of the distance between the fibres (Fig. 5.4). The resulting graphs clearly show that the measured intensity ratio increases with increasing distance. Thus, it was demonstrated that the *fibre-optics* micro-SORS sensor is able to achieve in a straightforward way information from a deeper layer, which is present under a turbid top layer.

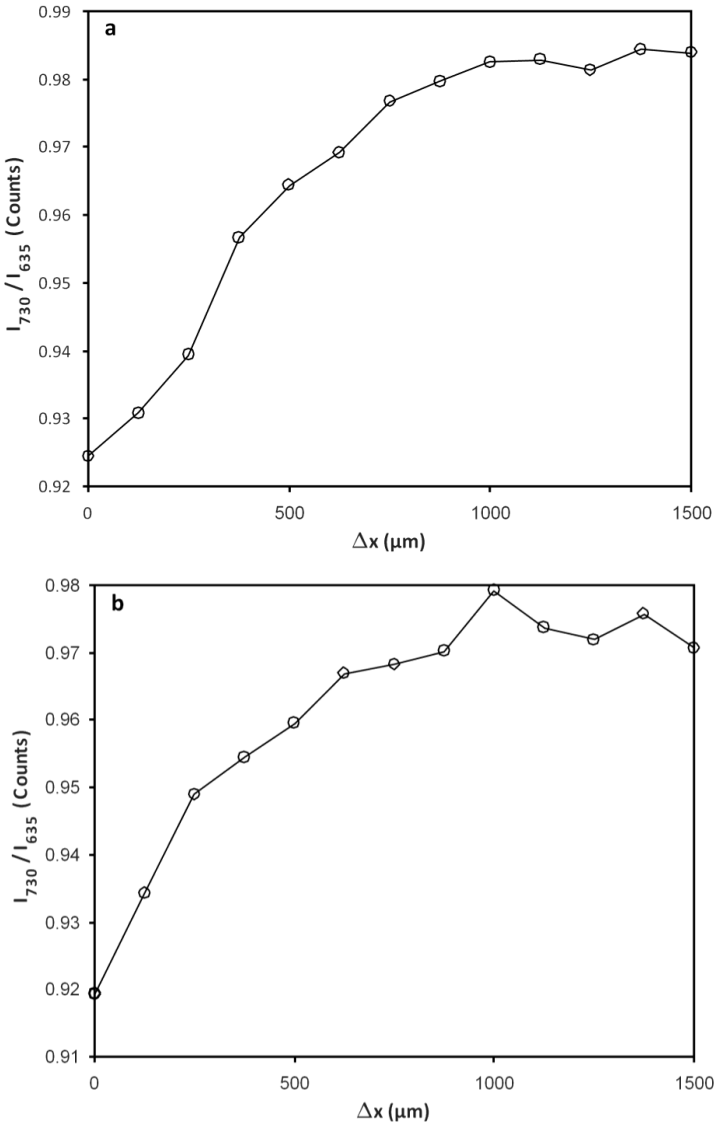

Figure 5.4. *Fibre-optics micro-SORS experiment: PVC tape on Teflon. Net Raman band intensity ratios are plotted as a function of the distance between the fibres. (a) Double layer of tape (300 µm); (b) single layer of tape (150 µm). For each datapoint, a fibre-optics Raman spectrum was recorded with 3 accumulations of 60 s (785 nm, ca. 20 mW at the sample).*

Moreover, when comparing both graphs, the influence of the thickness of the top layer can clearly be seen, as with thin layers the signal tends to increase at shorter interfibre distances. This could open possibilities to estimate non-destructively the layer thicknesses of turbid layers. The evolution of the intensity ratio as a function of the interfibre distance for the thin layer seems to be more subject to statistical variation.

The experiment was repeated in the case of the double layer of PVC on Teflon (Fig. 5.5) by changing the variant of glass fibre diameter (thinner fibres) and laser power. Also, in this case the resulting graph clearly demonstrated that the intensity ratio increased with the interfibre distance. Comparing the graphs illustrated in fig. 5.4 (a) and fig. 5.5, the experiment can be reproduced even by changing the laser and collecting spot size and thus, the interfibre distance, with some variations influenced by the fibre diameter. Moreover, the variation observed is also influenced by positioning difficulties when conducting the experiment.

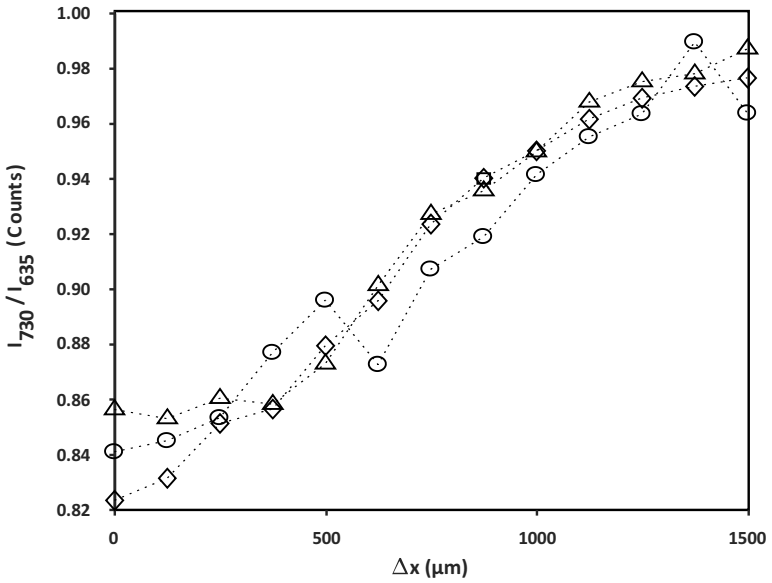

Figure 5.5. *Fibre-optics micro-SORS experiment: Double layer of PVC tape on Teflon. Net Raman band intensity ratios are plotted as a function of the distance between the fibres.*

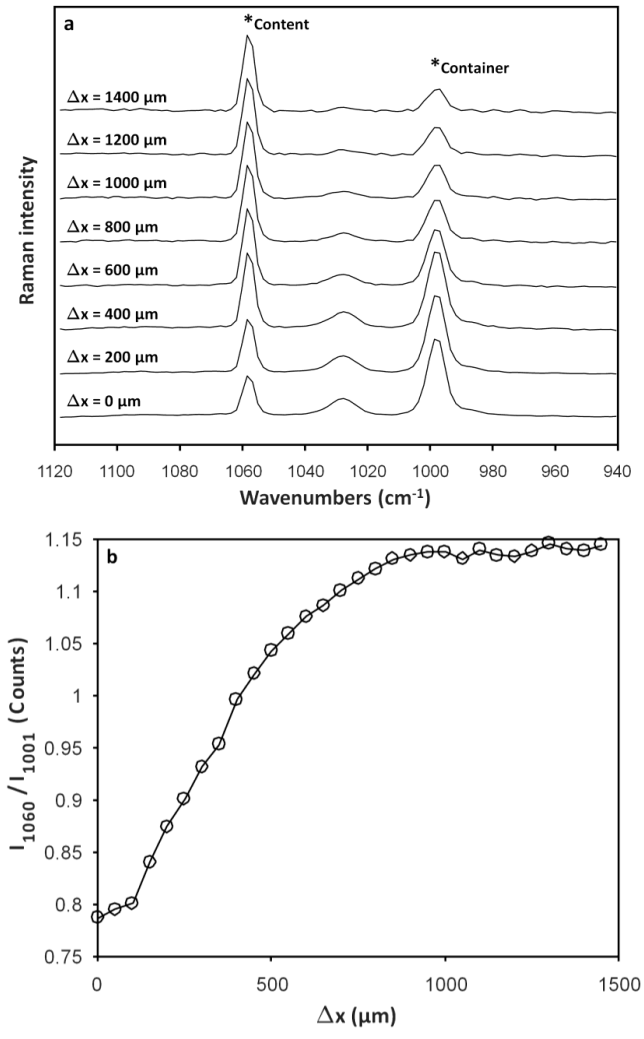

Figure 5.6. *Fibre-optics micro-SORS experiment: K_2CO_3 powder in a PS container. (a) Details of selected Raman spectra recorded with specific distances between the fibre (scaled to maximum intensity in this range and offset for clear visibility). The Raman bands that are used for the fibre-optics micro-SORS experiments are marked. (b) Plot of the Raman band intensity ratios as a function of the distance between the fibres; For each datapoint a fibre-optics Raman spectrum was recorded with 3 accumulations of 20 s (785 nm, ca. 20 mW at the sample).*

In the second sample, K_2CO_3 was analysed through the walls of a polystyrene (PS) container. This setup was selected as an example of the analysis of an inorganic salt in powder form. Spectra were recorded with increasing distances between the excitation and collection fibres (Δx=200 μm steps were used) (Fig. 5.6). From these experiments, it can be observed that, with increasing interfibre distance (Δx), the intensity of the aromatic ring breathing band of PS located at 1001 cm^{-1} decreases, while the intensity of the $\nu(CO_3^{2-})$ stretching vibration (1060 cm^{-1}) of the salt shows a smaller decrease. This is even more evident when plotting the band intensity ratios (Fig. 5.6 (b)), showing that also in this case it is possible to obtain information from the deeper layers and overcoming the turbid barrier of 500 μm.

The feasibility of using *fibre-optics* micro-SORS was also tested in the analysis of a liquid inside a turbid container. In this case, nitrobenzene ($C_6H_5NO_2$) was measured through a polystyrene (PS) beaker. In fig. 5.7 (a) the recorded spectra are presented. As the spectra are scaled towards the PS Raman band (1001 cm^{-1}), it is clearly seen how the intensity of the 1342 cm^{-1} band of nitrobenzene increases with increasing distance between the fibres of the sensor. Thus, it is demonstrated that with increasing interfibre distance increasingly deeper areas are probed. When plotting the Raman band intensity ratios (Fig. 5.7 (b)) a similar effect is observed. A 3-step pattern is observed when plotting the intensity ratios, which might suggest some chemical interaction between the nitrobenzene and the polystyrene container. Nitrobenzene corrodes quickly the polystyrene container and as a consequence the experiment should be quickly conducted.

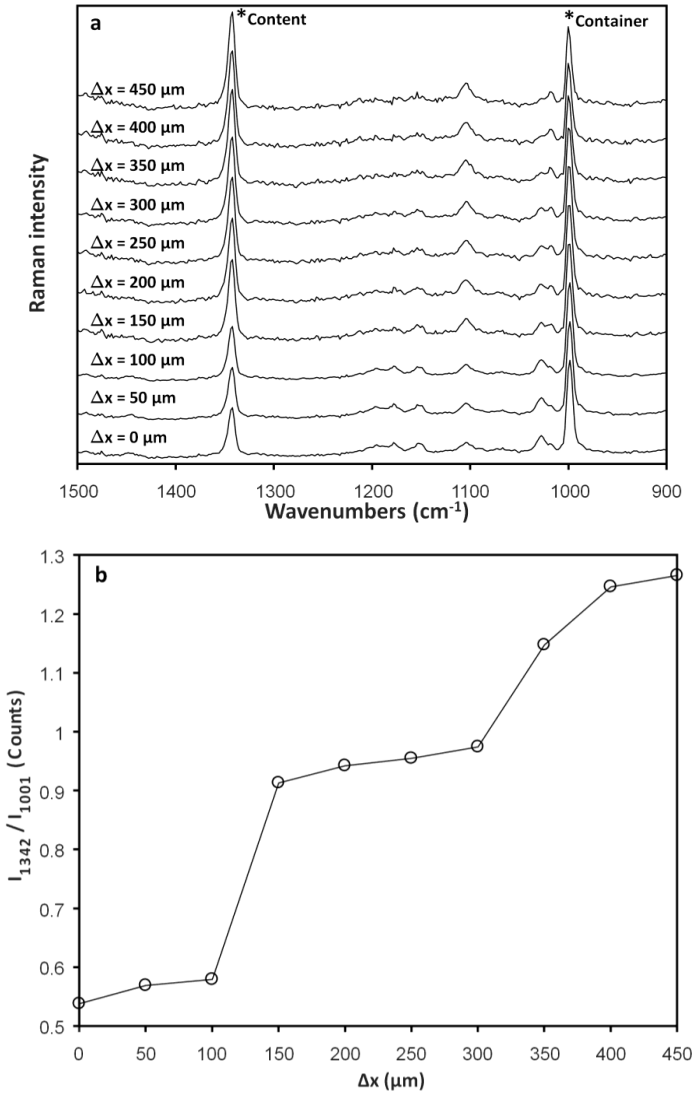

Figure 5.7. *Fibre-optics micro-SORS experiment: Liquid in a polystyrene container. (a) Raman spectra of nitrobenzene in a polystyrene container as recorded with specific distances between the fibres (scaled to maximum intensity in this range and offset for clear visibility). Raman bands used for the plot were marked; (b) Plot of the net Raman band intensity ratios as a function of the distance between the fibres. For each datapoint a fibre-optics Raman spectrum was recorded with 3 accumulations of 60 s (785 nm, ca. 20 mW at the sample).*

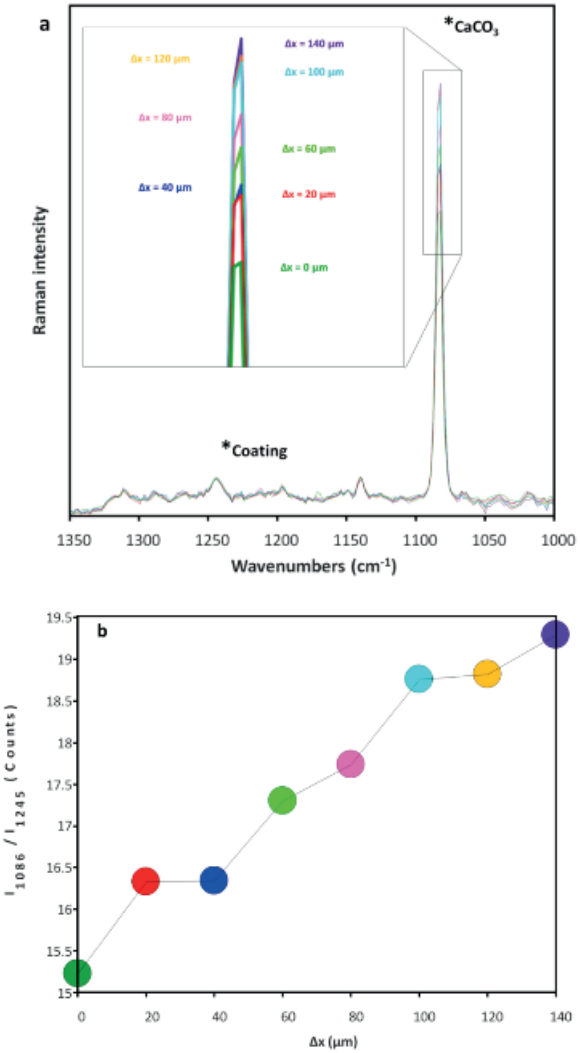

Figure 5.8. *Fibre-optics micro-SORS experiment: Coating on $CaCO_3$ rock. (a) Raman spectra as recorded with specific distances between the fibres. The Raman bands that are used for the fibre-optics SORS experiments are marked. For each datapoint, a fibre-optics Raman spectrum was recorded with 9 accumulations of 20 s (785 nm, ca. 20 mW at the sample). The spectra are intensity-scaled to the 1245 cm^{-1} Raman band of the coating. The inset shows the relative intensity of the $CaCO_3$-band, at 1086 cm^{-1} as a function of the interfibre distance. (b) Plot of the net Raman band intensity ratios as a function of the distance between the fibres.*

Finally, in order to evaluate the feasibility of *fibre-optics* micro-SORS for analysing thin layers, a sample consisting of an acrylic coating on a calcite rock was studied. The homogeneous thin coating (50 µm) on top of this sample is clearly less thick than the turbid layers used in previous samples (150, 300, 500 µm). Raman spectra were recorded with increasing distances between the fibres, between 0 and 140 µm (Δx = 20 µm steps were used) (Fig. 5.8 (a)). When normalising the spectra to the 1245 cm^{-1} Raman band of the coating, it is observed that the relative intensity of the $\nu(CO_3^{2-})$ stretching vibration (1086 cm^{-1}) of calcite increases with increasing distance between the fibres, i.e. an increasingly larger part of the deeper layer is being sampled. The same effect is observed when plotting the ratio as a function of the distance between the fibres (Fig. 5.8 (b)), demonstrating the micro-SORS capabilities of the fibre-optics sensor.

5.3.3 Critical evaluation of the *fibre-optics* micro-SORS sensor

In the previous paragraph, we demonstrated the effectiveness of the prototype fibre-optics sensor to perform micro-SORS experiments. In the current stage of development, we can also make a few remarks on the practical use of this concept.

First, in the current setup, the fibres that were used both have a diameter of 62.5 µm. During the experiments both fibres are brought into contact with the sample; this fibre diameter can be considered to be the equivalent of the laser spot size in conventional *full* micro-SORS experiments. However, in conventional experiments, the working distance of high magnification lenses is a limiting factor to the applicability; yet, in principle, it is possible to use glass fibres with smaller diameters. It can be appreciated that decreasing the fiber diameter will, on the one hand, increase the axial resolution that can be obtained with the micro-SORS experiments but, on the other hand, the signal intensity might be reduced. To achieve sufficient sensitivity, therefore, measurement times or the laser power should be increased accordingly but care has to be taken not to burn the sample, especially as diminishing the excitation fibre diameter inherently results in the delivery of higher power densities.

Another issue that requires attention is related to the fact that, in contrast with *full* micro-SORS, there is a physical contact between the sensor and the sample as the fibres are touching it during the experiment. However, as the bare fibres are very thin and tend to bend easily, we estimate there is little chance that this physical contact can affect the sample surface even if brittle materials are involved. The position of the sensor (exact zero and spatial offsets) and its effective contact with the sample surface has to be assured and influences the repeatability of the experiments, especially since bare fibres are flexible and it is not always easy to maintain the proper distance between the fibres. Moreover, these tiny fibres are very fragile and care has to be taken not to break or damage them. As the fibres are in contact with the sample surface, therefore, it must be appreciated that there is a risk of contaminating the fibre surfaces.

An additional downside is the inability to set the exact zero spatial offset, i.e., the full overlap between the illumination and Raman collection zones on a sample surface representing a conventional Raman measurement and typically used in scaled subtraction to retrieve pure signatures of sublayers. Instead, an approximation of this situation with fibres in contact with each other has to be used.

Finally, as was shown in fig. 5.3 (e), the fibres generate a signal in the final spectrum. In a Raman spectroscopic fibre-optics probe head, this effect could be reduced by including appropriate microfilters at the fibre tips, eg. a laser line filter on the laser fibre tip and Raman edge filter on the collection fibre tip. When the laser light from the excitation fibre enters the probe head it passes through a bandpass filter to eliminate the signal that is generated in the excitation fibre. Likewise, before the light enters the collection fibre a band blocking filter is used to eliminate the laser line. Any laser scattered light entering the collection fibre would generate interfering Raman and fluorescence induced by the collection fibre itself. In the fibre-optics micro-SORS sensor, this interference could also be reduced by working with shorter fibres. Moreover, if the effect is too large, appropriate spectral corrections for the dark signal can be implemented in the procedures. On a positive side, the simple setup renders itself amenable to miniaturisation of the probe head

and incorporation in a remote sensing arrangement that could be highly advantageous in situations where access to particular regions of the sample is restricted.

5.4 Conclusions

In this chapter, a prototype of an optical fibre-based sensor is proposed for *full* micro-SORS experiments. The advantages of this approach are that relative small laser spot sizes can be achieved in a relatively straightforward way and that the excitation and collection zones can be very close to each other. Thus, it is possible to retrieve the molecular composition of the sublayer/content concealed by a turbid top layer or container with a thickness ranging from 50 µm to 500 µm by using *full* micro-SORS. The effectiveness of the approach was demonstrated by analyzing a sandwich structure of polymer layers and the practical aspects of using this approach are discussed.

Raman spectroscopy is a well established technique, which includes a wide field of applications. Its non-destructive nature, along with other favourable characteristics, makes it one of the most appreciated techniques for the investigation of cultural heritage artifacts. The big advantage of Raman spectroscopy is that it can be employed non-invasively by bringing mobile (portable, handheld, palm size) instrumentation into the field. In chapters 3 and 4 the evaluation of the EZRaman-I dual Raman spectrometer and its use for analysing Patagonian rock art paintings are demonstrated. In chapter 5, the applicability of a novel fibre-optic sensor, is proposed based on the microspatially offset Raman spectroscopy (micro-SORS) approach. The latter will be useful for the identification of layered structures by probing specimens deeper than the surface and, consequently, it will contribute to the precise analysis of the different layers found in Patagonian rock art. This is anticipated to have a tremendous impact on the non-invasive investigation of stratified cultural heritage objects and sets the primary step towards the development of a pioneering, small-sized probe head.

As chapters 3, 4 and 5 are dedicated to point analysis, questions arise on the applicability of Raman spectroscopy for performing mapping experiments and to relate chemical information with its spatial distribution. Until now, in a non-invasive way, the EZRaman-I dual Raman spectrometer was tested under laboratory conditions on performing in situ Raman mappings on porcelain cards (small, flat objects) [27]. By using the 785 nm monochromator of the instrument and stepper motors, molecular images arising from the surface of the porcelain cards were retrieved successfully .

The challenge of the following chapter is the development of micro-SORS mapping for the identification of the stratigraphy of turbid and/or semi-transparent paint layers. The theoretical knowledge of micro-SORS, as described in chapter 2, together with the experience retrieved from the development of a novel micro-SORS approach as illustrated in the previous chapter will form the basis of the implementation of a more straightforward micro-SORS mode as will be described in chapter 6.

5.5 References

[1] H.G.M. Edwards, S.E.J. Villar, J. Jehlicka, T. Munshi, *Spectrochim. Acta A.* **2005**, *61*, 2273.

[2] M. Bouchard, D.C. Smith, *Spectrochim. Acta A.* **2003**, *59*, 2247.

[3] K. Maquelin, C. Kirschner, L.P. Choo-Smith, N. van den Braak, H.P. Endtz, D. Naumann, G.J. Puppels, *J. Microbiol. Meth.* **2002**, *51*, 255.

[4] J. De Gelder, K. De Gussem, P. Vandenabeele, L. Moens, *J. Raman Spectrosc.* **2007**, *38*, 1133.

[5] K. Kneipp, A.S. Haka, H. Kneipp, K. Badizadegan, N. Yoshizawa, C. Boone, K.E. Shafer-Peltier, J.T. Motz, R.R. Dasari, M.S. Feld, *Appl. Spectrosc.* **2002**, *56*, 150.

[6] D.S. Grubisha, R.J. Lipert, H.Y. Park, J. Driskell, M.D. Porter, *Anal. Chem.* **2003**, *75*, 5936.

[7] Bersani, D.; Conti, C.; Matousek, P.; Pozzi, F.; Vandenabeele, P. *Anal. Meth.* 2016, *8*, 8395-8409.

[8] A. Tournie, L.C. Prinsloo, C. Paris, Ph. Colomban, B. Smith, *J. Raman Spectrosc.* **2011,** *42*,399.

[9] A.M.A. Esam, H.G.M. Edwards, R. Cox, *J. Raman Spectrosc.* **2015**, *46*, 322.

[10] E.M.A. Ali, H.G.M. Edwards, M.D. Hargreaves, I.J. Scowen, *J. Raman Spectrosc.* **2010**, *41*, 938.

[11] A. Brookes, J.M. Dyke, P.J. Hendra, S. Meehan, *Spectrochim. Acta A* **1997,** *53*, 2313.

[12] J.K. Agbenyega, G. Ellis, P.J. Hendra, W.F. Maddams, C. Passingham, H.A. Willis, J. Chalmers, J. *Spectrochim. Acta A* **1990**, *46*, 197.

[13] S.K. Sharma, P.G. Lucey, M. Ghosh, H.W. Hubble, K.A. Horton, *Spectrochim. Acta A* **2003**, *59*, 2391.

[14] P. Vandenabeele, H.G.M. Edwards, J. Jehlicka, *Chem. Soc. Rev.* **2014**, *43*, 114.

[15] I. Martinez-Arkarazo, M. Angulo, L. Bartolome, N. Etxebarria, M.A. Olazabal, J.M. Madariaga, *Anal. Chim. A.* **2007**, *584*, 350.

[16] M.A. Legodi, D. de Waal, *Spectrochim. Acta A* **2007**, *66*, 135.

[17] P. Matousek, I. P. Clark, E. R. C. Draper, M. D. Morris, A. E. Goodship, N. Everall, M. Towrie, W. F. Finney, A. W. Parker, *Appl. Spectrosc.* **2005**, *59*, 393.

[18] C. Eliasson, N.A. Macleod, P. Matousek, *Anal. Chem.* **2007**, *79*, 8185.

[19] P. Matousek, N. Stone, *Chem. Soc. Rev.* **2016**, *45*, 1794.

[20] M.D. Keller, S.K. Majumder, A. Mahadevan-Jansen, *Optics Lett.* **2009**, *34*, 926.

[21] C. Conti, C. Colombo, M. Realini, G. Zerbi, P. Matousek, *Appl. Spectrosc.* **2014,** *68*, 686.

[22] P. Matousek, C. Conti, M. Realini, C. Colombo, *Analyst* **2016**, *141*, 731.

[23] M. Realini, A. Botteon, C. Conti, C. Colombo, P. Matousek, *Analyst* **2016**, *141*, 3012.

[24] Z. Di, B.H. Hokr, H. Cai, K. Wang, V.V. Yakovlev, A.V. Sokolov, M.O. Scully, *J. Mod. Opt.* **2014**, *62*, 97.

[25] K. Buckley, C. G. Atkins, D. Chen, H. G. Schulze, D. V. Devine, M. W. Blades, R. F. B. Turner, *Analyst* **2016**, *141*, 1678.

[26] C. Conti, M. Realini, C. Colombo, A. Botteon, M. Bertasa, J. Striova, M. Barucci, P. Matousek, *Philos. Trans. A Math. Phys. Eng. Sci.* **2016**, *374*. DOI: 10.1098/rsta.2016.0049.

[27] D. Lauwers, Ph. Brondeel, L. Moens, P. Vandenabeele, *Philosophical Transactions A* **2016**, *374*, 20160039.

Chapter 6 Development of *defocusing* micro-SORS mapping: Study of a 19th century porcelain card

Based on the paper: A. Rousaki, A. Botteon, C. Colombo, C. Conti, P. Matousek L. Moens, P. Vandenabeele, *Anal. Methods* **2017,** *9,* 6435.

In section β, the use of a portable Raman spectrometer for the analysis of rock art paintings in Patagonia (Argentina) was extensively described. This included the evaluation of the instrument and the suggestion of some new characteristics which could improve the quality of the in situ analysis under extreme conditions. As Raman spectroscopy is a surface technique and in order to overcome certain problems arising from the identification of components found on different layers of stratified works of art, a novel approach on probing subsurface regions is suggested. In chapter 5, the proof-of-concept of a fibre-optics micro-SORS approach has been demonstrated along with a critical evaluation of its applicability.

The previous chapter is dedicated to the point analysis of turbid and/or semi-tranparent layered structures. The question arises if it is possible to combine point measurments with information on the spatial distribution, in a non-invasive approach by combining a micro-SORS approach with Raman mapping.

In chapter 6, an alternative micro-SORS approach is now proposed, namely, defocusing microspatially offset Raman spectroscopy (defocusing micro-SORS). The advantage of this technique is that it uses an unmodified, commercially available Raman spectrometer and, thus, its use is more straightforward than other micro-SORS techniques, such as full micro-SORS and fibre-optics micro-SORS, which both require modified arrangements.

Defocusing micro-SORS is a recently developed technique that was proven to be potentially successful in cultural heritage research to investigate non-destructively the stratigraphy of turbid or semi-transparent paint layers [1-4]. However, until now this approach has not been applied to obtain imaging information with inhomogeneous real samples. In the current chapter, a defocusing micro-SORS mapping approach is demonstrated as a tool to study inhomogeneous painted stratigraphies on a 19th century porcelain card for which the depth information obtained with averaged defocusing sequences was combined with the lateral and spatial distribution achieved by mapping the painted zones. The effectiveness of the technique was verified by analysing an area with a partial overlap of red (vermilion), blue (Prussian blue), green (chrome yellow and Prussian blue), brown (vermillion and carbon black) pigmented zones, on top of a white (lead white) preparation layer.

6.1 Introduction

Raman spectroscopy has grown to be an established approach in the study of cultural heritage objects. [5-6] The technique has several favourable properties, such as its non-destructive character (provided the laser power is kept sufficiently low) and the possibility to use fibre-optics in a mobile setup for direct analysis of the artefacts. [7-8] The spectra that are obtained are usually relatively simple (compared with other techniques) and the interpretation is often performed by comparing the spectrum against a collection of reference spectra. Moreover, in a laboratory setup, the spectrometer is typically coupled with a microscope and an excellent spatial resolution down to 1 µm is obtained. [6]

In art analysis, the information achievable using Raman spectroscopy is well-appreciated and is often complemented with elemental data from other techniques such as X-ray fluorescence (XRF). [9-15]. XRF provides the elemental composition of a certain spot (typical diameter ca. 100 µm) of the artwork and by combining an array of point measurements it is possible to obtain

an elemental map of the artwork. [10, 16-17] Certain elements can be linked to well-known pigments. Unfortunately, as the X-ray beam penetrates the artwork, the different pigment layers generate a superimposed image, and it is not always clear which pigment layer generates a certain signal. In contrast, as Raman spectroscopy uses visual light, it typically does not penetrate deeply into the object and information from the surface layers is obtained. To study the stratigraphy of an artwork typically a minute sample is taken and, after embedding and polishing it, the different layers of the cross-section can be examined by (Raman-)microscopy. Unfortunately, in many cases, this approach is not valid due to the unavoidable (even though minimal) damage that is caused to the artwork. To obtain a complete view of the stratigraphy of an artwork, conservators often combine minute sampling with imaging techniques, such as UV-fluorescence and X-ray absorption (radiography) to obtain an over-all image of the artwork as well as to derive information about the underlying structures. For instance, as infrared radiation is strongly absorbed by carbonaceous materials, infrared reflectography can be used to visualise the underdrawing of a painting if this was established with carbon black.

Recently, a different Raman-spectroscopic based technique was proposed for the non-destructive analysis of turbid (diffusely scattering) media, such as pigment layers. This method is called micro-spatially offset Raman spectroscopy (micro-SORS) [1-4, 18] and is based on the recovering of the Raman signal generated at depth in the specimen by two key approaches: (i) *full* micro-SORS and (ii) *defocusing* micro-SORS. The former requires the laser to be focused on the sample by one lens while the data are collected by a different objective that is focused on the sample at a small distance away from the laser spot [4]. Alternatively, spatial offsets can also be set using the internal imaging optics of a microscope although the range of spatial offsets deployable in this arrangement is restricted by the field of view of the microscope [19, 20]. Although the full micro-SORS approach yields better results in terms of contrast between the different layers and achievable penetration depth, it is not always easily applicable in its unrestricted form utilising the external laser beam path. This is especially noted when using microscope objectives with higher magnifications (i.e. with short working distances between the paint surface and the objective) as the dimensions of the lenses form a practical limitation to the

achievable magnification. On the other hand, a prototype of a probe head for *full* micro-SORS experiments has been developed and demonstrated, which opens the way for *in situ* experiments [21-22].

Defocused micro-SORS experiments encounter fewer practical issues associated with its deployment since conventional Raman microscopes can be used without any modifications. During such an experiment at least two spectra are recorded. The first spectrum is recorded with the laser beam focused on the paint surface and for the defocused spectrum the laser beam is typically focused just above the surface [3]. The defocused spectrum is given from a larger area and has a relatively larger contribution of the deeper layers in the artwork, compared with the focused spectrum. An important step in the development of micro-SORS technology and in making it available for the scientific community dealing with cultural heritage objects is trying to combine this approach with Raman mapping so it will be possible to combine detailed spatial information with information on the different paint layers that are present in the artwork. To date micro-SORS mapping has only been demonstrated on artificially assembled systems using the *full* micro-SORS variant [23]. Here is demonstrated for the first time the utility of defocusing micro-SORS with a real object of art: a porcelain card. It is worth noting that, due to the card size (12 x 7 cm), the method is completely non-invasive; in fact, the specimen concerned was positioned directly under the Raman microscope objective so avoiding any cross-sectional analysis.

6.2 Experimental

The experiments were performed on a 19th century porcelain card (Fig. 6.1), often consisting of a thin layer of lead white ($2PbCO_3 \cdot Pb(OH)_2$) on top of cardboard. A lithographic technique is used to print the card and semi-transparent paint layers are applied on top of this. As this object is flat and made with a limited number of pigments, which are mostly good Raman scatterers, it is an ideal case for conducting *defocusing* micro-SORS experiments. Moreover, the porcelain card is a simple layered object, with non-transparent layers. Its simple structure can easily be verified with

invasive analysis in order to have comparable data. The thickness of the paint layers is estimated as ca. 15-20 µm.

Figure 6.1. *Porcelain card used in this study (12 x 7 cm).*

The measurments were performed with a Bruker Optics *'Senterra'* dispersive Raman spectrometer equipped with an Olympus BX51 microscope. The spectrometer allows the recording of point measurements and line scans as well as Raman mapping by using a diode laser (785 mm) or a green Nd:YAG (532 nm) laser. The power could be reduced stepwise (100%, 50%, 25%, 10%, 1% and 20%, 10%, 5%, 2%, 0.20% for the 785 nm and 532 nm laser, respectively) by entering filters in the beampath. Spectra can be obtained in the range of 60- 3709 cm^{-1} and 80- 3500 cm^{-1} for the 532 nm and the 785 nm lasers, respectively, with a spectral resolution of ~ 3-5 cm^{-1}. With a spectral resolution of ~ 9-18cm^{-1}, spectra can be obtained in the range of 58- 4454 cm^{-1} and 90- 3500 cm^{-1} for the 532 nm and the 785 nm lasers, respectively. The system is equipped with a thermoelectrically cooled CCD detector, operating at -65 °C. The spectrometer uses 5x, 20x, 50x, or 100x objective lenses to focus the laser beam on the sample and to collect the backscattered Raman signal. Corresponding spot sizes are ca. 50, 8, 4 and 2 µm, respectively. The instrument is controlled by OPUS® software.

The spectra were recorded with a red 785 nm laser in the spectral wavenumber range between 80 and ca 2600 cm^{-1}. This laser wavelength provides a good balance between fluorescence suppression and sensitivity and is frequently used for investigating paint layers. The laser power is software controlled and was set to 1 mW on the sample, while the laser spot size was generally ca. 8 µm when the sample is in focus (20x objective, NA = 0.4). Thus, the mapping step size can be kept sufficiently large to reach manageable mapping times, while achieving sufficient detail and sensitivity.

In a preliminary stage, the characterization of the pigments used in the card was performed. *Defocusing* micro-SORS experiments were then carried out in two steps as follows:

Table 6.1. *Integrated bands for each pigment.*

Pigment	Integrated band
Prussian blue	2172 – 2136 cm^{-1}
Vermillion	261 – 245 cm^{-1}
Carbon black	1645 – 1530 cm^{-1}
Lead white	1063 – 1035 cm^{-1}

Step (1): first, the relative band intensity change among the pigments was studied acquiring sequences of Raman spectra at imaged and two defocused positions (150 µm and 300 µm). These distances were selected based on point measurements (see further, section 6.3.1). The averaging procedure was performed to compensate for the (minimal) heterogeneity of the sample which is unavoidable in real art objects. Therefore, for each pigmented zone (blue, green, red and brown) three spectra were obtained (imaged, and 150 µm , 300 µm defocusing distances); each of these spectra is the combination (average) of ten spectra acquired at slightly different positions to account for any inhomogeneity. Then, a baseline correction was made and surface/subsurface ratios were calculated by integrating the most informative band for each compound with a net

band intensity (K-method in Opus software, ENet in [24]). The integrated bands are reported in Table 6.1. Moreover, a normalization was performed to highlight the band intensity increase of the subsurface pigment(s) (or surface compound decrease) at the defocused positions. Both the imaged and defocused spectra were acquired with acquisition times of 9 s with 9 accumulations.

Step (2): then, imaging acquisition was performed. An area of approximately 1.7 mm^2 was selected and three maps were acquired at the imaged position, 150 µm and 300 µm of the defocusing distances. The step size was 75 µm along the x and y axes with a total acquisition time for each map of 7.5 hours (9 s and 9 accumulations for each spectrum). The spectra were baseline corrected and the chemical images were obtained by recording the net intensity of the most informative band for each compound (Table 6.1). The pigment distributions are shown either without normalization or normalized to the lead white 1050 cm^{-1} band.

All the spectra (step 1 and 2) were acquired using a 50 µm confocal pinhole for imaged measurements and a 50 x 1000 µm slit for defocused positions. The data were processed in OPUS® software.

6.3 Results and discussion

The baseline-corrected Raman spectra of the pigments used for the card are shown in fig. 6.2. Prussian blue ($Fe_4[Fe(CN)_6]_3$) was used in the blue zones, a mixture of Prussian blue and a very small amount of chrome yellow ($PbCrO_4$) was used in the green zones, vermillion (HgS) was used in the red zones, vermillion and carbon black were used in the brown zones and lead white ($2PbCO_3 \cdot Pb(OH)_2$) was used in the white areas. In the metal paint used to add gold-coloured accents on the card no significant Raman signals were recorded. In all the coloured zones, the lead white band (1050 cm^{-1}) is present.

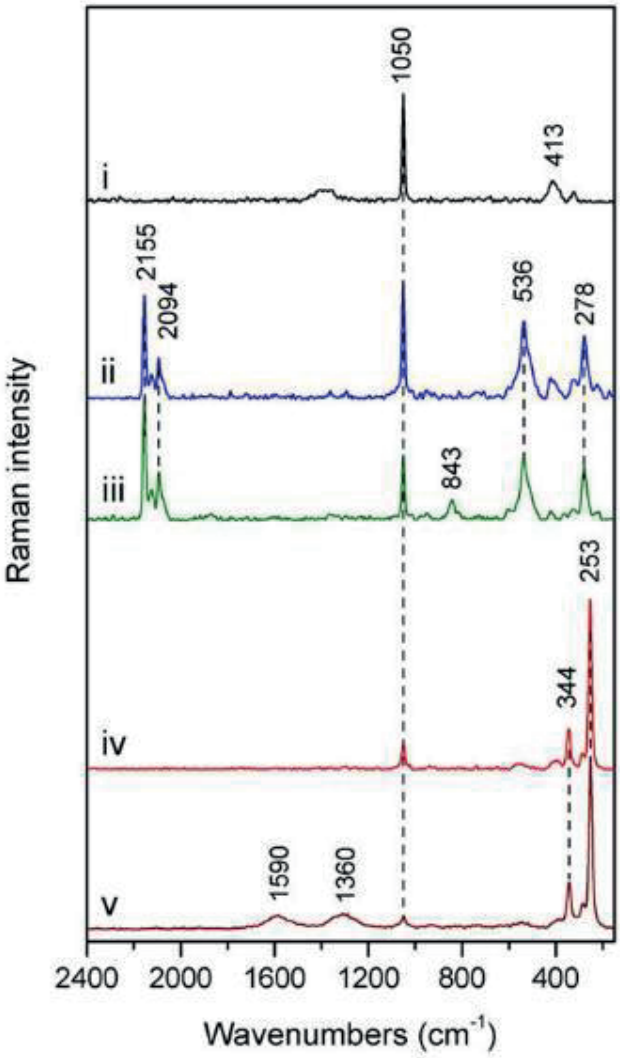

Figure 6.2. *Baseline-corrected Raman spectra recorded on the different coloured zones in the porcelain card. (i) White zone, containing lead white ($2PbCO_3 \bullet Pb(OH)_2$); (ii) blue area, containing Prussian blue ($Fe_4[Fe(CN)_6]_3$); (iii) green area, containing Prussian blue and a small amount of chrome yellow ($Fe_4[Fe(CN)_6]_3 + PbCrO_4$); (iv) red zone, containing vermillion (HgS); (v) brown zone, containing vermillion and carbon black (combusted organic material).*

6.3.1 Step 1 - *defocusing* micro-SORS sequences

In the first step, *defocusing* micro-SORS experiments were performed by recording several spectra (point measurements) in the different coloured areas, starting from the focal distance and increasing the working distances between the objective and the artwork. Among the tested distances, 150 µm and 300 µm provided the most informative spectra. With smaller distances the effect of defocusing was less evident, whilst with larger distances a severe loss of signal was observed.

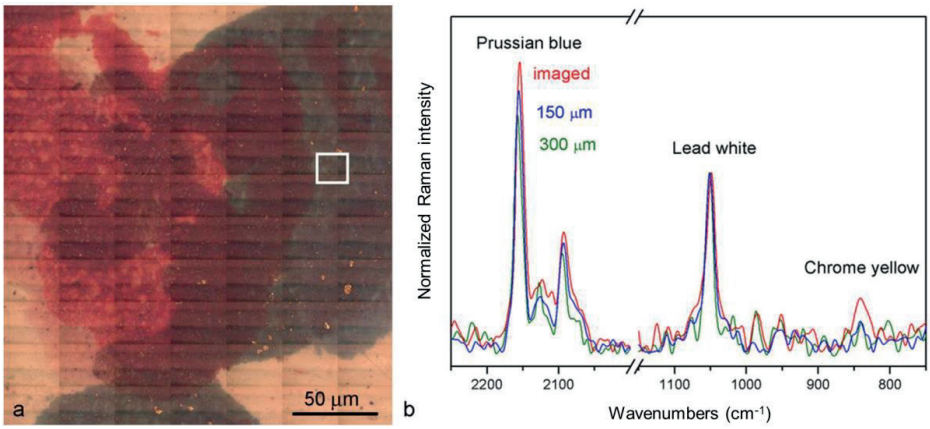

Figure 6.3. *(a) Porcelain card detail with the white square indicating the analyzed green zone; (b) averaged imaged and defocusing micro-SORS spectra normalized to the 1050 cm^{-1} lead white band.*

The results thereby obtained are exemplified below using the data collected in a green and in a brown area of the card. The averaged imaged spectrum of the green area (Fig. 6.3 (a)) exhibits the most characteristic bands of Prussian blue (2155 cm^{-1} and 2094 cm^{-1}) and the weak signal of chrome yellow at 843 cm^{-1} (Fig. 6.3 (b)). Moreover, the lead white band (1050 cm^{-1}) is present as well. The normalization to the 1050 cm^{-1} band of lead white of the averaged imaged and defocused spectra is reported (Fig. 6.3 (b)); the relative intensity of both Prussian blue and chrome yellow signals decreases upon increasing the defocusing distances. This outcome is consistent with lead white being used below the green paint.

The averaged imaged spectrum collected in the brown area (Fig. 6.4 (a)) shows the Raman bands of vermillion (253 and 344 cm^{-1}) and carbon black (ca. 1360 and 1590 cm^{-1}), in line with expectations, in addition to Prussian blue and lead white signals (Fig. 6.4 (b)).The normalization to the lead white signal allows the observation that vermillion, carbon black and Prussian blue decrease upon defocusing, highlighting that these compounds are located over the lead white layer (Fig. 6.4 (b)). When the same spectra are normalized to vermillion (Fig. 6.4 (c)) it is possible to observe that lead white and Prussian blue increase their signals with defocusing, suggesting that both pigments are located below the brown layer. A small overall shift in Raman band positions was observed over time due to calibration changes. This is not surprising as measurements were recorded in total over several days.

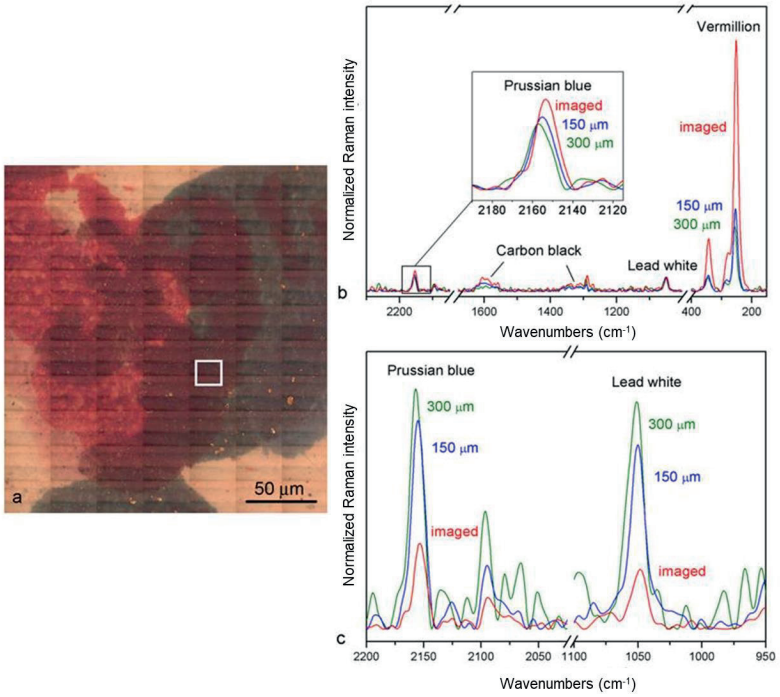

Figure 6.4. *(a) Porcelain card detail with the white square indicating the analysed brown zone; (b) averaged imaged and defocusing micro-SORS spectra normalized to lead white and (c) normalized to vermillion.*

To further explore the layers' stratigraphy two ratios (vermillion over Prussian blue and Prussian blue over lead white) were calculated and plotted over the defocusing distances (figs. 6.5 (a), (b)). The graphs clearly demonstrate that Prussian blue is located under vermillion (Fig. 6.5 (a)) and lead white under Prussian blue (Fig. 6.5 (b)). In conclusion, the stratigraphy of the brown area can be schematically represented as depicted in fig. 6.5 (c), where it can reasonably be supposed that chrome yellow is present in the middle layer.

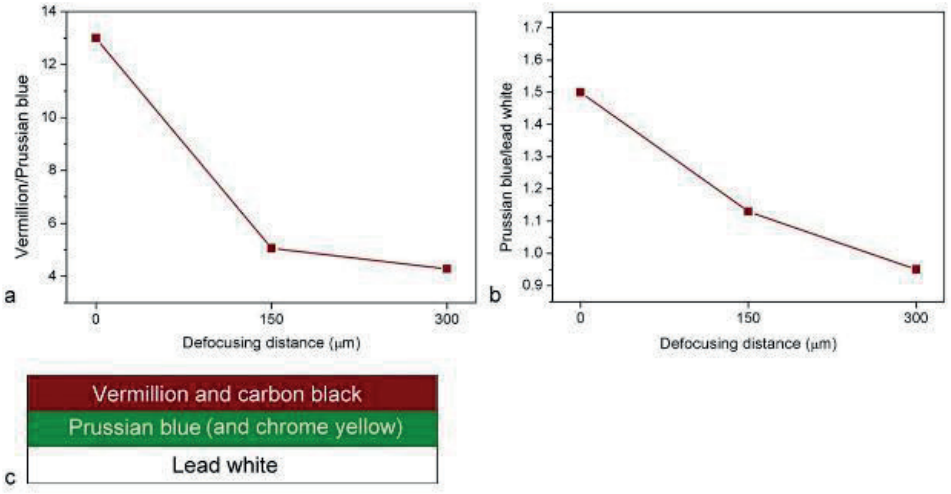

Figure 6.5. *(a) Vermillion over Prussian blue ratio and (b) Prussian blue over lead white ratio plotted over the degree of defocusing; (c) scheme of the stratigraphy suggested by the micro-SORS measurements.*

6.3.2 Step 2-*defocusing* micro-SORS mapping

In these experiments the ability of the *defocusing* micro-SORS arrangement to obtain information from underlying paint layers was demonstrated. However, micro-Raman spectroscopy is also well-appreciated for its good spatial resolution (typically down to ca. 1 µm, which is the order of magnitude of pigment grain sizes), and it would be of interest to be able to include information on the lateral and spatial distribution of the artists' materials in the analysis. The

advantages of mapping include the possibility to get images of the distribution overview of substances irregularly applied on the surface and, thanks to micro-SORS, the possibility to study the distribution of the substances that are present below the surface.

Recently, it was demonstrated on a mock-up sample that *full* micro-SORS can be deployed in a mapping set-up for measurement of an inhomogeneous layer (mimicking an underdrawing or whitewash covered artwork) under a uniform covering layer [23]. Although this approach was judged to be very promising, the influence of an inhomogeneous upper layer on a real object of art has still to be examined. Moreover, a further challenge is to obtain relevant results with *defocusing* micro-SORS, which is the less effective but also the simplest micro-SORS variant. For these reasons, a *defocusing* micro-SORS mapping experiment was performed on a selected zone of a porcelain card that includes red, green and brown paint (Fig. 6.6).

Figure 6.6. *(a) Porcelain card with indication of the mapped area (green square); (b) porcelain card detail of the mapped area (white square).*

In fig. 6.7 the distribution of vermillion, carbon black, Prussian blue and chrome yellow are reported. The maps are normalized to lead white and for each pigment the same absolute limits in the colour scale are set, so that focused and defocused maps can be easily compared. In line with the expectations, the distribution of vermillion, Prussian blue and carbon black in the imaged

Raman map clearly corresponds to the appropriately coloured zones (Fig. 6.7 (a), (d), (g)). Chrome yellow (Fig. 6.7 (j)) shows a considerably less clear image, and this is due to the small amount of the pigment and its inhomogeneous distribution in the green areas.

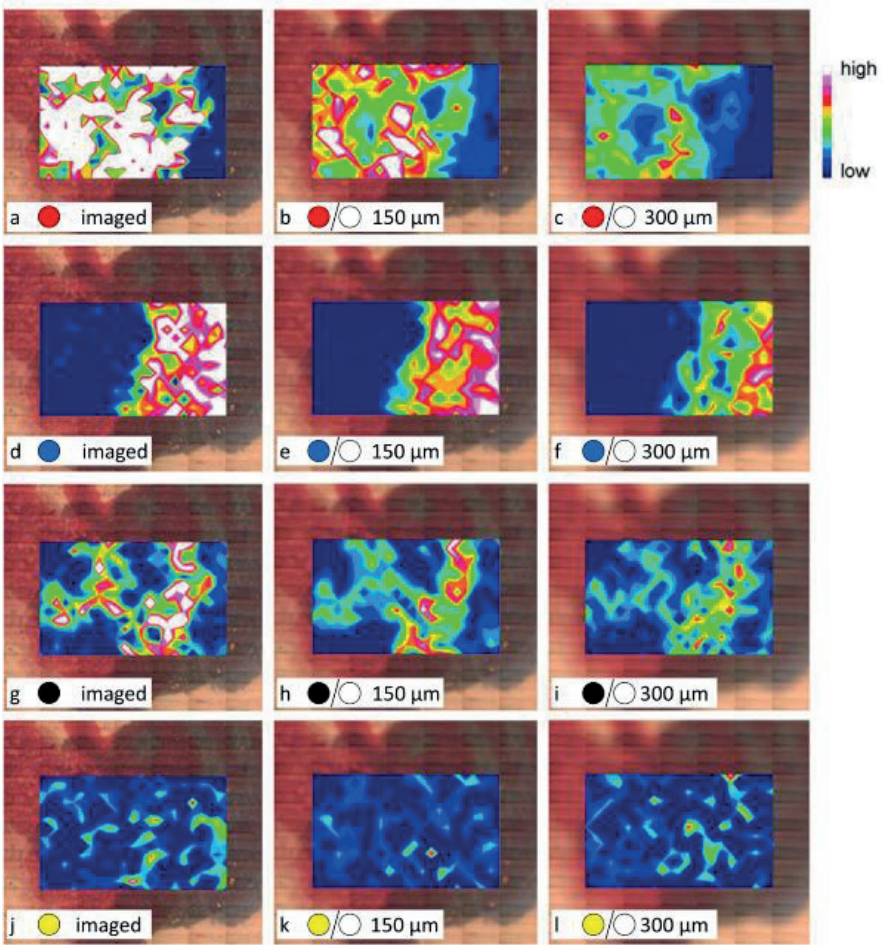

Figure 6.7. *Vermillion distribution normalized to lead white at (a) imaged position, (b) 150 µm and (c) 300 µm; Prussian blue distribution normalized to lead white at (d) imaged position, (e) 150 µm and (f) 300 µm; Carbon black distribution normalized to lead white at (g) imaged position, (h) 150 µm and (i) 300 µm; chrome yellow distribution normalized to lead white at (j) imaged position, (k) 150 µm and (l) 300 µm.*

With an increase in the defocusing distance, vermillion (Fig. 6.7 (b), (c)), Prussian blue (Fig. 6.7 (e), (f)) and carbon black (Fig. 6.7 (h), (i)) signals become progressively less intense, demonstrating that lead white is under all the coloured layers and its distribution is highly homogeneous. The chrome yellow distribution in the defocused maps (Fig. 6.7 (k), (l)) is not relevant due to the low signal-to-noise ratio in the spectra at the imaged position, and the complete loss of its signal at defocusing distances.

It is also worth considering the un-normalized maps. The un-normalized map of the Prussian blue at the imaged position (Fig. 8 (a)) reveals that this pigment has a less intense signal in the brown area than in the green zone. This could be an indication that the brown layer partially hides the Prussian blue pigment signal, which consequently originates from the lower depth position.

On the other hand, the distribution of Prussian blue normalized to lead white at the imaged position (Fig. 6.8 (b)) is more homogeneous in both the brown and green areas. This could be explained by the fact that the normalization to lead white automatically enhances the signals obtained from both the sublayers.

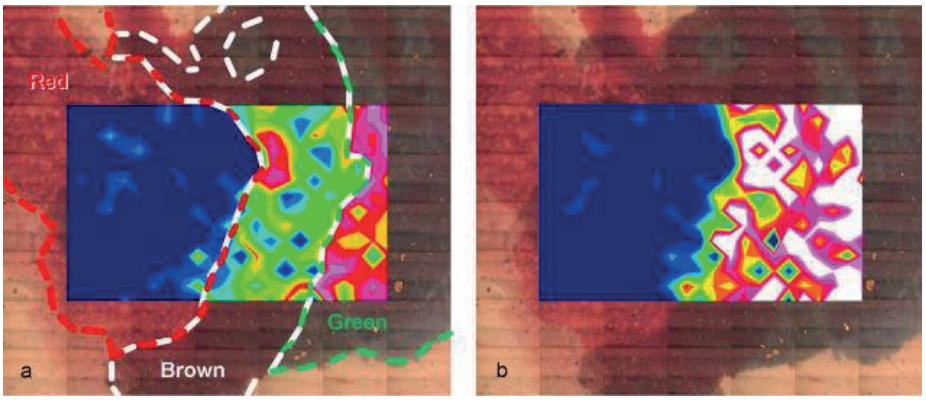

Figure 6.8. *Prussian blue distribution at imaged position; (a) non-normalized and (b) normalized to lead white. The broken lines are drawn as approximate curves as a visual guide to distinguish between the red, brown and green zones. The colour scales of the maps (a and b) are not comparable.*

The distribution of the (un-normalized) lead white pigment was also studied (Fig. 6.9). It should be noted that at the imaged position (Fig. 6.9 (a)) the lead white signal is more intense in the red area. Taking into account that lead white is present under all the coloured areas (as demonstrated by *defocusing* micro-SORS sequences), this outcome can be explained considering the different thickness of the layers: the red layer is probably thinner than that of the green one. Moreover, it should be noted that in the brown layer zone the lead white signal is even less intense and this can be reasonably ascribed to the overlapping of two layers, brown over green. Looking at the defocused distribution of lead white (Fig. 6.9 (b)-(c)), it can be noted that there are insignificant differences compared with the imaged distributions. This result is consistent with the presence of a homogeneously distributed lead white layer as background for the paint.

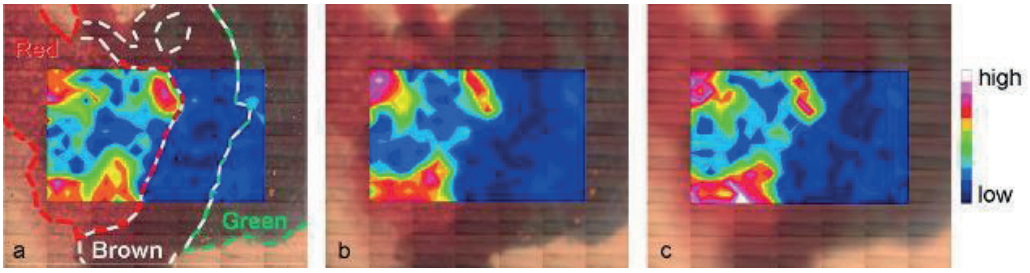

Figure 6.9. *Lead white distribution (un-normalized) at (a) imaged position, (b) 150 µm and (c) 300 µm defocusing distances. The broken lines are approximate curves as a visual guide to distinguish between the red, brown and green zones.*

In conclusion, the maps indicate that Prussian blue is below the brown layer and lead white is below all the layers. Therefore, the maps are consistent with the stratigraphy suggested in fig. 6.5 (c). Nevertheless, comparing the results obtained in steps 1 and 2 it is apparent that the spectra obtained in step 1 lead to a more precise enlightenment about the layer stratigraphy, since the relative intensity changes can be more accurately observed and top/bottom layer ratios can be better calculated. The limitation of step 1 is that the data acquired from the spectra refer to only a limited area of the sample.

With mapping (step 2) it is possible to get information about broad and inhomogeneous areas and about layers overlapping on a larger scale (the data here presented refers to an area of about 1.7 mm^2, but larger areas can be mapped). Substance distribution can also provide information about the thickness of the layers, the relative abundances of the pigments and their Raman scattering cross-sections.

6.4 Conclusions

Defocusing micro-SORS is a promising and straightforward approach to study the layered structure of painted artworks. Two methods were adopted and compared, the *defocusing* micro-SORS spectral sequence and the *defocusing* micro-SORS mapping. The former allowed one to reconstruct the layer stratigraphy of limited areas of the sample with high accuracy, calculating the relative intensity changes while defocusing; the latter provides data which are related to broad areas and which permit an overview of the whole stratigraphy. By comparing the results of focused and defocused Raman maps obtained non-invasively on the porcelain card, it was possible to combine stratigraphic information with the lateral and spatial distribution of the pigmented zones and to identify possible inhomogeneities in the paint layers.

When studying micrometre-thick layers one can use micro-spatially offset Raman spectroscopy (micro-SORS). In this way, the artefact can be examided non-invasively and the molecular information distributed in different layers can be revealed. Although full micro-SORS mapping has been demonstrated hitherto [23], defocusing micro-SORS mapping is suggested as a more straightforward approach as it does not require a specific set up. For the latter, more research should be conducted in order to achieve the optimal separation between layers.

The aim of the current PhD thesis combines the experimental data separated in two sections (section β working in situ, section γ probing into layered structures) in order to demonstrate and explore further the possibilities of non-invasive statigraphic Raman analysis. The question that is

posed in chapters 3 and 4: if it is possible to probe deeper than the surface using an approach free of sampling, is answered in chapters 5 and 6 by the illustration of 2 key modalities of micro-SORS. As the commercial portable Raman instruments are used for surface analysis (with penetration depending on the way that the probe head is focused on the surface and/or the laser wavelength), it is demonstrated in chapter 4 that superimposed layers can block the Raman signal of the pigmented areas or the subsurface regions of interest. In general terms, by using portable or benchtop Raman instrumentation, stratigraphic analysis without cross-sections taken from the object is forbidden. Micro-SORS is a promising approach to overcome the invasive nature of stratigraphic analysis by yielding results when analysing layered samples and/or objects. Moreover, micro-SORS techniques can be used for Raman mapping and, thus, the connection of chemical imformation with the spatial distribution of pigments, simultaneously for the x, y and z axis.

In the following chapter some conclusive remarks will be given and further possibilities and solutions will be discussed.

6.5 References

[1] C. Conti, C. Colombo, M. Realini, G. Zerbi, P. Matousek, *Appl Spectrosc.* **2014**, *68*, 686.

[2] C. Conti, M. Realini, C. Colombo, P. Matousek, *J Raman Spectrosc.* **2015,** *46*, 476.

[3] P. Matousek, C. Conti, M. Realini, C. Colombo, *Analyst* **2016,** *14*, 731.

[4] C. Conti, M. Realini, C. Colombo, P. Matousek, *Analyst* **2015,** *140*, 8127.

[5] P. Vandenabeele, H. G. M. Edwards, L. Moens, *Chem Rev.* **2007**, *107*, 675.

[6] R.S. Das, Y. K. Agrawal, *Vib. Spec.* **2011**, *57*, 163.

[7] B. Lydzba-Kopczynska, J.M. Madariaga, *J Raman Spectrosc.* **2016**, *47*, 1404.

[8] Ph. Colomban, J Raman Spectrosc. **2012**, *43*, 1529.

[9] B. H. Stuart, P. S. Thomas, *Heritage Sc.* **2017**, *5*, 10.

[10] P. Vandenabeele, M. K. Donais, *Appl Spectrosc.* **2016,** *70*, 27.

[11] R. Alberti, V. Crupi, R. Frontoni, G. Galli, M. F. La Russa, M. Licchelli, D. Majolino, M. Malagodi, B. Rossi, S.A. Ruffolo, V. Venuti, *J. Anal. At. Spect.* **2017**, *32*, 117.

[12] A. Rousaki, A. Coccato, C. Verhaeghe, B-O. Clist, K. Bostoen, P. Vandenabeele, L. Moens, *Appl Spectrosc.* **2016**, *70*, 76.

[13] L. Van de Voorde, M. Vandevijvere, B. Vekemans, J. Van Pevenage, J. Caen, P. Vandenabeele, P. Van Espen, L. Vincze, *Spectrochim Acta Part B* **2014**, *102,* 28.

[14] P. Vandenabeele, H.G.M. Edwards, J. Jehlička, *Chem Soc Rev.* **2014**, *8*, 2628.

[15] M. Veneranda, N. Prieto-Taboada, S.F.O. de Vallejuelo, M. Maguregui, H. Morillas, I. Marcaida, K. Castro, J. M. Madariaga, M. Osanna, *Env. Sc. Poll. Res.* **2017**, *24*, 19599.

[16] K. Janssens, G. Vittiglio, I. Deraedt, A. Aerts, B. Vekemans, L. Vincze, F. Wei, I. Deryck, O. Schalm, F. Adams, A. Rindby, A. Knochel, A. Simionovici, A. Snigirev, *X-Ray Spectrom.* **2000**, *29*, 73.

[17] H. Bartova, T. Trojek, T. Cechak, R. Sefcu, S. Chlumska, *Rad. Phys. Chem.* **2017**, *139*, 100.

[18] P. Matousek, I. P. Clark, E. R. C. Draper, M. D. Morris, A. E. Goodship, N. Everall, M. Towrie, W. F. Finney, A. W. Parker, *Appl Spectrosc.* **2005,** *59,* 393.

[19] Z. Di, B. H. Hokr, H. Cai, K. Wang, V. V. Yakovlev, A. V. Sokolov, M. O. Scully, *J Mod Opt.* **2014**, *62*, 97.

[20] K. Buckley, C. G. Atkins, D. Chen, H.G. Schulze, D. V. Devine, M. W. Blades, R. F. B. Turner, Analyst **2016,** *141*, 1678.

[21] M. Realini, A. Botteon, C. Conti, C. Colombo, P. Matousek, *Analyst* **2016,** *141*, 3012.

[22] P. Vandenabeele, C. Conti, A. Rousaki, L. Moens, M. Realini, P. Matousek, *Anal Chem.* **2017,** *89*, 9218.

[23] A. Botteon, C. Conti, M. Realini, C. Colombo, P. Matousek, *Anal Chem.* **2017,** *89*, 792.

[24] D. Lauwers, Ph. Brondeel, L. Moens, P. Vandenabeele, *Phil. Trans. R. Soc. A.* **2016,** *374*, 20160039.

Section δ: Epilogue

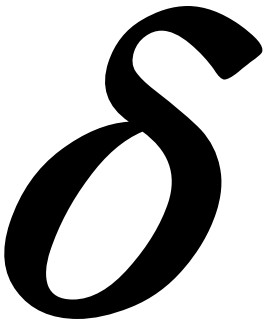

Chapter 7 Summary, conclusions and future perspectives

Documentation of cultural heritage objects is the cornerstone of archaeometrical research. The pigments and techniques used by an artist(s) in a certain era, imply and define the societal and technological progress. Moreover, studying the state of preservation of artistic objects is highly important as this can contribute towards their better conservation which can lead to the expansion of the life of the work of art. The latter is considered quite critical to allow future generations to enjoy their beauty.

A combination of a range of scientific disciplines constitutes what is known today as archaeometry. Natural sciences are brought together with humanities in order to create a scientific field dedicated to physicochemical analysis and in context interpretation of artefacts of human expression found through the centuries. One of the most well-appreciated scientific tools for art analysis is Raman spectroscopy. The latest technological advances have improved the technique while simultaneously it was brought from the laboratory into the field. New instrumentation and approaches improved the quality of the retrieved information and thus have made Raman spectroscopy one of the leading techniques in cultural heritage analysis.

This PhD thesis is dedicated to Raman spectroscopy and its applications with a special focus on the non-invasive and non-destructive analysis of layered structures in works of art. Furthermore, *state-of-the-art* Raman approaches are discussed and new insights are proposed with the aim to set a base for the analysis of paint layers.

Raman spectroscopy, both with benchtop and portable instrumentation, has several possibilities when applied to cultural heritage objects. The applications and different approaches are well described in the literature together with its advantages as well as possible drawbacks (chapter 2). In general, the analytical protocols used for the identification of different organic and

inorganic components found in art objects aim towards a non-invasive and non-destructive approach. The possibilities of portable Raman spectroscopy were demonstrated in the case of Patagonian rock art paintings. Shelters from hunter-gatherer populations found in three provinces in Argentinian part of Patagonia (Neuquén, Río Negro, Chubut) were investigated using this approach. This highly novel research describes the first use of portable Raman instrumentation for the on-site study of prehistoric rock art paintings in Patagonia (chapter 3). This study resulted in one of the most comprehensive investigations published on analysing rock art in different environments. The portable *EZRaman-I Dual* Raman spectrometer was evaluated for its applicability under extreme conditions and its performance for the identification of pigments, alteration products and substrata.

The results from the measurement campaign in the Patagonian field, revealed not only the pigments used, but also it helped to evaluate the preservation state of these magnificent rock paintings found in different provinces with different ambient/environmental conditions (chapter 4). Portable Raman spectroscopy can serve as a first choice technique for the molecular characterization of paintings from rock art shelters and to differentiate between the original components (pigments) and the post-depositional materials (weathering products). Post-depositional degradation is present as a relatively thin turbid layer that either covers part of the rock paintings or the entire artwork and rock support and it may be dispersed on the surface. Moreover, the local population seems, in some cases, to have painted on already degraded surfaces. With Raman spectroscopy being predominantly a surface sensitive technique the signal from the pigmented layers can be overwhelmed by signals from the superficial layers . Sandwiched layers are, however, not only a result of degradation processes and layered structures can be found in nearly every cultural heritage artefact. Until recently, the only way of molecularly probing deeper than the surface was by sampling.

A novel approach for non-invasive, non-destructive molecular stratigraphic analysis of micrometre thick layers is meticously illustrated in this PhD thesis (chapter 5). *Fibre-optics* microspatially offset Raman spectroscopy (*fibre-optics* micro-SORS) is proposed as an alternative

to the micro-SORS technique. The new micro-SORS sensor, which utilizes bare glass fibres for transferring the laser radiation and collecting the Raman signal, is a very promising approach with a wide field of applications including cultural heritage studies. The lightweight and compact configuration of *fibre-optics* micro-SORS gives an opportunity to further miniaturise the set-up and to develop a pioneering Raman probe head.

As an addition to micro-SORS point measurements for stratigraphic analysis, subsurface Raman mapping is also developed using a different variant of the micro-SORS technique, namely, *defocusing* micro-SORS (chapter 6). The latter is one of the most simple approaches towards micro-SORS as it uses an unmodified commercially available Raman spectrometer. Although the results of *defocusing* micro-SORS are very promising, more research now needs to be done to achieve a better separation of the different layers.

This PhD thesis combines the concepts of direct and stratigraphic analysis, in order to propose pioneering solutions in the field of Raman spectroscopy and cultural heritage studies. This research tries to overcome a possible limitation of traditional Raman spectroscopy by using micro-SORS to obtain information that originates from beneath the surface. Recent developments of the micro-SORS technique have set the starting point for the development of new approaches. This PhD research should be considered as the first solid step for further investigations and fundamental research on two axes: (a) improvement of Raman spectroscopy for the analysis of prehistoric rock art paintings and suggestion of new strategies and (b) the understanding of the physical and chemical phenomena in micro-SORS (*full*, *defocusing* and *fibre-optics*) in order to establish a better approach optimizing the hardware and software (and data-processing) of the technique. Some of the future research objectives could then be:

a. For rock art painting investigations:

a1. More fundamental research should be performed on ochres and earth pigments in relation to their Raman signals. Doped matrices, structural distortions, geological formation,

degradation, high temperatures, etc. can introduce several changes to the recorded Raman spectrum (wavenumber shift, band broadening and the appearance of new Raman bands). Samples synthesised according to traditional practices (thermal treatment, incorporation of organics, etc.) should be analysed as well, in order for the structural changes to be investigated and correlated with material processing methods.

a2. In parallel, fundamental investigations should be conducted also on the degradation products. The understanding of the formation of weathering crusts (depending upon the environment and chemical pollution) and their absolute Raman band interpretation will help towards the establishment of a more definitive identification of the components. Furthermore, the comparison of raw materials e.g. pebbles, rock deposits or other geological minerals coming from different places that may have served as source of pigments should be conducted.

a3. The incorporation of different lasers (e.g. 1064 nm) and lighter Raman instrumentation in the field in order to retrieve more information (also from organics, e.g. binders, dyes) and increase the mobility of the equipment. The selection of different lasers is considered very important as fluorescence will be in some cases suppressed and the signals of weak Raman scatterers can be enhanced by changing the laser wavelength.

a4. The incorporation of other techniques such as Mössbauer spectroscopy, an ideal technique for the iron oxides, and also X-ray diffraction (XRD) for the identification of crystalline phases, can contribute towards the positive identification of all the inorganic compounds found on rock art paintings. Moreover, luminescence dating can be an alternative to radiocarbon dating of oxalate crusts or ^{14}C chronology for the span of human occupation of the archaeological site (excavated layers). The solar bleaching of surfaces prior to their being covered with paint is a potential basis for such an investigation.

a5. As a final goal, the comparison of the results (for pigments, degradation and substrata) between different scientific groups and different sites.

b. Molecular probing of layered materials is anticipated to have a considerable impact in various scientific fields ranging from art analysis, archaeology, geology, biomedical science, pharmacology etc. A thorough investigation of micro-SORS can bring the technique from a limited number of specialised laboratories towards widely-used mobile, *in situ* investigations. For the latter, several milestones need to be achieved:

b1. Further development of *fibre-optics* micro-SORS. As this approach was only recently established, it needs to be further studied e.g. the influence of the fibres (type, diameter, etc.) needs to be examined as well as improvemnets made to the experimental set-up such as protecting the brittle fibres.

b2. Towards a better understanding of the fundamentals of micro-SORS, a series of experiments should be based on well-defined, synthetic samples. In this way, the evaluation of the chemical build-up of a sandwich structure can be made by using an experimental set-up where different parameters can be modified independently, before applying the technique to the unknown complex system. Data-processing needs to be optimised and the possibilities of micro-SORS mapping should be further explored.

b3. Incorporation of different lasers in the micro-SORS technique. Using a 1064 nm laser could bring new insights into this research and assist towards the identification of layers that are not completely turbid, these being semi-transparent or transparent.

b4. Comparison of different micro-SORS approaches and evaluation towards mobile use. Strengths and weaknesses of the different micro-SORS approaches should be evaluated in terms of performance and data processing but also depending on how they can be implemented in mobile Raman spectrometers.

b5. Application of micro-SORS in the lab and *in situ*. The applicability of the different micro-SORS approaches can be implemented in *state-of-the-art* studies where it is relevant to obtain molecular information from layers covered with non-transparent materials. Some of these applications could involve the investigation of prehistoric rock art (as highlighted here in this PhD thesis), artworks by René Magritte and the surrealist painters, highly stratified artworks like the Ghent Altarpiece by the Van Eyck brothers, geological applications etc.

The current PhD thesis aimed at introducing novel approaches to study layered cultural heritage materials by Raman spectroscopy focused primarily upon its *in situ* application for the study of Patagonian rock art. Next to this, some modifications of micro-SORS were proposed to make them more accessible for archaeometrical applications. Whereas there are still many aspects which require further analysis before this approach can be more widely applicable it is hoped that this current work will have created a solid base for these future studies.

Chapter 8 Samenvatting, conclusies en toekomstperspectieven

Het documenteren van het cultureel erfgoed is een hoeksteen van archeometrisch onderzoek. De pigmenten en technieken die door een artist in een bepaalde periode gebruikt werden, beïnvloeden enerzijds en anderzijds zijn uitingen van de technologische vooruitgang. Bovendien is het onderzoek naar de bewaring van kunstvoorwerpen erg belangrijk, omdat dit bijdraagt tot een betere conservatie, wat dan weer de levensduur van het kunstwerk kan verlengen. Dit is noodzakelijk om ook toekomstige generaties van de schoonheid van kunst te kunnen laten genieten.

De combinatie van een hele reeks analytische technieken dragen bij tot wat we 'archeometrie' noemen. Natuurwetenschappen worden samengebracht met menswetenschappen om een wetenschappelijk domein te vormen dat gewijd is aan de fysicochemische analyse en de contextuele interpretatie van (kunst) vormen van menselijke expressie door de eeuwen heen. Eén van de preferentiële technieken in kunstanalyse, is Ramanspectroscopie. De techniek werd één van de primaire technieken in erfgoedonderzoek, omwille van technologische evoluties en omdat de techniek uit het laboratorium naar in situ analyses kon overgebracht worden.

Dit doctoraatsonderzoek is gewijd aan Ramanspectroscopie en zijn toepassingen, met specifieke aandacht voor niet-invasieve en niet-destructieve analyse van gelaagde structuren in kunstobjecten. Bovendien worden speerpunt toepassingen binnen de Ramanspectroscopie bediscussieerd en nieuwe inzichten worden voorgesteld, om de basis te leggen voor de analyse van verflagen.

Ramanspectroscopie kent veel toepassingen binnen de analyse van cultureel erfgoed, waarbij zowel mobiele apparatuur als laboratoriumtoestellen ingezet worden. De toepassingen en verschillende benaderingen worden uitgebreid beschreven in de literatuur, samen met de voor-

en nadelen van de techniek (Hoofdstuk 2). Over het algemeen gebruikt men een niet-invasieve en niet-destructieve benadering in de analytische protocollen voor de identificatie van organische en anorganische componenten in kunstvoorwerpen. De mogelijkheden van draagbare Ramanspectroscopie werden gedemonstreerd in het geval van beschilderde rotskunst uit Patagonië. Met deze benadering werden verblijfplaatsen onderzocht van jager-verzamelaars, in drie provincies in Patagonië, Argentinië (Neuquén, Rio Negro, Chubut). Dit erg vernieuwend onderzoek omvat voor het eerst het gebruik van draagbare Ramaninstrumentatie voor de in situ analyse van prehistorische rotsschilderingen in Patagonië (Hoofdstuk 3). Deze studie resulteerde in één van de meest geconcentreerde gepubliceerde onderzoeken van rotskunst in verschillende omgevingen. Het gebruik van de draagbare *EZRaman-I Dual* Raman spectrometer werd geëvalueerd voor zijn toepasbaarheid onder extreme omstandigheden en de performantie voor de identificatie van pigmenten, degradatieproducten en onderliggende lagen.

De meetcampagne in Patagonië liet niet enkel toe om de gebruikte pigmenten te identificeren, maar het hielp ook om de conservatietoestand van deze schitterende rotsschilderingen – uit verschillende provincies met wisselende klimatologische omstandigheden – te evalueren (Hoofdstuk 4). Draagbare Ramanspectroscopie kan dienen als eerstelijnstechniek voor de moleculaire karakterisering van rotsschilderingen en om het onderscheid te maken tussen originele pigmenten en post-depositionele verweringsproducten. Deze verwering is aanwezig als een relatief dunne, niet-transparante laag die de beschilderingen en de rots (drager) al dan niet volledig bedekt. Bovendien lijkt de oorspronkelijke bevolking in sommige gevallen op oppervlakken gewerkt te hebben, die al bedekt waren met een degradatielaag. Tijdens Raman-analyses kan het signaal van de pigmenten overstemd worden door de bovenliggende lagen. Gelaagde structuren zijn echter niet enkel het gevolg van degradatieprocessen: ze kunnen in haast elk erfgoedobject teruggevonden worden. Tot voor kort was staalname de enige manier om de moleculaire samenstelling van bedekte lagen te bestuderen.

Een vernieuwende benadering voor de niet-invasieve en niet-destructieve moleculaire stratigrafische analyse van micrometer-dikke lagen wordt uitgebreid geïllustreerd in dit

doctoraatswerk (Hoofdstuk 5). Glasvezel micro-ruimtelijk verplaatste (*microspatially offset*) Ramanspectroscopie (glasvezel micro-SORS) wordt voorgesteld als een alternatieve benadering voor micro-SORS. Deze nieuwe micro-SORS sensor die glasvezels (zonder filters) gebruikt om het laserlicht en het Ramansignaal over te brengen is een veelbelovende benadering met een breed gamma aan toepassingen, waaronder kunstanalyse. De lichte en compacte configuratie van glasvezel micro-SORS, laat toe om de meetopstelling verder te miniaturiseren en een vernieuwde meetsonde te maken.

Aanvullend op micro-SORS puntmetingen, werd ook Raman mapping van bedekte lagen ontwikkeld, door gebruik te maken van een andere variant van de micro-SORS techniek, namelijk gedefocusseerde (*defocusing*) micro-SORS (Hoofdstuk 6). Dit is één van de meest eenvoudige benaderingen voor micro-SORS, gezien het een standaard commerciële Ramanspectrometer gebruikt. Hoewel de resultaten van *defocusing* micro-SORS veelbelovend zijn, verder onderzoek is noodzakelijk om de verschillende lagen beter te kunnen onderscheiden.

Dit doctoraatsonderzoek combineert rechtstreekse analyse en stratigrafische analyse, om zo vernieuwende oplossingen voor te stellen binnen het Ramanspectroscopisch onderzoek en de erfgoedanalyse. Dit onderzoek probeert een beperking van traditionele Ramanspectroscopie weg te werken, namelijk door te pogen om informatie te verkrijgen, die ontstaat onder het oppervlak van het kunstwerk. Recente ontwikkelingen van de micro-SORS techniek leidden tot nieuwe benaderingen. Dit doctoraat moet beschouwd worden als de eerste stap naar verdere toepassingen en fundamenteel onderzoek, langs twee assen: (a) verbetering van Ramanspectroscopie voor de analyse van prehistorische rotskunst en de suggestie van nieuwe strategieën en (b) het begrip van de fysische fenomenen in micro-SORS om tot een betere benadering te komen, waarbij zowel hard- als software (dataprocessing) verbeterd worden. Enkele toekomstige onderzoeksdoelstellingen zouden kunnen zijn:

a. Voor het onderzoek naar rotsschilderingen:

a1. Meer fundamenteel onderzoek is nodig naar het Ramansignaal van okers en aardpigmenten. Gedopeerde matrices, structurele distorsies, de geologische genese, degradatie, hoge temperaturen, etc. kunnen verschillende veranderingen in het Ramanspectrum veroorzaken (bandverschuiving, bandverbreding, of het ontstaan van nieuwe Ramanbanden). Reconstructies, in overeenstemming met traditionele gebruiken (thermische behandelingen, het mengen met organische producten, etc.) zullen ook bestudeerd moeten worden, om zo de structurele veranderingen te bestuderen.

a2. Daarnaast moet fundamenteel onderzoek uitgevoerd worden naar de degradatieproducten. Het begrijpen van de vormingsmechanismen van een verweringskorst (afhankelijk van de omgeving en de pollutie) en de interpretatie van hun Raman bandposities zal bijdragen tot een stabiel interpretatieprotocol. Bovendien moet de vergelijking gemaakt worden met ruw materiaal zoals keien, rotsafzettingen en andere geologische structuren afkomstig van verschillende plaatsen.

a3. De introductie van verschillende lasergolflengtes (vb. 1064 nm) in het onderzoek, en lichtere Ramaninstrumentatie in het veldonderzoek zou ons in staat stellen om meer informatie te bekomen (inclusief organische moleculen, zoals bindmiddelen en lakken) en zal de techniek mobieler maken. Door verschillende lasers te kunnen selecteren, kan fluorescentie in sommige gevallen onderdrukt worden en kunnen de signalen van zwakke Raman verstrooiers versterkt worden.

a4. Het onderzoek naar rotsschilderingen kan gebaat zijn door ook andere technieken hierin te betrekken, zoals Mössbauer spectroscopie, wat een methode is die uitermate geschikt is voor de analyse van ijzeroxides, of X-stralen diffractie (XRD) om kristallijne fasen te analyseren. Bovendien kan luminescentie als dateringstechniek gebruikt worden als alternatief voor ^{14}C datering van de oxalaatkorst of van houtskoolresten tijdens de periode

van menselijke bewoning (opgegraven lagen). Luminescentie maakt gebruik van het feit dat de lagen werden gebleekt in zonlicht, voordat ze bedekt werden met verf.

a5. Als finaal doel dienen de resultaten (voor pigmenten, degradatieproducten en grondlagen) van verschillende onderzoeksgroepen en verschillende sites met elkaar vergeleken worden.

b. Moleculaire analyse van gelaagde materialen kan een behoorlijke impact hebben in verschillende wetenschappelijke velden, zoals o.a. kunstanalyse, archeologie, geologie, biomedische wetenschappen, farmacie, etc. Een diepgaand onderzoek naar micro-SORS kan de techniek meer toegankelijk maken, van een beperkt aantal gespecialiseerde laboratoria, onder meer in *in situ* onderzoeken. Daarvoor dienen een aantal stappen genomen te worden:

b1. Verdere ontwikkeling van glasvezel micro-SORS. Gezien deze benadering pas recent ontwikkeld werd, dient dit verder geoptimaliseerd te worden. Zo dient de invloed van de glasvezels (type, diameter, etc.) onderzocht te worden en moet de experimentele set-up verbeterd worden (o.a. het beschermen van de broze glasvezels).

b2. Om de fundamentele principes van micro-SORS beter te begrijpen, moeten er een reeks analyses uitgevoerd worden op goed-gedefinieerde teststalen. Er kunnen analyses uitgevoerd worden met een meetsonde waarbij de verschillende parameters onafhankelijk van elkaar kunnen gevarieerd worden, zodat de invloed van de verschillende eigenschappen nauwkeurig bepaald kan worden, vooraleer deze op een onbekend staal toegepast worden. De dataverwerking dient geautomatiseerd te worden en de mogelijkheden voor micro-SORS mapping dienen verder geëvalueerd worden.

b3. Het gebruik van verschillende lasers voor de micro-SORS techniek. Het gebruik van een 1064 nm laser kan nieuwe inzichten met zich meebrengen en zou kunnen bijdragen in de analyse van lagen die niet volledig opaak zijn (dus transparant of semi-transparant).

b4. De vergelijking van verschillende micro-SORS benaderingen en de evaluatie naar de combinatie met mobiele apparatuur. De sterktes en zwaktes van de verschillende micro-SORS benaderingen dienen geëvalueerd te worden, zowel qua performantie, qua gebruiksgemak als qua dataverwerking.

b5. Toepassing van micro-SORS in het laboratorium zowel als *in situ*. De toepasbaarheid van de verschillende micro-SORS benaderingen kan geïmplementeerd worden in baanbrekende studies, waar het relevant is om moleculaire informatie te bekomen van lagen die bedekt zijn met niet-transparante materialen. Sommige van deze toepassingen zouden het onderzoek naar prehistorische schilderkunst kunnen omvatten(zoals in dit doctoraatsproefschrift voorgesteld), kunstwerken van René Magritte en de surrealisten, erg gelaagde kunstwerken, zoals het Lam Gods, geologische toepassingen, etc.

Dit doctoraat had tot doel om nieuwe benaderingen te introduceren voor de analyse van gelaagde kunstwerken met Raman spectroscopie. We focusten op *in situ* toepassingen voor de studie van rotskunst uit Patagonië. Daarnaast werden enkele aanpassingen voor micro-SORS voorgesteld, om de techniek meer toepasbaar te maken voor archeometrische toepassingen. We zijn ervan overtuigd dat veel aspecten verder onderzoek vergen, voordat deze benadering breed toepasbaar is, maar we hopen met dit werk een stevige basis gecreëerd te hebben voor verdere studies.

Publications and contributions

List of articles

1. A. Rousaki, E. Vargas, C. Vázquez, V. Aldazábal, C. Bellelli, M. Carballido Calatayud, A. Hajduk, O. Palacios, L. Moens, P. Vandenabeele, On-field Raman Spectroscopy of Patagonian Prehistoric Rock Art: Pigments, Alteration Products and Substrata, Trend. Anal. Chem., 2018, accepted.

2. A. Rousaki, A. Botteon, C. Colombo, C. Conti, P. Matousek, L. Moens, P. Vandenabeele, Development of defocusing micro-SORS mapping: a study of a 19th century porcelain card**,** Anal. Methods 9 (2017) 6435-6442.

3. P. Vandenabeele, C. Conti, A. Rousaki, L. Moens, M. Realini, P. Matousek, Development of a fiber-optics microspatially offset raman spectroscopy sensor for probing layered materials, Anal. Chem. 89 (2017) 9218-9223.

4. A. Rousaki, C. Vázquez, V. Aldazábal, C. Bellelli, M. Carballido Calatayud, A. Hajduk, E. Vargas, O. Palacios, P. Vandenabeele, L. Moens, The first use of portable Raman instrumentation for the in situ study of prehistoric rock paintings in Patagonian sites, J. Raman Spectrosc. 48 (2017) 1459–1467.

5. A. Coccato, M. Costa, A. Rousaki, B.-O. Clist, K. Karklins, K. Bostoen, A. Manhita, A. Cardoso, C. Barrocas Dias, A. Candeias, L. Moens, J. Mirão, P. Vandenabeele, Micro-Raman spectroscopy and complementary techniques (hXRF, VP-SEM-EDS, µ-FTIR and Py-GC/MS) applied to the study of beads from the Kongo Kingdom (Democratic Republic of the Congo)**,** J. Raman Spectrosc. 48 (2017) 1468–1478.

6. A. Rousaki, A. Coccato, C. Verhaeghe, B.–O. Clist, K. Bostoen, P. Vandenabeele, L. Moens, Combined spectroscopic analysis of beads from the tombs of Kindoki, Lower Congo Province (Democratic Republic of the Congo), J. Appl. Spectrosc. 70 (2016) 76-93.

7. A. Rousaki, C. Bellelli, M. Carballido Calatayud, V. Aldazabal, G. Custo, L. Moens, P. Vandenabeele, C. Vázquez, Micro-Raman Analysis of Pigments from Hunter-Gatherer Archaeological Sites of North Patagonia (Argentina), J. Raman Spectrosc. 46 (2015) 1016-1024.

List of book chapters

1. A. Rousaki, L. Moens, P. Vandenabeele, Archeological investigations (Archaeometry), in: J. Popp (Ed.), Micro-Raman Spectroscopy Theory and Application, Physical Sciences Reviews, De Gruyter, Berlin, Germany, 2018, submitted.

2. P. Vandenabeele, A. Rousaki, M. Costa, L. Moens, H.G.M. Edwards, Pigments and colourants, in: H.G.M. Edwards, P. Vandenabeele (Eds.), Raman Spectroscopy in Archaeology and Art History (Vol. 2), Royal Society of Chemistry, Cambridge, UK, 2018 (In Press).

List of conference contributions

1. **"Unfolding the Prehistoric World: Portable and Benchtop Raman Spectroscopy for the Analysis of Rock Art"**
IFRAO 2018 – 20th International Rock Art Congress, August 29 - September 2, 2018, Valle Camonica, Darfo Boario Terme (BS), Italy (***oral presentation, accepted***), A. Rousaki, L. Moens, P. Vandenabeele

2. **"Analysis of painted pre-Islamic pottery from the Kur River Basin (Fars, Iran) using Raman Spectroscopy"**

   XIII International GeoRaman Conference, June 10-14, 2018, Catania, Italy ***(poster presentation, accepted),*** P. Pincé, A. Rousaki, S. Lycke, P. Vandenabeele

3. **"Towards the non-invasive identification of layered structures by Raman Spectroscopy"**

   XIII International GeoRaman Conference, June 10-14, 2018, Catania, Italy ***(oral presentation, accepted),*** P. Vandenabeele, A. Rousaki, B. Vanderhaeghe, M. D'Hiet, C. Conti, P. M., L. Moens

4. **"Project Cástulo (Linares, Spain): archaeometric approach by MRS, EDXRF, hXRF and GC-MS"**

   XIII International GeoRaman Conference, June 10-14, 2018, Catania, Italy ***(oral presentation, accepted),*** A. Sánchez, P. Vandenabeele, J. Tuñón, D. Parras, S. Lycke, B. Ceprián, M. Montejo, A. Rousaki, M. Barrocas, D. Saelens, M. Castro

5. **"Espectroscopía Raman in situ: Pigmentos, sustratos y alteraciones en el Arte Rupestre Norpatagónico"**

   VII Congreso Nacional de Arqueometria (CNA 2018): Materialidad, Arqueologia, Patrimonio (VII Archaeometry National Congress - Argentina: Materiality, Archaeology, Patrimony), 17-20 April 2018, San Miguel de Tucumán, Argentina ***(poster presentation),*** A. Rousaki, E. Vargas, C. Vázquez, V.Aldazábal, C. Bellelli, M. Carballido Calatayud, A. Hajduk, O. Palacios, L. Moens, P. Vandenabeele

6. **"Combined Spectroscopic Analysis on the Cork Masterpiece of the Pantheon of Rome Made By Antonio Chichi"**

   inArt 2018, 3nd International Conference on Innovation in Art Research and Technology, 26-29 March 2018, Parma, Italy ***(poster presentation),*** A. Rousaki, S. Lycke, P. Monsieur, M. Martens, L. Moens, P. Vandenabeele

7. **"Confocal Micro-Raman Spectroscopy for the Study of Natural Fibres"**
inArt 2018, 3nd International Conference on Innovation in Art Research and Technology, 26-29 March 2018, Parma, Italy ***(poster presentation),*** A. Rousaki, B. Braem, L. Moens, P. Vandenabeele

8. **"Raman Spectroscopy in Archaeometry"**
2nd Pan-Hellenic Conference on Digital Cultural Heritage-EuroMed 2017, 1-3 December 2017, Volos, Greece ***(keynote lecture),*** A. Rousaki, L. Moens, P. Vandenabeele

9. **"Development of a Fibre Optics Micro-SORS Sensor for Probing Layered Cultural Heritage Objects"**
RAA 2017, 9th International Congress on the Application of Raman Spectroscopy in Art and Archeology, October 24-26, 2017, Évora, Portugal, **Best Poster Award** ***(poster presentation)***, A. Rousaki, C. Conti, L. Moens, M. Realini, P. Matousek, P. Vandenabeele

10. **"Micro-Raman Spectroscopy for the Analysis of Ceramics from Ecuador"**
RAA 2017, 9th International Congress on the Application of Raman Spectroscopy in Art and Archeology, October 24-26, 2017, Évora, Portugal ***(poster presentation)***, A. Rousaki, E. Odelli, V. Dominguez, C. Vázquez, O. Palacios, D. Bersani, L. Moens, P. Vandenabeele

11. **"Depicted on Stone: Raman Spectroscopy for the Analysis of Rock Art Paintings"**
RAA 2017, 9th International Congress on the Application of Raman Spectroscopy in Art and Archeology, October 24-26, 2017, Évora, Portugal, p. g. 50 ***(oral presentation)***, A. Rousaki, L. Moens, P. Vandenabeele

12. **"Portable and Handheld Raman Instrumentation: Investigation of Materials from Patagonian Rock Art Paintings"**
RAA 2017, 9th International Congress on the Application of Raman Spectroscopy in Art and Archeology, October 24-26, 2017, Évora, Portugal ***(poster presentation),*** A. Rousaki, A.

Arnaboldi, A. Culka, C. Vázquez, V. Aldazábal, C. Bellelli, M. Carballido Calatayud, A. Hajduk, E. Vargas, O. Palacios, S. Bruni, J. Jehlička, L. Moens, P. Vandenabeele

13. **"The first use of portable Raman instrumentation for the analysis of Patagonian prehistoric rock art paintings: pigments, accretions and substrata"**
TECHNART 2017, Non-Destructive and Microanalytical Techniques in Art and Cultural Heritage, May 2 - 6, 2017, Bilbao, Spain p. g. 137 ***(oral presentation),*** A. Rousaki, C. Vázquez, V. Aldazábal, C. Bellelli, M. Carballido Calatayud, A. Hajduk, E. Vargas, O. Palacios, A. Culka, J. Jehlička, L. Moens, P. Vandenabeele

14. **"Unraveling the composition of coloured glass by the comparison of complementary spectroscopic methodologies: the case of beads from the Kongo Kingdom"**
TECHNART 2017, Non-Destructive and Microanalytical Techniques in Art and Cultural Heritage, May 2 - 6, 2017, Bilbao, Spain p. g. 301 ***(poster presentation),*** B. Laforce, A. Rousaki, A. Coccato, M. Costa, B. Clist, K. Karklins, K. Bostoen, B. Vekemans, L. Moens, J. Mirão, L. Vincze, P. Vandenabeele

15. **"The First Use of Portable Raman Instrumentation for the in situ Study of Prehistoric Rock Paintings in North Patagonian Sites"**
XIIth International GeoRaman Conference, June 9-15, 2016, Novosibirsk, Russia, p. g. 127 ***(poster presentation),*** A. Rousaki, C. Vázquez, V. Aldazabal, Cristina Belleli, M. Carballido Calatayud, A. Hajduk, O. Palacios, P. Vandenabeele, L. Moens

16. **"Raman (532 and 785 nm) study of glass beads from the Kongo Central province, Democratic Republic of Congo (DRC)"**
XIIth International GeoRaman Conference, June 9-15, 2016, Novosibirsk, Russia, p. g. 89 ***(poster presentation),*** A. Coccato, A. Rousaki, M. Costa, B. Clist, K. Bostoen, L. Moens, P. Vandenabeele

17. **"Analysis of Glass Beads from the Democratic Republic of Congo by Means of a Non-Destructive Multi-Analytical Approach"**

SAfA 2016, the Society of Africanist Archaeologists , 23rd Biennial Meeting, 26 June-2 July 2016, Toulouse, France, p. g. 12 (Book of Posters) **(*poster presentation),*** M. Costa, A. Coccato, A. Rousaki, C. Verhaeghe, B. Clist, K. Bostoen, L. Moens, J. Mirão, P. Vandenabeele

18. **"A Protocol to evaluate how Good Varnishes protect Silver Gilding Against Atmospheric Pollutants"**

ChemCH 2016, 4th International Congress Chemistry for Cultural Heritage, Brussels, July 6-8, 2016, p. g 81 ***(poster presentation),*** A. Rousaki, P. Vandenabeele, J. Sanyova, H. Dubois, L. Moens

19. **"Evaluation of the Protective Capacity of Coatings on Silver Foil Exposed to H_2S, HCl and H_3CCOOH as a Model for the Ghent Altarpiece Gilded Frames"**

inArt 2016, 2nd International Conference on Innovation in Art Research and Technology, 21-25 March 2016, Ghent, Belgium, p.g 208 ***(poster presentation),*** A. Rousaki, P. Vandenabeele, J. Sanyova, H. Dubois, L. Moens

20. **"Combined historical, physical anthropology, archaeological, and archaeometrical approaches to understand glass beads from the tombs of Mbanza Nsundi, Kongo Central province, Democratic Republic of Congo (DRC)"**

inArt 2016, 2nd International Conference on Innovation in Art Research and Technology, 21-25 March 2016, Ghent, Belgium, p.g 61 ***(oral presentation),*** A. Coccato, A. Rousaki, B. Clist, K. Bostoen, P. Vandenabeele

21. **"Análisis In Situ de Pinturas Rupestres de Sitios de Norpatagonia, Utilizando un Equipo Raman Portátil"**

XIX del CNAA, XIX Congreso Nacional de Arqueología Argentina, San Miguel de Tucumán, Tucumán, Argentina, 08-12 Agosto 2016, p. g. 195 ***(poster presentation),*** C. Vázquez, A. Rousaki, V. Aldazabal, A. Hajduk, O. Palacios, P. Vandenabeele, L. Moens, E. Vargas

22. **"Combined spectroscopic analysis of beads from the tombs of Kindoki, MbanzaNsundi, Lower Congo"**

RAA 2015, 8th International Congress on the Application of Raman Spectroscopy in Art and Archeology, September 1-5, 2015, Wroclaw, Poland, p.g. 68 ***(oral presentation),*** A. Coccato, A. Rousaki, C. Verhaeghe, B.-O Clist, K. Bostoen, P. Vandenabeele, L. Moens

23. **"Micro-Raman analysis of prehistoric rock art in Patagonia (Argentina)"**

RAA 2015, 8th International Congress on the Application of Raman Spectroscopy in Art and Archeology, September 1-5, 2015, Wroclaw, Poland, p. g. 72 ***(oral presentation),*** A. Rousaki, A. Coccato , C. Bellelli , M. Carballido Calatayud, O. Palacios, G. Custo, L. Moens, P. Vandenabeele, C. Vázquez

24. **"Optimization of TXRF for the analysis of paint samples"**

Technart 2015, Non-destructive and Microanalytical Techniques in Art and Cultural Heritage, April 27-30, 2015 Monastero dei Benedettini, Catania, Italy, p. g. 225 (P1-63) ***(poster presentation),*** A. Coccato, A. Rousaki, L. Moens, P. Vandenabeele

25. **"Spectroscopic Investigations on Portable Icons from Historical Saint Paul's Church of Thessaloniki Charitable Men Fellowship"**

Technart 2015, Non-destructive and Microanalytical Techniques in Art and Cultural Heritage, April 27-30, 2015, Catania, Italy, p. g. 433, (P2-78) ***(poster presentation)***

A. Rousaki, D. Lazidou, T. Zorba, T. Fardi, D. Nikolis, N. Bonobas, I. Nazlis, E. Pavlidou, D. Lampakis, E. Likartsi, K. Paraskevopoulos

26. "Spectroscopic analysis of the Ghent Altarpiece"

Cultural Programm of the Symposium : "Mechanisms of Innate Immunity, Cell Death and Inflammation", 25 & 26 September 2014, Het Pand, Gent, Belgium ***(oral presentation)***, P. Vandenabeele, A. Coccato, D. Lauwers, A. Rousaki, L. Moens

27. "Archeometrical Study of the Ghent Altarpiece I"

Ghent Altarpiece, International Study Day, 10 September 2014, Aula Academica, Voldersstraat 9, Ghent, Belgium ***(oral presentation),*** P. Vandenabeele, A. Coccato, D. Lauwers, A. Rousaki

List of field campaigns

09/04/2018-25/04/2018 Portable Raman and XRF campaign of Cástulo archaeological site, in Linares, Jaén, Spain (FWO-project K207718N)

14/11/2017-23/11/2017 Portable Raman and hXRF analysis on the cork masterpiece of the Pantheon of Rome made By Antonio Chichi, Ghent University, Ghent, Belgium.

18/09/2017 Portable Raman and hXRF analysis of a single altar stone from the goddess Nehallenia, Koninklijke Musea voor Kunst en Geschiedenis (KMKG), Brussels, Belgium.

20/2/2016-8/3/2016 Portable Raman campaign in Patagonia, Argentina (FWO-project K204416N)

2014-2016 Portable Raman measurements under the concerted research action "Archaeometrical Study of the Ghent Altarpiece" (GOA-BOF), B/13340/02, Museum voor Schone Kunsten (MSK), Ghent, Belgium.